Development of Green Electrode Fabrication Technologies for Low Cost and High Performance Lithium Ion Batteries

Author

Ling, Min

Published

2015

Thesis Type

Thesis (PhD Doctorate)

School

Griffith School of Environment.

DOI

10.25904/1912/1809

Development of Green Electrode Fabrication Technologies for Low Cost and High Performance Lithium Ion Batteries

Min Ling

B.Sc., M.Sc.

Griffith School of Environment

Griffith Sciences

Griffith University

Submitted in fulfilment of the requirements of the degree of Doctor of Philosophy

March 2015

ABSTRACT

Rechargeable lithium ion batteries (LIBs) are playing a dominant role in powering enormous numbers of portable electronic products and modernizing our everyday life. In the past decade, intense investment, research and development have been devoted to improving the major components of LIBs such as active materials, separators and electrolytes to further the application of LIBs for high energy consumption devices. The currently available LIBs however, cannot meet all requirements primarily because of low electronic/ion conductivity of electrodes. Furthermore, cost, safety, and environmental issues continue to impede further development of LIBs. In particular, the traditional electrode fabrication process commonly involves the consumption of toxic organic solvents such us NMP.

To address all these issues, this thesis attempts to develop green electrode fabrication technologies for low cost and high performance LIBs by selection and modification of low cost and sustainable natural binders and removing the adoption of the toxic organic solvents.

To convert the traditional LIB electrode production process from an organic solvent-based process into a green and water-based production technology, the water-soluble polymer *Eastman AQ^{TM} 55S* (EAQ) was chosen as a binder for graphite anodes in LIBs. The chemical bonds between the carboxyl groups on the oxidized graphite surface and the hydroxyl groups on the EAQ polymer surface offer strong binding force and provide excellent Li ion conductivity, enhancing cell performances. The EAQ-based electrode can withstand 1.6 pound peel force, which is nearly twice the force applied to conventional PVDF-based electrode. The resultant EAQ-based

electrode delivered a capacity of ca. 360 mAh/g compared to 250 mAh/g for PVDF-based electrodes.

Another water-based electrode fabrication system was developed for Si anode materials. This was challenging as Si nanoparticles possess the largest specific capacity (4200 mAh/g) but experience substantial volume expansion (ca. 300%) during lithiation/delithiation. The two main benefits of the gum arabic (GA) binder involve performance enhancement: hydroxyl groups in polysaccharide increase the binding force and glycoproteins improve the mechanical properties as seen in *Fibre-Reinforced Concrete* (FRC) to prevent cracks resulting from the volume expansion of lithiated Si electrodes. A stable cycling performance was demonstrated at various *C* rates using the GA binder while a promising long-term performance of 1000 cycles was observed when limiting the specific capacity to 1000 mAh/g at 1 *C*.

To expand applicability, this GA binder has been applied to Lithium-Sulfur (S) batteries which are one of the most promising and challenging energy storage systems. The resulting S@GA electrode demonstrates significantly better electrochemical performance compared to the S@PVDF and S@Gelatin electrodes. The S@GA electrode delivered an initial capacity of 1386 mAh/g at *C*/5, and 843 mAh/g at *C*/5 and 504 mAh/g at 1 *C* throughout 500 cycles when sulfur loading was 55 wt% in sulfur/carbon composites. To the best of our knowledge, the GA binder in this work has a better cycling performance than previous used bio-derived and non-bio-derived binders in Li-S batteries.

To produce high areal loading Si anodes and high volumetric capacity for the LIBs, the GA is modified via a simple *in situ* esterification with polyacrylic acid (PAA) at 150 ^{o}C under vacuum to establish a cross-linking binding network. The esterification reaction between hydroxyl groups in GA and carboxylic acid groups in

PAA reinforced mechanical strength and lithium ion diffusion coefficient. Furthermore, the micron-sized pores formed during the process prevented the crack formation and propagation by relieving the stress on the electrode due to the dramatic volume change of Si particles during charge/discharge processes. The crack-blocking effect helped the GA-PAA composite binder-based Si electrode achieve high volumetric capacity of ca. 2898 Ah/L, which is nearly five times that of graphite electrode (ca. 600 Ah/L).

Sodium alginate (SA) and 3,4-propylenedioxythiophene-2,5-dicarboxylic acid (ProDOT) were used to synthesized multi-functional polymer binder SA-ProDOT using a cyclohexane/DBSA/water micro-emulsion system. The tailored electronic structure of the SA-ProDOT facilitated n-type lithium doping under the battery environment. A long-term cycle with specific capacity of ca. 120 mAh/g at 1 *C* for more than 400 cycles was achieved without conductive additives when SA-ProDOT was applied as the binder for $LiFePO_4$ cathodes. The optimized performances compared with SA, SA plus carbon black (CB) and PVDF plus CB were due to the improved mechanical property, Li-ion conduction, diffusion coefficient and lower electro-chemical impedance. The synthesized SA-ProDOT is promising for universal application in low cost and environmentally benign manufacturing of LIBs.

STATEMENT OF ORIGINALITY

This work has not previously been submitted for a degree or diploma in any university. To the best of my knowledge and belief, the thesis contains no material previously published or written by another person except where due reference is made in the thesis itself.

(Signed)_____

Name of Student: Min Ling

March 2015

TABLE OF CONTENT

ACKNOWLEDGEMENTS

The writing and completion of this dissertation would not have been possible without the guidance and support of a few very special people in my life.

My principle supervisor, A/Prof. Shanqing Zhang, always offers me his genius research insight and gives me inspiration and encouragement to further achievements. My sincere thanks also go to my associate supervisors Prof. Huijun Zhao, Dr. Milton Kiefel, Dr, Peng Zhang and my external supervisor Dr. Gao Liu for their guidance and support at all critical moments. During 2013, I studied after Dr. Gao Liu in the Lawrence Berkeley National Lab in US where I learned state-of-the-art LIB technologies and communicated widely many top academics.

I would also like to express my gratitude to Dr. Jingxia Qiu for her training and guidance in the lab. I would like to extend my thanks to all team members: Mr. Sheng Li, Mr. Yazhou Wang, Ms. Tianling Li, Mr. Xingxing Gu and Mr. Tiefeng Liu who have accompanied me day and night to overcome all sorts of barriers and difficulties in the lab. I also want to thank my colleagues, Dr. Yanbao Fu, Dr. Hui Zhao, Dr. Mingyan Wu, Ms. Fan Yang, Dr. Yibing Li, Dr. Xiaolu Liu, Mr. Tao Sun Lindi Wu and Mr Zhijin Tan for their help and friendship. My sincere appreciation also goes to ENV, EFRI and CCEE, especially Dr. Yun Wang, Dr. Robert Liu, Dr. William Wen, Ms. Belinda Hachem and Dr. Clare Morrison for their great help.

I want to thank Ms. Ying Yu and Mr. Xiangyun Song for their training and expertise with SEM and TEM at the University of Queensland and Lawrence Berkeley National Lab, respectively.

Finally, I would like to express my deep gratitude to my parents for their love, supports from my brother and happiness from my niece Xuan.

ALL PAPERS INCLUDED ARE CO-AUTHORED

Acknowledgement of Papers included in this Thesis

Section 9.1 of the Griffith University Code for the Responsible Conduct of Research ("Criteria for Authorship"), in accordance with Section 5 of the Australian Code for the Responsible Conduct of Research, states:

> To be named as an author, a researcher must have made a substantial scholarly contribution to the creative or scholarly work that constitutes the research output, and be able to take public responsibility for at least that part of the work they contributed. Attribution of authorship depends to some extent on the discipline and publisher policies, but in all cases, authorship must be based on substantial contributions in a combination of one or more of:
>
> - conception and design of the research project
> - analysis and interpretation of research data
> - drafting or making significant parts of the creative or scholarly work or critically revising it so as to contribute significantly to the final output.

Section 9.3 of the Griffith University Code ("Responsibilities of Researchers"), in accordance with Section 5 of the Australian Code, states:

> Researchers are expected to:
>
> - Offer authorship to all people, including research trainees, who meet the criteria for authorship listed above, but only those people.
> - Accept or decline offers of authorship promptly in writing.
> - Include in the list of authors only those who have accepted authorship
> - Appoint one author to be the executive author to record authorship and manage correspondence about the work with the publisher and other interested parties.
> - Acknowledge all those who have contributed to the research, facilities or materials but who do not qualify as authors, such as research assistants, technical staff, and advisors on cultural or community knowledge. Obtain written consent to name individuals.

Included in this thesis are papers in *Chapters 2, 3, 4, 5 and 6* which are co-authored with other researchers. My contribution to each co-authored paper is outlined at the

front of the relevant chapter. The bibliographic details/status for these papers including all authors, are:

Chapter 2: Ling, M., Qiu, J., Li, S., Zhao, H., Liu, G. & Zhang, S. (2013) 'An environmentally benign LIB fabrication process using a low cost, water soluble and efficient binder', *Journal of Materials Chemistry A* 1, 11543-11547.

Chapter 3: Ling, M., Xu, Y., Zhao, H., Gu, X., Qiu, J., Li, S., Wu, M., Song, X., Yan, C., Liu, G. & Zhang, S. (2015) 'Dual-functional gum arabic binder for silicon anodes in lithium ion batteries', *Nano Energy* 12, 178-185.

Chapter 4: Chapter 4: Acacia Senegal Inspired Bi-functional Binder for Longevity of Lithium Sulfur Batteries (2015, prepared).

Chapter 5: Ling, M., Zhao, H., Xiao, X, Shi, F., Wu, M., Qiu, J., Li, S., Song, X., Liu, G. & Zhang, S. (2014) 'Low cost and environmentally benign crack-blocking structures for long life and high power Si electrodes in lithium ion batteries', *Journal of Materials Chemistry A* 3, 2036-2042.

Chapter 6: Ling, M., Li, S., Qiu, J., Yan, C, Kiefel, M, Liu, G. & Zhang, S. A Multi-functional SA-ProDOT Binder for Lithium Ion Batteries (2015, submitted to Nano Letters, manuscript ID: nl-2015-00795w).

Appropriate acknowledgements of those who contributed to the research but did not qualify as authors are included in each paper.

(Signed) _____ (Date)_____

Name of Student: Min Ling

(Countersigned) _____ (Date)_____

Supervisor: Shanqing Zhang

PUBLICATIONS

Chapter Publications

This thesis consists of three published papers, Chapters 2, 3 and 5 which are co-authored with other researchers. My contribution to each co-authored paper is outlined at the beginning of each relevant chapter.

Chapter 2: Ling, M., Qiu, J., Li, S., Zhao, H., Liu, G. & Zhang, S. (2013) 'An environmentally benign LIB fabrication process using a low cost, water soluble and efficient binder', *Journal of Materials Chemistry A* 1, 11543-11547.

Chapter 3: Ling, M., Xu, Y., Zhao, H., Gu, X., Qiu, J., Li, S., Wu, M., Song, X., Yan, C., Liu, G. & Zhang, S. (2015) 'Dual-functional gum arabic binder for silicon anodes in lithium ion batteries', *Nano Energy* 12, 178-185.

Chapter 4: Acacia Senegal Inspired Bi-functional Binder for Longevity of Lithium Sulfur Batteries (2015, prepared).

Chapter 5: Ling, M., Zhao, H., Xiao, X., Shi, F., Wu, M., Qiu, J., Li, S., Song, X., Liu, G. & Zhang, S. (2014) 'Low cost and environmentally benign crack-blocking structures for long life and high power Si electrodes in lithium ion batteries', *Journal of Materials Chemistry A* 3, 2036-2042.

Chapter 6: Ling, M., Li, S., Qiu, J., Yan, C, Kiefel, M, Liu, G. & Zhang, S. A Multi-functional SA-ProDOT Binder for Lithium Ion Batteries (2015, submitted to *Nano Letters*, manuscript ID: nl-2015-00795w).

Additional Publications

I have been actively involved in a number of other research projects, leading to the following co-authored publications, which are not part of my thesis itself. The bibliographic details for these papers are:

1. Qiu, J., Zhang, P., **Ling, M.**, Li, S., Liu, P., Zhao, H. & Zhang, S. (2012) 'Photocatalytic Synthesis of TiO_2 and Reduced Graphene Oxide Nanocomposite for Lithium Ion Battery', *ACS Applied Materials & Interfaces* 4, 3636-3642.

2. Li, S., Qiu, J., **Ling, M.**, Peng, F., Wood, B. & Zhang, S. (2013) 'Photoelectrochemical Characterization of Hydrogenated TiO_2 Nanotubes as Photoanodes for Sensing Applications', *ACS Applied Materials & Interfaces* 5, 11129-11135.

3. Zhang, P., Qiu, J., Zheng, Z., Liu, G., **Ling, M.**, Martens, W., Wang, H., Zhao, H. & Zhang, S. (2013) 'Free-standing and bendable carbon nanotubes/TiO_2 nanofibres composite electrodes for flexible lithium ion batteries', *Electrochimica Acta* 104, 41-47.

4. Li, S., Wang, Y., Lai, C., Qiu, J., **Ling, M.**, Martens, W., Zhao, H. & Zhang, S. (2014) 'Directional synthesis of tin oxide@graphene nanocomposites via a one-step up-scalable wet-mechanochemical route for lithium ion batteries', *Journal of Materials Chemistry A* 2, 10211-10217.

5. Li, S., Wang, Y., Qiu, J., **Ling, M.**, Wang, H., Martens, W. & Zhang, S. (2014) 'SnO2 decorated graphene nanocomposite anode materials prepared via an up-scalable wet-mechanochemical process for sodium ion batteries', *RSC Advances* 4, 50148-50152.

6. Zhao, H., Zhou, X., Park, S.-J., Shi, F., Fu, Y., **Ling, M.**, Yuca, N., Battaglia, V. & Liu, G. (2014) 'A polymerized vinylene carbonate anode binder enhances performance of lithium-ion batteries', *Journal of Power Sources* 263, 288-295.

Conference Presentations

1. The 5th Australia-China Conference on Science, University of Wollongong (UOW), Australia, 21-23 July 2014. **Poster**: *Functionalized natural sodium alginate polymer as the conductive polymer binder for lithium ion batteries.*
2. The 6th International Conference on Advanced Lithium Batteries for Automobile Applications, Argonne National Laboratory, 9-11 September 2013. **Poster**: *An environmentally benign LIB fabrication process using a low cost, water soluble and efficient binder.*
3. The 7th U.S.-China Electric Vehicle and Battery Technology Workshop sponsored by U.S. Department of Energy and China Ministry of Science and Technology, Lawrence Berkeley National Lab, U.S. 4-5 April 2013.

Invited Presentation

1. ECS 224th Meeting, San Francisco, California October 27 – November 1, 2013，

   Oral: *An environmentally benign LIB fabrication process using a low cost, water soluble and efficient binder.*

KEY WORDS

Natural binders

Water-soluble binders

Gum arabic

Polyacrylic acid

Eastman AQ™ 55S

Graphite anode

Silicon anode

Lithium ion phosphate cathode

Lithium-sulfur battery

Fibre reinforcement

Condensation reaction

Crosslinking structure

Functionalization

Multi-functions

Lithium ion conductivity

Electronic conductivity

Volume expansion

Crack-blocking

Environmental-benign

Chemical bonding

Energy density

Powder density

ACRONYMS

LIBs	Lithium-ion batteries
EVs	Electric vehicles
HEV	Hybrid electric vehicle
FCs	Fuel cells
ICEs	Internal combustion engines
$LiPF_6$	Lithium hexafluorophosphate
LFP	$LiFePO_4$
Si	Silicon
S	Sulfur
EC	Ethylene carbonate
DEC	Diethylene carbonate
DMC	Dimethyl carbonate
FEC	Fluorinated ethylene carbonate
R_s	Electrolyte resistance
R_{ct}	Charge-transfer resistance
SEI	Solid electrolyte interphase
CV	Cyclic voltammetry
EIS	Electrochemical impedance spectroscopy
SEM	Scanning electron microscopy
EDS	Energy dispersive spectrometer
TEM	Transmission electron microscopy
TGA	Thermogravimetric analysis
XPS	X-ray photoelectron spectroscopy
XRD	X-ray diffraction spectroscopy

NMR	Nuclear magnetic resonance
SPM	Scanning probe microscopy
BET	Brunauer Emmett Teller
FTIR	Fourier transform infrared spectroscopy
PTFE	Poly(tetrafluoroethylene)
PVDF	Polyvinylidene fluoride
GA	Gum arabic
SA	Sodium alginate
ProDOT	3,4-propylenedioxythiophene-2,5-dicarboxylic acid
PAA	Polyacrylic acid
CMC	Carboxymethyl Cellulose
PAN	Polyacrylonitrile
PEG	Polyethylene glycol
PVA	Polyvinyl alcohol
PMMA	Poly methyl methacrylate
SBR	Styrene butadiene rubber
Equation	Eq

LIST OF FIGURES

LIST OF TABLES

CHAPTER 1: INTRODUCTION

1.1 General background

Today the world faces energy challenges on two main fronts: moving electricity production from fossil fuels to sustainable energy sources, and shifting ground transportation towards electrical power sources, i.e. using electric vehicles (EVs) instead of vehicles driven by internal combustion engines (ICEs).[1-3] The power level of sustainable energy fluctuates with time, hence the use of sustainable energy for electricity production requires the availability of suitable technology for energy storage, i.e. batteries. Significant progress have been made in recent years in the development of technology for sustainable energy, e.g. photo-thermal receivers, better wind turbines and photovoltaic cells, the development of storage devices still lags far behind. The research on batteries which can store up long stability sustainable power, prolonged cycle life and meet environmental restrictions is an important challenge for modern electrochemistry.[4-9]

Another essential demand of modern society is to reduce the use of oil for transportation as soon as possible due to non-regenerable resources. Hence, there is general agreement among leading economics, politicians, major car manufacturers and the scientific technological community that we have to move towards more wide spread use of EVs. The highest energy density (ca. 800 Wh/kg) is found in by fuel cells (FCs). However, it seems that FC technology is not advanced enough for practical EV application due to problems related to catalysis in direct FCs, and serious issues in hydrogen storage.[10-14]

To date, all commercialized EVs are powered by lithium ion batteries (LIBs) packs. Hence, LIBs are the most promising candidate for application and development in EVs. The US Environmental Protection Agency (EPA) has estimated the energy

cost for commercialized EVs, hybrid electric vehicles (HEV) and gasoline vehicles. The EVs can significantly decrease the cost from ca. $2300 to $500 annually (Table 1.1). The range and recharging time is however, still an issue. EVs, e.g. the *Tesla Roadster*, can travel 245 miles per charge, more than double that of prototypes. The Roadster can be fully recharged in ca. 3.5 hours from a 200 V, 70 amp from a home installed outlet. Except the drive range and recharging time, it is not clear whether the cost saving on gasoline in EVs over their lifetime will offset their higher purchase prices. Hence, the cost of the EVs is urgently to be reduced, especially the battery packs. Moreover, assuming that battery costs will decrease and gasoline prices increase, the EVs will dominate the vehicles market in the near future.[15-19]

Table 1.1 Comparison of fuel efficiency and costs for all the electric cars rated by the EPA for the U.S. market as of January 2015.[20-24]

	Vehicle	Model year	EPA rated combined fuel economy	Annual energy cost
Electric Vehicles	BMW i3	2014	124 mpg(1)-e(27 kWh /100 mile)	$500(2)
	Scion iQ EV	2013	121 mpg-e(28 kWh /100 mile)	$500
	Chevrolet Spark EV	2014	119 mpg-e(28 kWh /100 mile)	$500
	Honda Fit EV	2013	118 mpg-e(29 kWh /100 mile)	$500
	Fiat 500e	2013/14	116 mpg-e(29 kWh /100 mile)	$500
	Nissan Leaf	2013	115 mpg-e(29 kWh /100 mile)	$500
	Volkswagen e-Golf	2015	116 mpg-e(29 kWh /100 mile)	$550
	Nissan Leaf	2014/15	114 mpg-e(30 kWh /100 mile)	$550
	Mitsubishi i	2012/13	112 mpg-e(30 kWh /100 mile)	$550
	Smart electric	2013	107 mpg-e(32 kWh /100 mile)	$600

	drive			
	Kia Soul EV	2015	105 mpg-e(32 kWh /100mile)	$600
	Ford Focus Electric	2012/13	105 mpg-e(32 kWh /100 mile)	$600
	BMW Active E	2011	102 mpg-e(33 kWh /100 mile)	$600
	Tesla Model S AWD -85D	2015	100 mpg-e(34 kWh/100 mile)	$600
	Nissan Leaf	2011/12	99 mpg-e(34 kWh/100 mile)	$600
	Tesla Model S	2013/14	95 mpg-e(35 kWh/100 mile)	$650
	Tesla Model S AWD -P85D	2015	93 mpg-e(36 kWh/100 mile)	$650
	Tesla Model S	2012/15	89 mpg-e(38 kWh/100 mile)	$700
	Tesla Model S AWD	2014	89 mpge-(38 kWh/100 mile)	$700
	Mercedes-Benz B-Class Electric Drive	2014	84 mpg-e(40 kWh/100 mile)	$700
	Toyota RAV4 EV	2012/13	76 mpg-e(44 kWh/100 mile)	$850
Hybrid Electric Vehicles	Toyota Prius (HEV)	2010/13	50 mpg	$1050
Internal Combustion Engine	Ford Taurus FWDFFV (gasoline only)	2013/14	23 mpg	$2300

Notes: (1) Mile per gallon (mpg)

(2) All estimated fuel costs based on 15,000 miles annual driving and regular gasoline price of US$3.49 per gallon.

1.2 Lithium-ion batteries

1.2.1 Working mechanism

Lithium ion battery pack is constituted of several electrochemical cells that are connected in series and/or in parallel to provide the required voltage and capacity, respectively. Each cell consists of a positive and a negative electrode separated by electrolyte solution containing dissociated lithium salts. Polymer binder, as a network producer, is one of the major components in an electrode. Since the binder is used to conjugate active materials and conducting particles together onto the current collector, the coating morphology is formed on the active materials and current collector. The properties of polymer binders therefore are critical in the electrochemical performance of the electrodes, especially for conductivity and long-term cycle stability. Rechargeable LIBs involves a reversible insertion/extraction of lithium ions into/from a host matrix, i.e. the lithium insertion compound, during the lithiation/delithiation processes. The lithium lithiation/delithiation process takes place with ions through the electrolyte and binder and is accompanied by a reduction/oxidation reaction of the host matrix. When the cells are connected externally, the lithium ions transfer to the cathode, thereby delivering electrons and enabling the current to be collected by the user. (Figure 1.1).

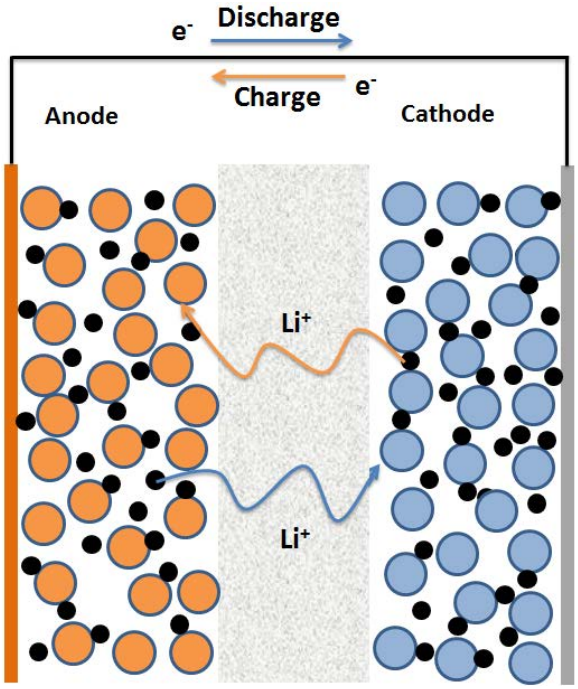

Figure 1.1 Schematic representation of the operation for lithium ion batteries.

1.2.2 Basic concepts

1.2.2.1 Potential

The open-circuit voltage V_{oc} of a lithium ion battery is related to the gap in the lithium chemical potential between the cathode ($\mu_{Li(c)}$) and anode ($\mu_{Li(a)}$) as:

$$V_{oc} = \frac{\mu_{Li(c)} - \mu_{Li(a)}}{F} \qquad (1)$$

where F is the Faraday constant. Figure 1.2 is a schematic of the relative electron energies in the electrodes and the electrolyte of a thermodynamically stable battery cell with an aqueous electrolyte. The electrolyte window is the energy separation E_g of the lowest unoccupied molecular orbital (LUMO) and the highest occupied molecular orbital (HOMO) of the electrolyte. As shown in Figure 1.2, Thermodynamic stability considerations require the redox energies of the cathode and anode to stay within the band gap E_g of the electrolyte.

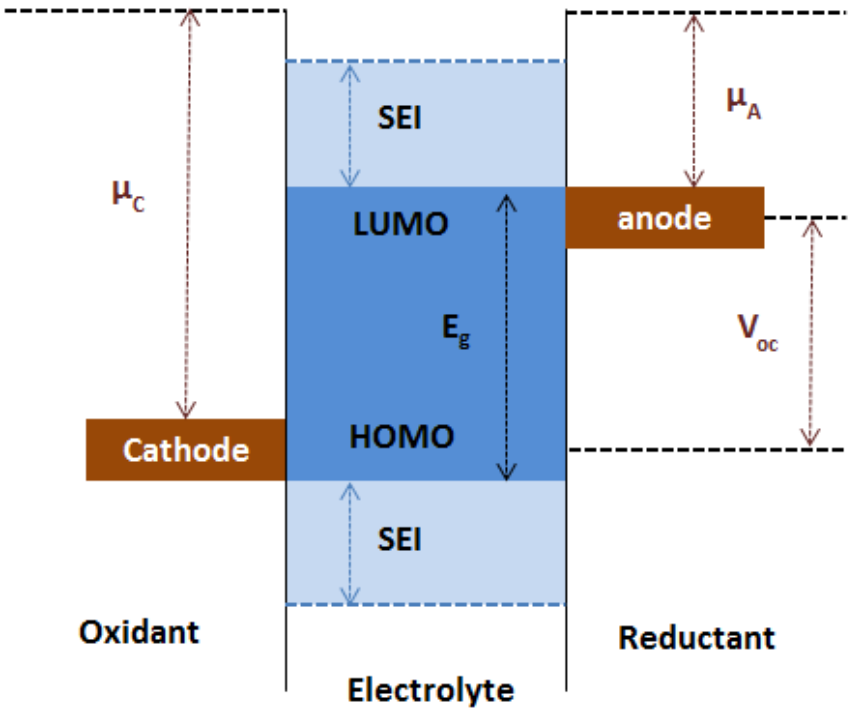

Figure 1.2 Schematic open-circuit energy diagram of a lithium cell. HOMO and LUMO refer to the highest occupied molecular orbital and lowest unoccupied molecular orbital in the electrolyte, respectively.

When the μ_A is above the LUMO of the electrolyte, a reduction will takes place at anode unless a passivation layer creates a barrier to electron transfer. Also, a cathode with a μ_c below the HOMO will cause the oxidation. Therefore, it's critical to limit the potentials μ_A and μ_c to be within the electrolyte window, i.e. the open circuit voltage V_{oc}.

$$eV_{oc} = \mu_A - \mu_C \leq E_g \qquad (2)$$

Where *e* is the magnitude of the electron charged.

For rechargeable lithium ion batteries, cathodes and anodes are defined as the higher potential and lower potential electrode, respectively. Generally, the electrochemistry performance can be investigated through a half-cell with lithium metal as reference electrodes. Hence, the active materials are always working as

cathode materials in the half-cell. Normally, the cathode materials in half cells show a potential higher than 2 V, while the anode materials show a potential vs. Li^+/Li lower than 2 V in contrast to Li^+/Li.

The theoretical specific capacity (*Q*) of active materials can be calculated by the follow Equation 3:

$$Q = \frac{nF}{M} \quad (3)$$

Where *n* is the number of moles of electrons transferred in the electrochemical reaction, and *M* is the molecular weight of the active materials.

1.2.2.2 Energy density

Specific energy (*SE*, Wh/kg)/energy density (*ED*, Wh/L) are used to represent the amount of energy stored in a specific device per unit mass/ volume, respectively. The details are as the following equations:

$$SE = \frac{E \times Q}{1000} \quad (4)$$

$$ED = \frac{E \times Q \times m}{1000 \times V} \quad (5)$$

Where *E* is the voltage (V) of the cell, *Q* is specific capacity (mAh/kg), *m* is the weight of the cell (kg) and *V* is the volume of the cell (L).

1.2.2.3 Power density

Specific power (*SP*, W/kg)/ power density (*PD*, W/L) are used to represent the abilities of the cell to deliver power per unit mass/volume, respectively.

$$SP = \frac{SE}{t} \quad (6)$$

$$PD = \frac{ED}{t} \quad (7)$$

Where *t* refers to the discharge time (h)

1.2.2.4 Rate capability

The *C* rate generally describes battery loads or battery charging current. Normally, a medium high rate is between 2 and 10. While *C* rate higher than 10 *C*, it is referred as a high rate. For instance, 1 *C* means a current allowing a full lithiation/delithiation in 60 minutes.

1.2.2.5 Irreversible capacity

Irreversible capacity refers to how much capacity lost after cycle, which can describe the cycling stability of batteries. The details are as follows.

$$\text{Irreversible capacity} = n^{th}\ Charge - n^{th}\ Discharge \quad (8)$$

$$\text{Irreversible capacity loss} = \frac{n^{th}Charge - n^{th}Discharge}{n^{th}Charge} \times 100\% \quad (9)$$

1.2.2.6 Coulombic efficiency

Coulombic efficiency (η) equals to the ratio of discharge capacity to charge capacity.

$$\eta = \frac{n^{th}Discharge}{n^{th}Charge} \times 100\% \quad (10)$$

1.2.3. Status and remaining challengers

Primary lithium batteries were commercialized during the 1970s. In their early stages, it turned out to be failure to develop rechargeable Li batteries with Li-metal as anodes. These included Li-TiS_2, Li-MoS_2 and Li-Li_xMnO_2 systems. These systems did not succeed due to safety problems and the prolonged charging time. The LIBs technology emerged since the introduction of graphite as the anode material in substitute of Li metal.

During the early stages of LIBs, it was demonstrated that transition metal oxides and sulphides could work as excellent reversible cathode materials for LIBs. Initially, the application of layered $LiNiO_2$ is a cathode due to its qualified specific capacity. However, requirements were not met for safety reasons due to the collapsed delithiated Li_xNiO_2 structure. Afterwards, the Li_xCoO_2 was tested to be more stable than Li_xNiO_2 cathode. For safety reasons, delithiation for commercial applications has been controlled below 0.5 for Li_xCoO_2 to avoid structure collapse.[25,26] Ascribed to a strong edge-shared Mn_2O_4 octahedral framework, the spinel $Li_xMn_2O_4$ exhibits good structural stability during the lithiation/delithiation process. Nevertheless, the ca. 80% reversible Li ion at ca. 4 V versus Li/Li^+ limits the capacity to ca. 120 mAh/g. Also, due to the Jahn-Teller distortion in ca. 3V region, the additional capacity at 3 V cannot be used in practical cells.[27,28] Polyanion (XO_4^{y-}: X = P, S, Si, As, Mo, W) have been extensively studied as cathode materials in lithium ion batteries since the introduction of $LiFePO_4$ by Goodenough et al. Iron and manganese-based polyanion compounds are particularly promising candidates ascribed to their advantages of being environmentally benign, abundant, and inexpensive, etc. However, these polyanion materials have the crucial disadvantage of having poor electronic and ionic conductivities.[29,30]

For anode materials, graphite is one of the most widely used anodes due to the following features, e.g. low cost and long cycle life and flat&low voltage plateau,. Besides the modification of graphite, many efforts have been devoted to non-carbon materials for high capacity anodes. These include: carbon nanotubes (1100 mAh/g)[31], carbon nanofibres (450 mAh/g),[32,33] graphene (960 mAh/g),[34,35] tin (993 mAh/g),[36] transition metal oxides (500-1000 mAh/g),[37] SiO (1600 mAh/g),[38] and silicon (Si) (4200 mAh/g).[39] Poor electron transport, high volume change, and capacity fading are the main limitations of these materials that must be overcome before commercialization.

When examining LIBs technologies that are suitable today for EV applications, it seems that the best system is silicon-$LiFePO_4$, due to its high specific capacity and good safety features. Lithium iron phosphate (LFP) has been considered a promising cathode material that could dominate large scale EV markets due to its low cost, safely and high theoretical capacity (170 mAh/g). However, the low ion conductivity and electronic conductivity inhibit its further commercialization.[40-48] In the last decade, Si has been researched intensively as promising LIB anode material for LIBs in the last decade due to its ten times higher theoretical gravimetric specific capacity of current commercialized graphite, low lithiation/delithiation potential, the natural abundance of elemental Si, safety and environmental benignity. However, Si-based anodes also experience, ca. 300% volume expansions, during lithiation/delithiation processes, which commonly pulverize, crack and break electrical contact between the Si particles with conductive additive and the current collector, resulting in rapid capacity loss.[39,49-57]

The power density of these active materials with bulk sizes is generally low due to high level of polarization at high charge/discharge rates. This high polarization

is believed to result from slow lithium diffusion or low electric conductivity in the active material. Compared with complicated and costly nano-manipulation processes, the engineering of polymer binder is the most promising and practical approach as it can fine-tune the mechanical and electronic characteristics of the electrodes. To date, polymers with tailored electronic properties, binding strength, wettability, flexibility and even self-healing abilities have been proposed to replace conventional polyvinylidene difluoride (PVDF) binder.[5,58]

1.3 The properties of binders

The binder is one of the major elements in LIBs. A qualified polymer binder should fill the following requirements: 1) it acts as both dispersing agent and as a thickener in the dispersion process; 2) for the mechanical properties, it connect the particles together and with the current collector; 3) it's critical to keep electronic conductivity since the coating on the surface of the active materials; 4) in the ionic conductivity, the ions is only allowed to migrate to the active materials through the binder polymer; and 5) chemical and physical stabilities. These properties are significantly dependent on the thin layer generated by the polymer chains at the surface of the AM and conducting agent particles. It is in this area that research efforts should focus to better understand and further optimize electrode performance through tailoring of the binder properties.[59]

To date, the trend of developing new binders developed includes (1) seeking new electronic conductive binder with high adhesion force to accommodate the large volume expansion and shrinkage of active materials during lithiation/delithiation processes, (2) replacing the environmentally hazardous volatile organic solvents for the electrode manufacturing, and (3) enhancing the adhesion strength between the binder and other components of the electrode. Table 1.2 shows a number of excellent binders developed to date. The binder properties including the molecular structure and the glass transition temperature are presented. Besides binding capability, various functions can be achieved through the burgeoning binding systems. The water-based polymers (e.g. CMC, PAA, PEO, PVA, SBR, gum arabic, alginate) were proven to form more uniform distribution and present better dispersion properties than organic-based binder system. Meanwhile, the diversified active groups (e.g. carboxyl, hydroxyl, ester, nitrile groups) can facilitate chemical bonding with active materials

and the current collector which result in improved mechanical integrity of the electrodes. Furthermore, based on the active groups, functionalization of the backbone of the binders can achieve multiple-functions, i.e. high lithium ion diffusion coefficient and electronic conductivities.[60]

Table 1.2 The binders developed to date for LIBs.

Category	Binder	Molecular structure	Glass transition temperatrure (T_g/^{o}C)
Chemical products	Polyvinylidene fluoride (PVDF)	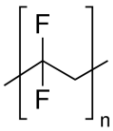	-35
	Poly(tetrafluoroethylene) (PTFE)	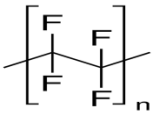	115
	Polyethylene glycol (PEG)	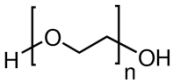	-53 to -45
	Polyacrylic acid (PAA)	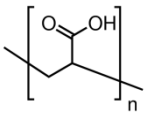	106
	Polyvinyl alcohol (PVA)	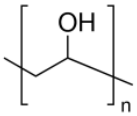	85
	Polyacrylonitrile (PAN)	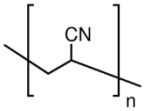	95
	Polyamide (PA)	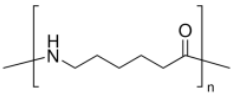	47-60
	Poly methyl methacrylate (PMMA)	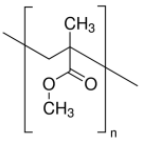	105
	Styrene butadiene rubber (SBR)	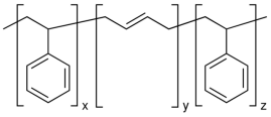	-65
Natural products	CMC	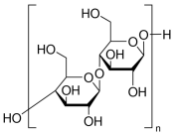	N/A

Alginate	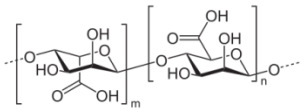	N/A
Gum arabic	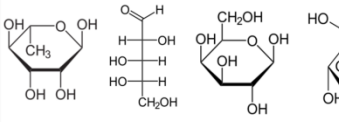 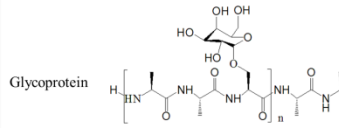	N/A
Chitosan	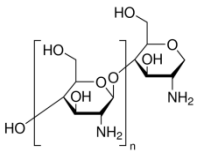	N/A
Xanthan	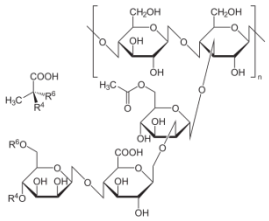	N/A

1.3.1 Mechanical properties

Research on the function of the binder in maintaining the mechanical integrity of electrodes is critical to the prospective LIB progress.[61,62] In a traditional conductive additives-filled binder system, the filler particles could improve the mechanical strength of the composite within limits. As the conductive additive content is increased past the threshold, the mechanical properties of the polymer binder system based electrodes will collapse. Gao's group claimed that as the conductive additive content increases in the electrode composite, the conductivity increased until a weight ratio of up to ca. 0.9. The conductivity decreased when the weight ratio increased to 1. Hence, there is an optimized ratio for this conventional binder system to produce the highest and most efficient binding performance.[63]

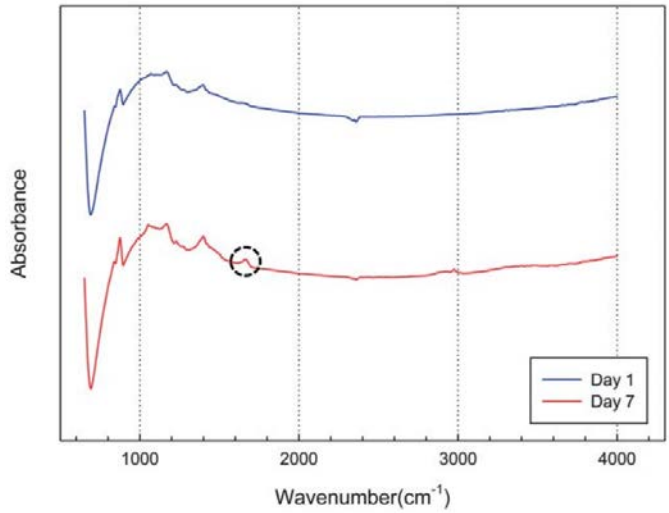

Figure 1.3 FTIR spectrum of the slurries as a function of the wave number.[64]

The long-term stability of the PVDF binding system has also been evaluated by Cho et al. As presented in Figure 1.3, due to the C=C stretching vibrations resulting from CH=CF- of the PVDF binder, the FTIR spectroscopy for the slurry after 7 days has the peak wave number between 1645 and 1650 cm^{-1}. The formation of double bonds was predicted after broken of C-F bonds and it is presumed that the binder polymer degrades over time. Therefore, the stability of the binder is critical in maintaining the performance of LIBs.[64]

The higher crystallinity of PVDF was also proven to contribute to the mechanical strength of the electrode. According to the research by Yoo et al., PVDF preferentially adsorbs onto the crystalline edges of the graphite anode. The highly crystalized graphite surface will result in prominent exposure of graphite crystalline edges. An increase in the number of nucleation sites for PVDF will be generated at the interface between graphite particles and polymer, leading to increased binding strength.[65] The PVDF binder's performance at elevated temperatures was studied by Markevich et al. They reported on the effect of the PVDF binder on the stability of composite $LiCoO_2$ electrodes at elevated temperatures in 1 M $LiPF_6$ EC/EMC

solutions. At the contact points between the active mass and the binder. the formation of surface Co_3O_4 and the dissolution of Co ions at elevated temperatures are accelerated (Figure 1.4). The presence of water (and/or HF) is the cause for the accelerated dissolution of Co ions. Hence, the $LiCoO_2$ cathode could oxidizes the solvents at elevated temperatures thus forming CO_2.[66]

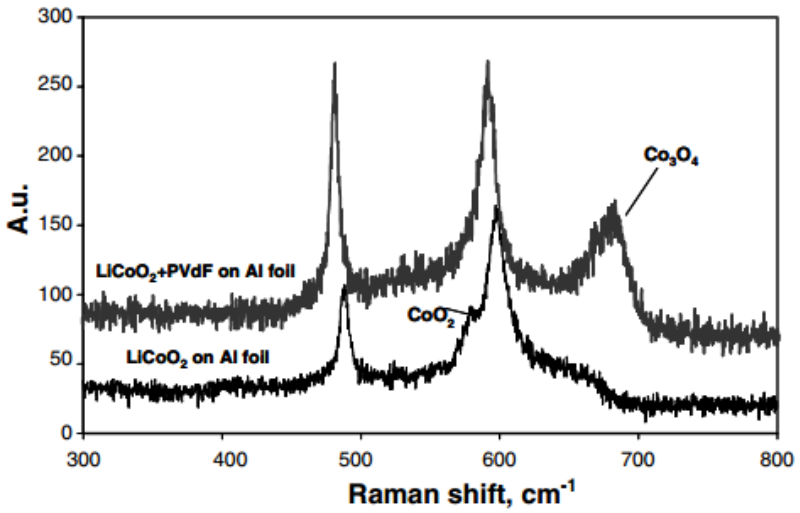

Figure 1.4 Raman spectra of $LiCoO_2$ electrodes with/without PVDF binder after being stored for 2 weeks at 60 ^oC in standard electrolyte solutions, 1 M $LiPF_6$ in EC/EMC.[66]

1.3.2 Lithium ion conduction

Some of the key performance metrics, e.g. the charge/discharge rate, practical capacity and cycling stability are determined by the diffusion properties of LIBs. The governing equation which describes the diffusion process is the Fick's law (Eq. 1 in Table 1.3). The proportionality factor *D* is the diffusivity or diffusion coefficient. (Eq. 3-5 in Table 1.3) Diffusion is governed by random jumps of atoms or ions in both liquids and solids, leading to position exchange with their neighbours. The kinetics of this process follows an Arrhenius relationship and is temperature dependant. (Eq. 2 in

Table 1.3). In liquids, the temperature dependence of the diffusion is much lower than in solids.

Table 1.3 Governing equations for diffusion and diffusion coefficients.[60]

No.	Title	Equation
1	Fick's law	$j_i = -D_i \nabla c_i \frac{\partial c_i}{\partial \tau} = \nabla \cdot (D \nabla c_i)$
2	Arrhenius equation	$rate \approx exp(-\frac{\Delta G}{k_B T})$
3	Diffusivity in Liquid	$D_i = \frac{k_B T}{6\pi\mu R_0}$
4	Diffusivity in solid	$D_i = a_l^2 \Gamma$: $a_l is$ the jump length, $\Gamma = \upsilon^0 exp(-\frac{\Delta G}{k_B T})$
5	Temperature dependence of diffusivity in solid	$D_i = D^0 \exp(-\frac{H^M}{k_B T})$ *describes non-defect mediated interstitial diffusion*
6	Temperature dependence of diffusivity in solid	$D_i = D^0 \exp\left(-\frac{H^F + H^M}{k_B T}\right)$ *describes vacancy mediated diffusion*

Diffusion mechanisms for solids can be sorted into two categories: vacancy/defects-mediated mechanisms, and non-vancancy/non-defect-mediated mechanisms. Much larger activation energies are needed than for non-vancancy mediated mechanisms. They are corresponding to-Schottky pairs and Frenkel pairs in crystals, respectively. Because ionic transport occurs from the motion of vacancies, ionic solids with Schottky defects (corresponding to the defect-mediated diffusion in Table 1.3) have lower ionic conductivities and higher activation enthalpies. Ionic crystals with Frenkel disorder (corresponding to the interstitial mechanism in Table 1.3) show higher ionic conductivities and lower activation enthalpies because ionic

transport occurs primarily from the motion of interstitial species. The diffusion is mainly through an interstitial mechanism due to the small radius of Li-ions (5.9×10^{-11} m). When compared to electrons (radius of an electron: 10^{-22} m), Li-ion is still relatively large. The radius of a Li-ion is ten orders of magnitude. The potential generated by the neighbouring ions would also strongly hinder the motion of Li ions. Diffusion should be the rate-determining process compared to electronic conduction in a lithiation/delithiation process.

Table 1.4 Bonding potentials in LIBs.[60]

Cell Component	Bond type	Bond length (Å)	Bond strength (kJ/mol)
Anode (graphite, in-plane)	Covalent	1.46	374
Anode (graphite, inter-plane)	Van der Waals	3.55	5.9
Cathode (spinel, $LiMn_2O_4$)	Ionic	1.96 (Li-O)	426.48 (Li-O)

The structure is well defined and diffusivity can be modelled with a first-principles calculation in crystalline solids. (Eq. 4 in Table 1.3) Bonding potentials and defects in a crystal strongly affects the diffusion properties. The effects are expressed as enthalpy (H) and a pre-factor D^o (Eqs. 5 and 6 in Table 1.3). Bond types and potentials of the typical materials applied in LIBs are summarized in Table 1.4. Ionic and covalent bonds are the two strongest chemical bonds. Ionic atoms are created through electron-transfer between two species. Despite the van der Walls interaction showing a longer interaction range, the Lennard-Jones potential is relatively weak. For graphite anode, a Li-ion can easily diffuse parallel to the graphene layers during intercalation rather than perpendicular. The values of Li-ion diffusivity in different materials are summarized in Table 1.5.

Table 1.5 Diffusivity of Li ions in the active materials at room temperature.[60]

Active material	D_{Li} (cm^2/s)
$LiCoO_2$	10^{-10} to 10^{-8}
$LiMn_2O_4$	10^{-11} to 10^{-9}
$LiFePO_4$	10^{-14} to 10^{-15}
Natural graphite	10^{-9} to 10^{-10}

A cross-linked comb-copolymer, consisting of ethylene oxide (EO), 2-(2-methoxyethoxy) ethyl glycidyl ether (MEEGE), and allyl glycidyl ether (AGE), (Figure 1.5) was comparatively studied to demonstrate morphology effect. It's believed that the introduction of MEEGE to PEO appreciably enhances the ionic conductivity due to the contribution of the fast side chain motion of the MEEGE structure as well as the decrease in the crystallinity of the PEO sequence. The increase of MEEGE composition in the binder copolymers resulted in decrease of interfacial resistances. Consequently, the discharge capacity of the LPB also enhanced with increasing the MEEGE composition. The introduction of the branched-side-chains of the polymer backbone to the binder polymers in composite cathodes could facilitate interfacial charge transport processes and enhances ionic conductivity.[67]

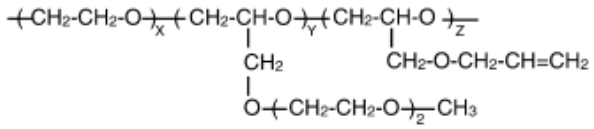

P(EO/MEEGE/AGE)

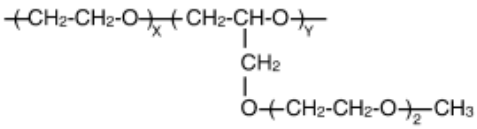

P(EO/MEEGE)

Figure 1.5 Chemical structure of P(EO/MEEGE/AGE) and P(EO/MEEGE).[67]

The electrolyte uptake effect was evaluated by styrene-butadiene (ST-BD) and 2-ethylhexyl acrylate-acrylonitrile (2EHA-AN) copolymer in a typical electrolyte solution (EC/DEC = 1/2, 1 M $LiPF_6$). The Lithium ion conductivity of the ST-BD copolymer is 9.45×10^{-8} $S\cdot cm^{-1.}$ The lithium ion conductivity of the 2EHA-AN copolymer is 1.25×10^{-5} $S\cdot cm^{-1}$ (Table 1.6). The polymer structure of the binders is one of the determine factor to the lithium ion conduction after swollen by electrolyte. According to the impedance profiles for each binder electrolyte, the 2EHA-AN-based polymer electrolyte exhibited the room temperature conductivity in the range of 10^{-4}-10^{-5} S cm^{-1}, which was 3-4 times higher than that of the ST-BD copolymer-based electrolyte. Therefore, the two conceivable ion transport mechanisms can be concluded as follows: (1) ion migrates through the cavity among binder polymers, and/or (2) ion migrates through the polymer coating via interaction with the polymer chains (Figure 1.6)[68]. The factors controlling electrolyte uptake have also been investigated by Gao's group. The enhanced polarity of the polymer binder was believed to improve the electrolyte uptake. The better swelling in the electrolyte is due to the increased polarity of the polymer, which is evidenced by the water contact angle measurements.[69]

Table 1.6 The ionic conductivity at 30 ^{o}C and Arrheius parameters of ionic conduction for (a) electrolyte (EC/DEC = 1/2, 1M LiPF6), (b) ST-BD copolymer and (c) 2EHA-AN = 85/15 wt%).[68]

	Molecular structure	Li concentration (μg/g)	σ (S/cm)
(a) Electrolyte			7.90E-03
(b) ST-BD copolymer	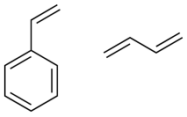	810	9.40E-08
(c) 2EHA-AN copolymer	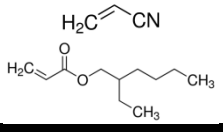	3,300	1.20E-05

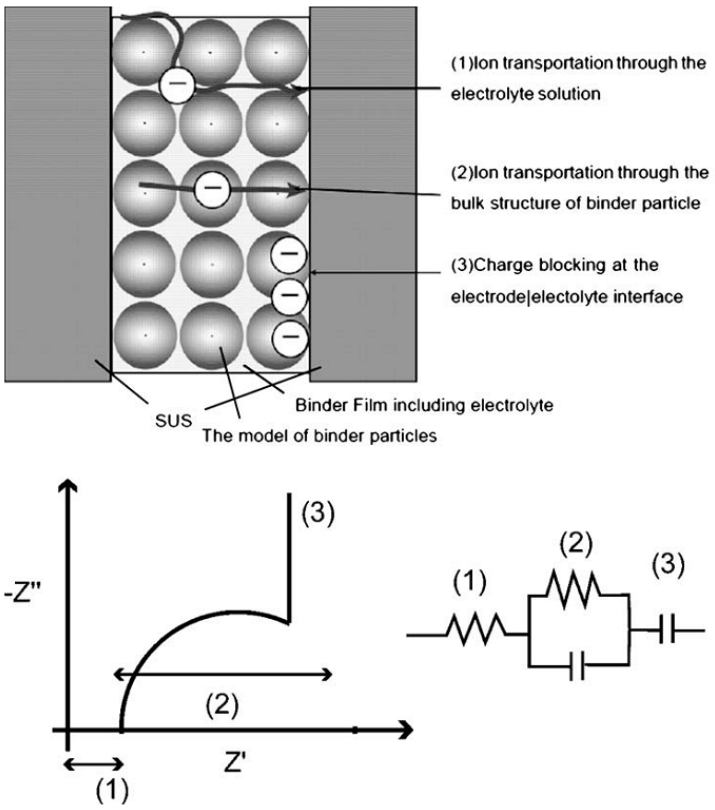

Figure 1.6 The Li ion transport mechanism in the binder film (1) ion transfer through the electrolyte, (2) ion transfer by the bulk structure of binder particle, and (3) ion transfer as a condenser.[68]

1.3.3 Electronic conduction

The electron transfer mechanism is one of the most critical properties of a battery system. According to quantum mechanics, the differences in electrical properties of materials derive from the different band structures. Generally, an insulator has a completely filled valence band and an empty conduction band with a large band gap. In contrast, conductors have a partially filled valence band (metal) or overlapped bands, which allow electrons transport in the crystal when an external electrical connection is applied. The band gap and conductivity at room temperature of various battery materials used for LIBs are summarized in Table 1.7. Materials having a non-zero band gap usually have low conductivity. Considering the ion conductivity, the overall conduction can be considered as the sum of ion and electron transport. Hence, ionic conduction is also important for semiconductors and insulators in lithium ion batteries.[60] The electrical conductivity of the binder is critical in ensuring the battery performance because of the active materials in the electrodes are always coated or surrounded by the polymer binders.

Table 1.7 Room temperature electronic conductivity for various LIBs components.[60]

Cell component	Materials	Band gap (eV)	Electronic conductivity (S/cm)
Current collector (anode)	Copper	0	5.8×10^{5}
Current collector (cathode)	Aluminum	0	3.4×10^{5}
Anode	Graphite	0	$(2\text{-}1)\times10^{3}$
Cathode	$LiCoO_2$	0.5-2.7	$\sim10^{-4}$
	$LiMn_2O_4$	0.28-2.2	$\sim10^{-6}$
	$LiFePO_4$	0.3-1	$\sim10^{-9}$

Since swelling of PVDF in the electrolyte can increase the space between the conductive carbon particles, the electrical conductivity will decrease when the

electrode is immersed in the electrolyte. To increase cycling performance in LIBs, most researchers generally focus on optimization of active materials. However, the following factors should also be valued including the homogeneous and efficient carbon black (CB) distribution and optimized ratios of binder and CB.[70] The electronic conductivity of the traditional CB/PVDF binder system has been studied with varying weight ratios of CB/PVDF using a four-point probe direct current method. Before the network is completely formed at ca. 0.2:1 CB:PVDF, the conductivity improves rapidly. The fully formed CB network appears with a plateau between an CB:PVDF ratio of 0.2:1 and 0.8:1. When further increasing the ratio, the conductivity decreases due to insufficient binding capability to maintain the CB network structure. Hence, it can be concluded that the addition of CB could increase the conductivity while simultaneously weakening the conductive network.[71] In contrast to the conventional organic solvent binder-based electrode, water-based binder systems have more uniformly distributions. Low electric resistance is one of the benefits derived from the uniform distribution of the electrodes. Considering the morphology effect, the introduction of the branched-side-chains to the polymer backbone of the binder polymers for the composite cathodes was investigate to be beneficial to the interfacial charge transport processes.[67]

Besides the traditional binder system, conjugated polymers such as poly(3-hexylthiophene) (P3HT) and poly(thiophene)s was investigated in various devices, e.g. field-effect transistors, solar cells, and light-emitting diodes. P-doped poly(thiophene)s have been verified to possess improved electronic conductivity. The modification of poly(thiophene)s has been conducted by attaching oliggo ethylene. The side chain is also proven beneficial for the lithium ion diffusion coefficient. However, the electronic conductivity dropped by an order of magnitude compared to

the polymers with longer side-chains.[72,73] Recently, A multi-functional PFFOMB polymer binder with tailored electronic structure which composed of conjugated structure and carbonyl groups has also been successfully applied to high specific capacity silicon anode materials.[62]

1.4. Application of binders for cathodes

1.4.1. Layered $LiMO_2$ (M = Co, Ni, Mn)

PVDF is a commercialized polymer binder which still attracts research attentions due to its stability and universality. Through a study of the PVDF binder system on $LiCoO_2$, a detrimental impact of the contact between PVDF and $LiCoO_2$ on the stability was revealed. At the contact points between the active material and the binder, the formation of surface Co_3O_4 and the dissolution of Co ions is accelerated.[66] $LiNi_{0.8}Co_{0.15}Al_{0.05}O_2$ was chosen as a promising cathode material because of its high specific energy/power density. To improve the cycle performance, the cooperation between $LiNi_{0.8}Co_{0.15}Al_{0.05}O_2$, PVDF and acetylene black (AB) was investigated. The PVDF to AB ratio and the total amount of inactive material make a significant impact on the specific capacity, porosity, Coulombic efficiency, and rate capability. In contrast, the electronic conductivity of the laminate does not impact the rate performance of the electrode as much as generally believed.[60 71] Figure 1.7 shows the variations of the electronic conductivity of the electrode versus total inactive material content at different PVDF/AB ratios. When the PVDF/AB ratio is 5:1, it is observed that an increasing in the electronic conductivity with increasing total inactive material content from 3% to 10%. Then a conductivity plateau appears due to the conductivity limitations of the PVDF/AB ratio at 5:1 ratio. A continuous increase in the electronic conductivity with the total inactive material content is detected for the electrode with

other PVDF/AB ratios. The electronic conductivity starts to decline at a PVDF/AB ratio of 5:5, which is believed to arise from the poor connectivity between particles as a result of binder shortage.[74]

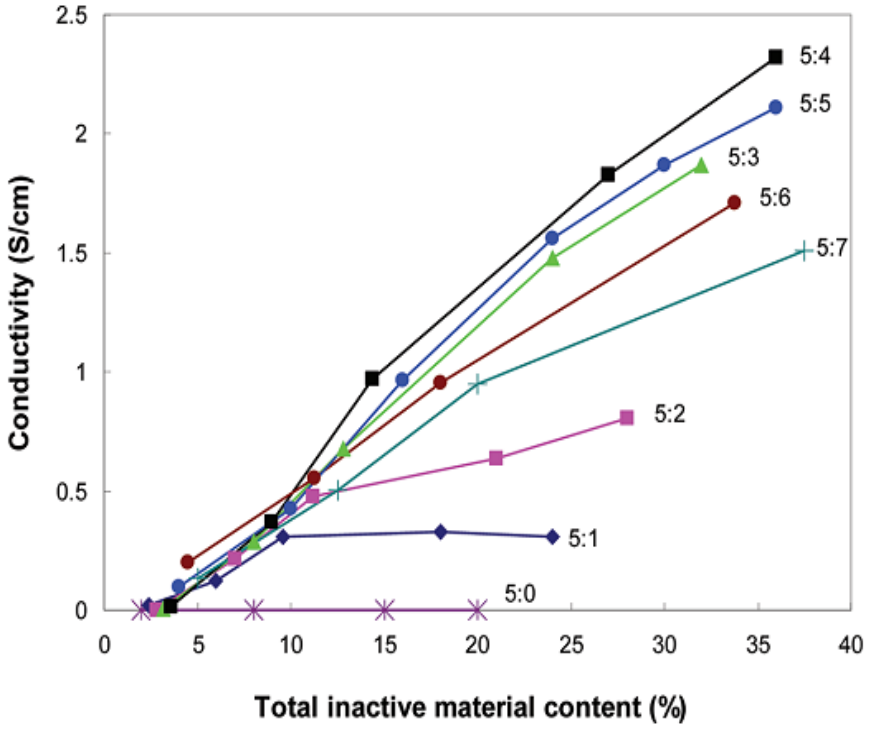

Figure 1.7 Variations in electronic conductivity of the $LiNi_{0.8}Co_{0.15}Al_{0.05}O_2$ composite electrodes with inactive material content at different PVDF/AB ratios.[74]

Moreover, water-based binders have been examined in terms of their binding strength, conductivity, distribution and dispersion properties. Through mathematical analysis, the distribution of binders in dried water-based and organic-based $LiCoO_2$ electrode sheet was evaluated. The migration of the binder to the top surface of an electrode sheet is primarily caused by the flow of solvent during drying according to migration-controlled drying kinetics. Because of the lower evaporation rate of NMP, the distribution of the water-based SBR-CMC is much uniform than PVDF-based electrode (Figure 1.8). Distribution and dispersion effects on the $LiCoO_2$ electrode were investigated using water-based styrene butadiene rubber (SBR) and sodium

carboxymethyl cellulose (CMC). Concluded from dispersion analyses, CMC is efficient in dispersing $LiCoO_2$, and the dispersion improves when the fraction of SBR in the binder is reduced. Nevertheless, the electrode is more uniform with more SBR, which results in improved adhesion strength and decreased surface resistance of the electrode sheets.[75] Meanwhile, other water-based polymer binders, e.g. poly(butyl acrylate)-based (PBA), polyacrylonitrile-based (PA) and poly(ethylene glycol) (PEG), were evaluated on $LiCoO_2$ and have improved rate capabilities and cycle stability in contrast to organic-based PVDF binder.[76] It is worth noting that the wate-based PEG polymer binder can maintain over 30 mg/cm^2 active material loading, which deliver 4.53 mAh/cm^2 at C/2 rate.[77]

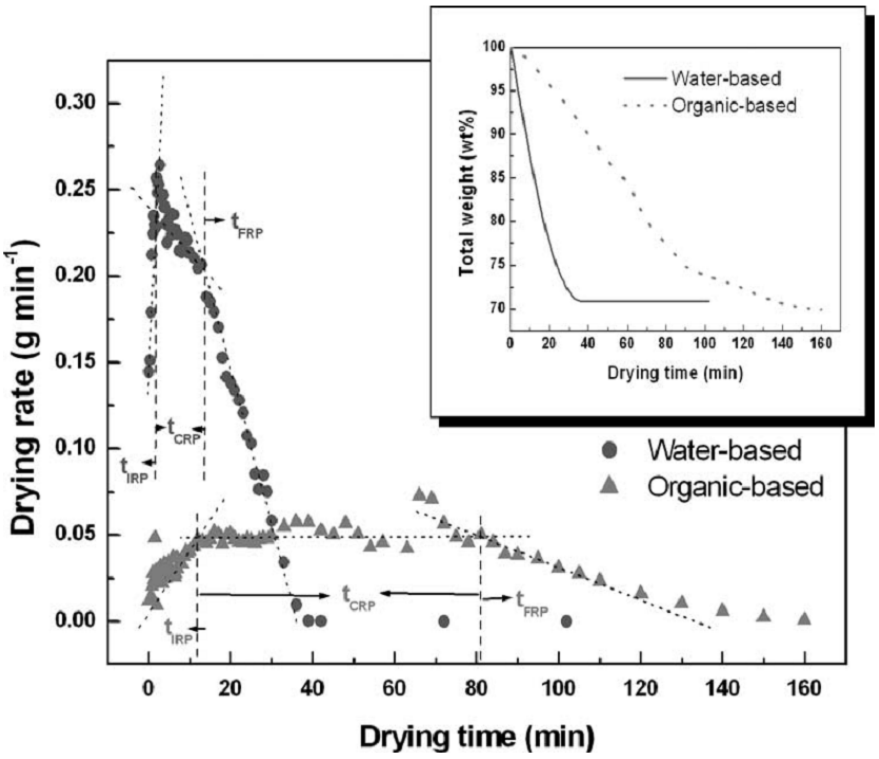

Figure 1.8 The total weight and drying rate as a function of time for the water-based and organic-based $LiCoO_2$ electrode sheets.[75]

The effect of binders on electrochemical properties in LIBs was also evaluated on layered $LiNi_{1/3}Mn_{1/3}Co_{1/3}O_2$ (NMC) cathode material between water and organic-based polymers. The performance of the NMC electrodes with CMC, PVDF, and alginate from brown algae binding system was comparatively studied. As a result, the CMC-based NMC electrodes have the best performance, followed by that of alginate and PVDF binders, respectively. One of the advantages of CMC is the lower charge transfer resistance and lower activation energy evidenced by electrochemical impedance spectroscopy (EIS). The activation energy values for CMC, alginate, and PVDF-based electrodes were calculated to be 27.4 kJ mol^{-1}, 33.7 kJ mol^{-1}, and 36 kJ mol^{-1}, respectively.(Figure 1.9)[78] The CMC binder system were also applied in $LiNi_{0.4}Mn_{1.6}O_4$ cathode material. Compared with electrodes using PVDF, CMC-based electrodes display better discharge capacities at all rates. Furthermore, CMC binders could achieve stable electro-chemical performance even when the voltage is as high as 5 V. To investigate the electrochemical stability of CMC at high voltage during the cycling, electrodes of CMC (CMC:CB = 3:1) and PVDF (PVDF:CB = 3:1) were tested on charge to 5 V without the existence of active materials. Note that no floating step was used at 3 V. The corresponding profiles indicate that CMC electrodes show less electrochemical activity than PVDF electrodes which is a sign of a higher stability at 5 V.[79]

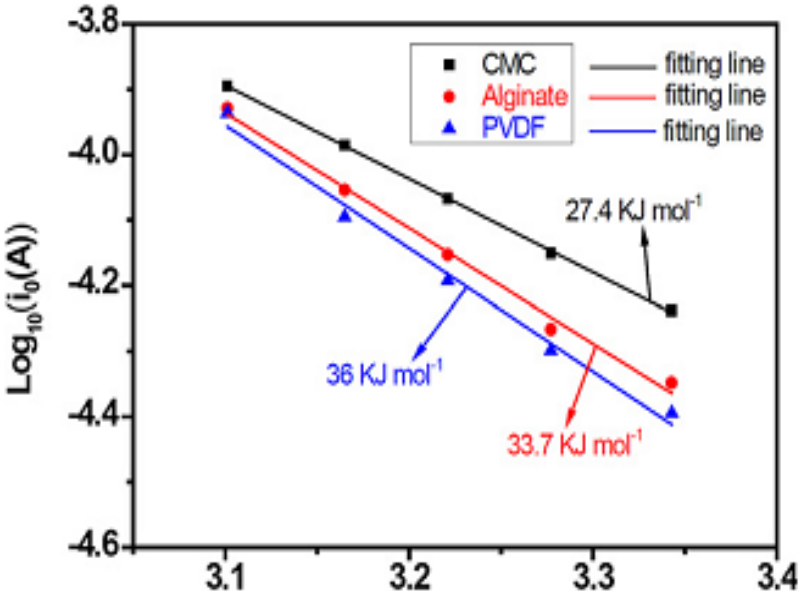

Figure 1.9 Arrhenius plots of Log i_o versus 1/T for NMC electrodes with CMC, alginate and PVDF as binders at the discharge state of 3.7 V. The lines are the linear fitting results.[78]

Based on a urethane acrylate binder, electrodes of NMC were prepared via a thermally initiated free-radical polymerization process. Interestingly, the electrode with urethane acylate-based binder experienced a slightly higher charging voltage (ca. 0.05V) in the first cycle compared with the PVDF binder. However, this difference turns out to be negligible since the second cycle. It can be concluded that although higher energy is required for the electrolyte to initially permeate the cross-linked poly urethane acylate binder, it has a minimal impact on the electrochemical properties of the electrodes. Also, EIS profiles of the NMC/Li cell in the fully discharged state show that the interfacial impedance is slightly higher in the urethane acylate-based binder case. Based on the cycling results discussed above, the higher interfacial impedance observed for the acylate-based binder will not greatly affect the cell performance.[80]

1.4.2. Olivine $LiFePO_4$

Organic soluble PVDF has been modified to achieve higher electrochemical performance for $LiFePO_4$ cathode. The electrochemical performance of the $LiFePO_4$/C electrodes with poly(-methyl methacrylate) (PMMA), poly(vinylidene fluoride) (PVDF) and poly(vinylidenefluoride-co-hexafluoropropylene) (PVDF-HFP) as binders were compared. The structure is demonstrated in Figure 1.10. Galvanostatic lithiation/delithiation profile showed that the PVDF-HFP binder had the highest rate capability and cyclic performance. The better rate performance and cycling stability of the $LiFePO_4$/C electrode containing PVDF-HFP binder could be ascribed to the higher lithium ions diffusion coefficient due to lower glass transition temperature(T_g).[81]

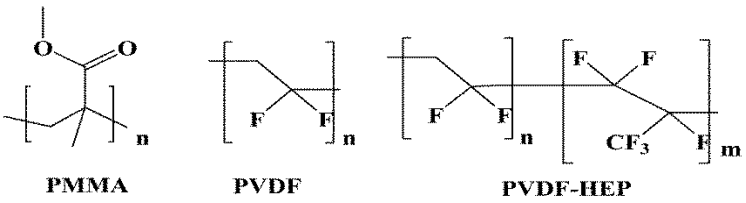

Figure 1.10 Molecular structure of PMMA, PVDF and PVDF-HEP.[81]

Guerfi et al. developed a water-soluble elastomer-based polyer binder for $LiFePO_4$ cathodes. In contrast to PVDF, they speculated that the elastomer polymer have a different way of binding as illustrated in Figure 1.11. The elastomer showed high flexibility and good adhesion capability. The cycle performance was also investigated and compared to PVDF-based cathodes at 25 and 60 ^{o}C. A lower irreversible capacity loss was achieved for the elastomer-based cathode. The elastomer-based $LiFePO_4$ reached 120 mAh/g at 10 C at 60 ^{o}C.[82]

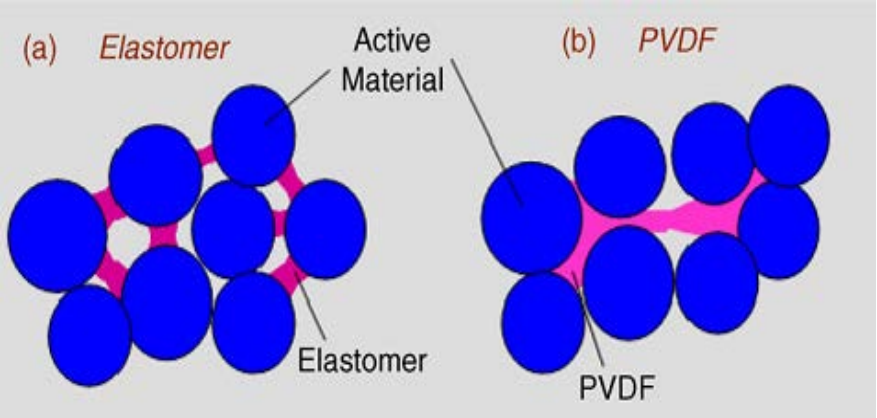

Figure 1.11 Schematic images of binding structure between: (a) elastomer and (b) PVDF.[82]

The water soluble polyacrylic acid (PAA) with carboxyl groups was also investigated on $LiFePO_4$ electrodes. In contrast to organic-based PVDF binder, the better dispersion and distribution properties in aqueous solution bestowed lower resistance and better charge transfer capability during lithiation/delithiation. Better reversibility was also evidenced by cyclic voltammetry (CV) tests. As shown in Figure 1.12, the electrode prepared in aqueous solvent showed a smaller difference than that in NMP (0.53V) between the oxidation peak and reduction peak potential, i.e. 0.19V. The current appearing before the peak in the aqueous based electrode increased more quickly than that in NMP, which indicated that the electrode prepared in the aqueous solvent has better reversibility.[83] Zhang et al. also proven that PAA could provide high adhesion strength to ensure good electrical connection between active materials and current collector. Compared to the PVDF binder, meanwhile, PAA could suppress swelling of $LiFePO_4$ cathodes after immerse in electrolyte solution. Figure 1.13 shows that the value of R_{ct} with PAA binder based battery is smaller than the that prepared based on PVDF.[84]

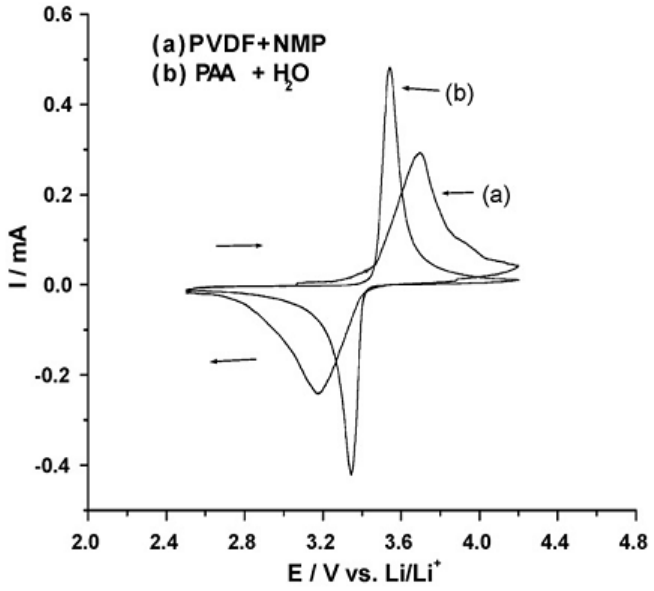

Figure 1.12 Cyclic voltammograms of LFP electrodes at 0.1 mV/s. The electrode was prepared in NMP by using (a) PVDF and (b) PAA as binders.[83]

Based on LFP, The neutralized derivatives polyacrylic acid (PAAX) (X = Li, Na, and K) was comparatively studied in contrast to conventional PVDF binder. The electrochemistry performance showed that the application of PAAX binders can significantly improve the initial Coulombic efficiency, reversible capacity, and cyclability of $LiFePO_4$ cathodes compared to electrodes based on PVDF binder. Based on PAALi binder system, graphite/LFP full cells cycled 847 cycles with 70% capacity retention, which was a significant improvement over the electrodes with PVDF (223 cycles). This study demonstrated the promising application of neutralized PAA as binder for LFP/graphite full cell, instead of environmentally hazardous organic solvents, i.e. NMP.[85]

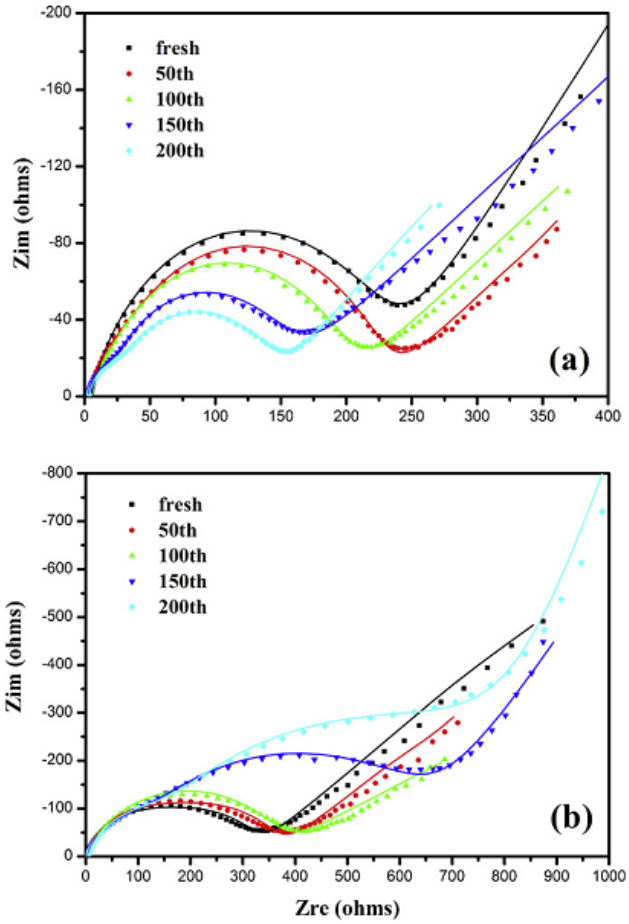

Figure 1.13 Nyquist plots of the LFP/Li half cell (a) made with PAA. (b) made with PVDF after different cycle numbers.[84]

Lux et al. innovatively investigated the performance of PVDF and CMC binder on LFP cathode through voltage profiles as performed in Figure 1.14. Concluded from the PVDF-based profile, the increase of the ohmic drop and the short of the voltage plateau during cycling resulted in a sharp decrease in the discharge capacity. In contrast, based on the CMC binder, the discharge current increase shortened the voltage plateau rather than increased the initial ohmic drop. The dry temperature at elevated 170 ^{o}C was also believed to be benefit for the long term stability for the LFP electrode.[86] It was showed that LFP prefers to interact with SBR compared to other binders such as CMC based on the analyses of zeta potential, sedimentation, and rheology. The order of the addition of binder is critical to the dispersion property. It is

suggested that it is better to mix CMC with LFP prior to the addition of SBR. For the electrode prepared via the above suggested process, improved cycle performance is achieved.[87] According to the work by Oh et al., perfluorosulfonate ionomer as a binder could compensate for electrolyte decomposition from the electrode porous space as lithium ions are intercalated into lithium-deficient LFP particles, especially during rapid discharge.[88]

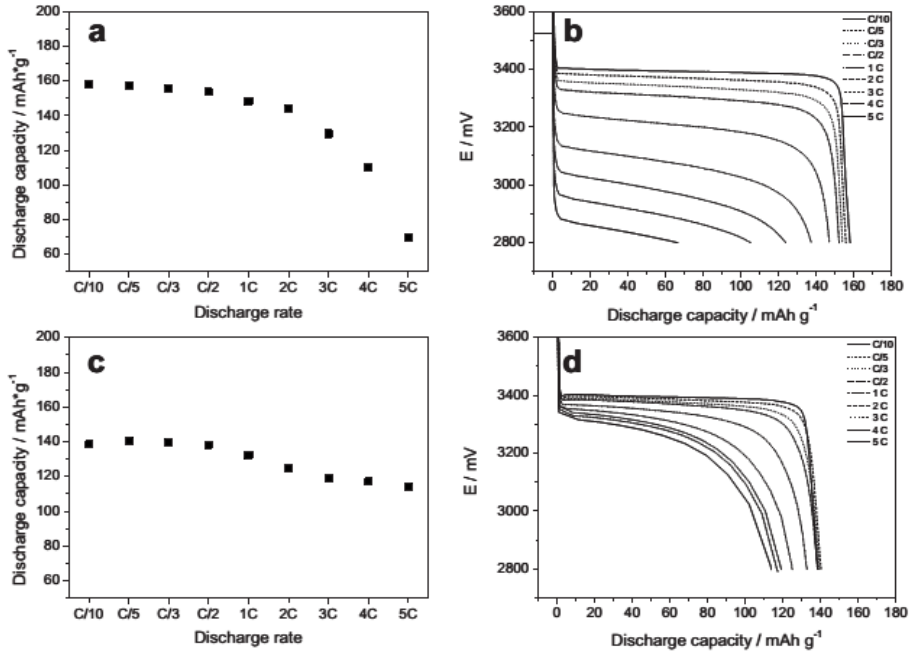

Figure 1.14 Rate performance and discharge voltage profiles of LFP electrodes using (a,b) PVDF binder and (c,d) CMC binder.[86]

1.4.3. Spinel $LiMn_2O_4$

For binder research of spinel $LiMn_2O_4$ cathode material, work has mainly focused on comparisons between organic and water-based binders. The surface distribution effects of highly oriented pyrolytic graphite (HOPG) were studied by using three different binders: gelatin, CMC and PVDF as shown in Figure 1.15. The entire substrate was coated by gelatin to form a nanometre-thick homogeneous film.

By contrast, the CMC formed thread-like patterns rather than a homogeneous film. The threads seemed to be interconnected and rather fragile. The structure of PVDF seemed much stronger than that of CMC. In an attempt to optimize gelatin properties as a binder, the properties were also measured with different pH value. The binding ability is the best when the pH value is fixed at 9. However, the surface modifying effect is better when the pH value is 12.[89]

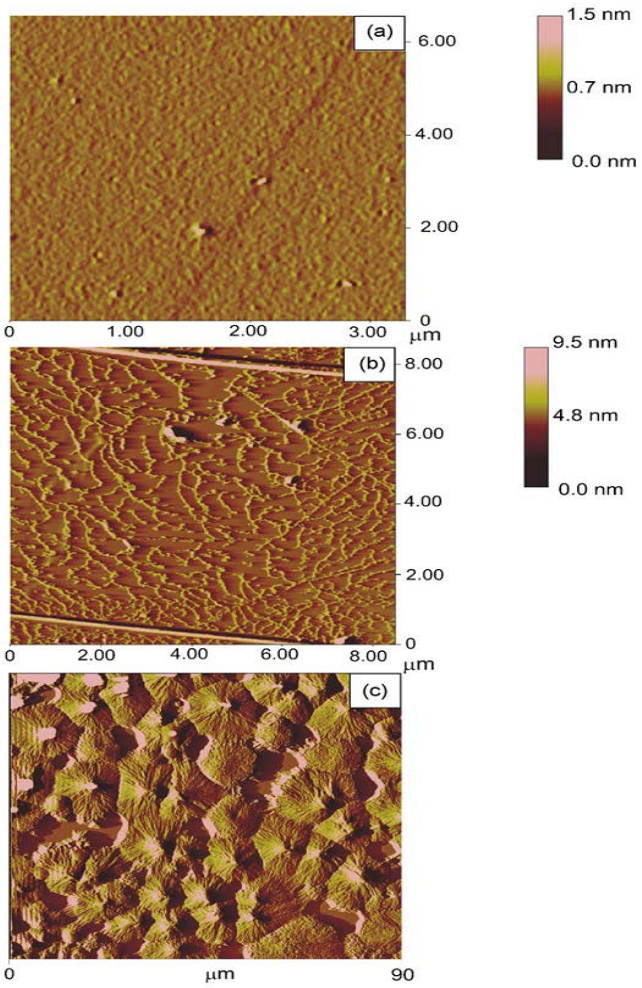

Figure 1.15 AFM images of different binders on the surface of a highly oriented pyrolytic graphite (HOPG): (a) HOPG dipped into gelatin solution at pH 12 for 1 h, (b) HOPG dipped into 1 wt% of CMC solution, and (c) HOPG was dipped into 1wt% of PVDF solution in NMP.[89]

Zhang et al. investigated the physical and chemical properties of PVDF, CMC and PAA binders in terms of crystallinity, functional group analysis and thermal properties. The crystallinities of the binder were examined by XRD (Figure 1.16a). It is worth noting that the PVDF has a better crystallinity than PAA and CMC because it is a semicrystalline polymer with a polymorphism. According the SEM images, PVDF is composed of small spherical particles which gathered together like roe (Figure 1.16b). This regular shape implies that PVDF have the features of crystal. According to Figure 1.16c and d, irregular shape particles were observed for PAA and CMC, which indicate that PAA and CMC are amorphous substances.[90]

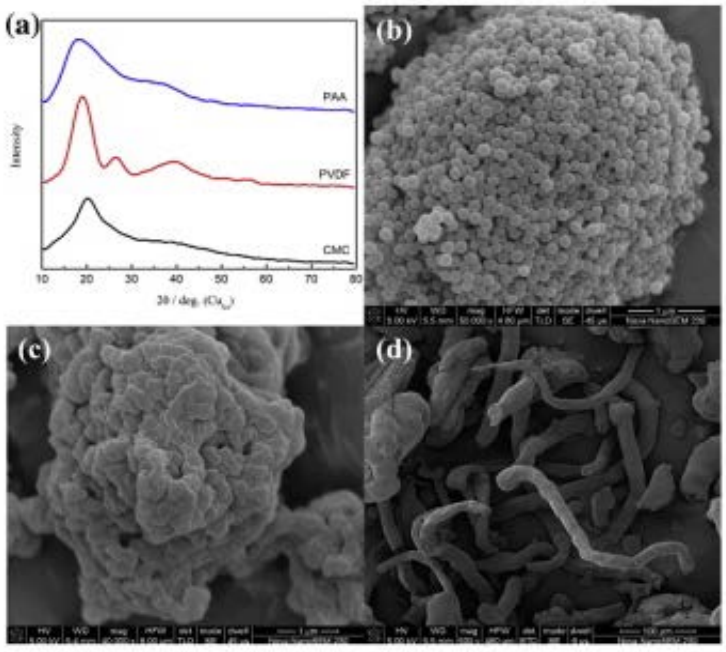

Figure 1.16 (a) X-ray diffraction patterns of the three binders: PAA, PVDF and CMC; SEM images for (b) PVDF, (c) PAA and (d) CMC pristine solid powders.[90]

The differences in as-formed crystallinity may strongly influence the morphologies of polymer films after dissolving the binders in solvent and then drying. The main chains of PVDF partially aggregated together to form the crystallite region during drying. Hence, the effective amount of the polymer which is effectively

applied to bind the electrode materials is decreased. In contrast, the application PAA binder can cover the $LiMn_2O_4$ active materials uniformly and thus improving the cycle performances due to the decrease in electrolyte decomposition.

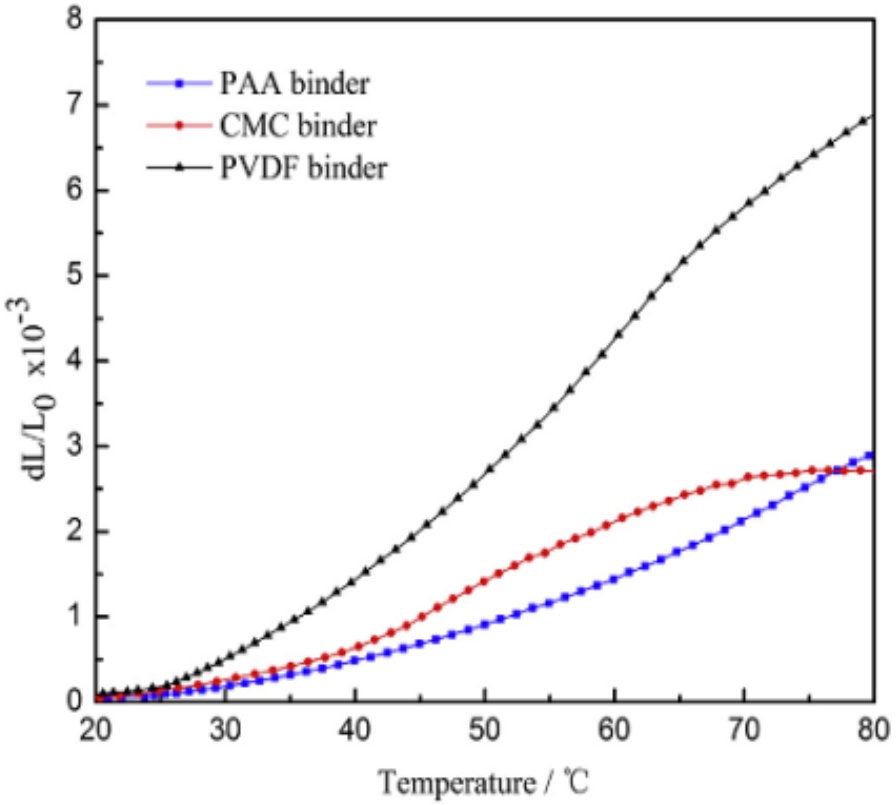

Figure 1.17 Thermal expansion rate curves of PAA, PVDF and CMC binders at the temperature range from 20 ^{o}C to 80 ^{o}C.[90]

The thermal expansion rate of the polymers was also evaluated. Figure 1.17 showed the thermal expansion rate curves of the three binders between 20 ^{o}C and 80 ^{o}C, which is the normal operation temperature range of LIBs. PVDF binders have a larger thermal expansion rate d_L/L_0 (d_L for the length of the sample at a given temperature, L_0 for the original length of the sample) than CMC and PAA binders. Since PAA and CMC polymers involves not only van der Waals force but also hydrogen bonds, the intermolecular force of PVDF polymer is weaker with only van

der Walls force. When the temperature increased, the PVDF binder had the largest volume expansion, which tends to trigger safety problems. Thermal diffusivity of the polymers was also tested to indicate the impact on safety performance. The PAA binders had the largest thermal diffusivity of 3.1×10^{-3} cm^2/s, which is ca. three times larger than that of the CMC and PVDF binders.[90]

$LiMn_2O_4$ cathodes with four different binder systems, i.e. PAA binders/NMP solvent, PVDF binders/NMP solvent, PAA binders/H_2O solvent and CMC binders/H_2O solvent, were prepared, and their adhesion strengths, swelling properties, morphologies and electrochemical properties were studied. It was concluded that the $LiMn_2O_4$ cathode with PAA/NMP system had the best cycle performances at both 25 ^oC and 55 ^oC. The better capacity retention of the $LiMn_2O_4$ cathode with the PAA/NMP system could be ascribed to strong binding ability, appropriate swelling property and homogeneous distribution of particles inside the electrode.

1.4.4. Other cathodes

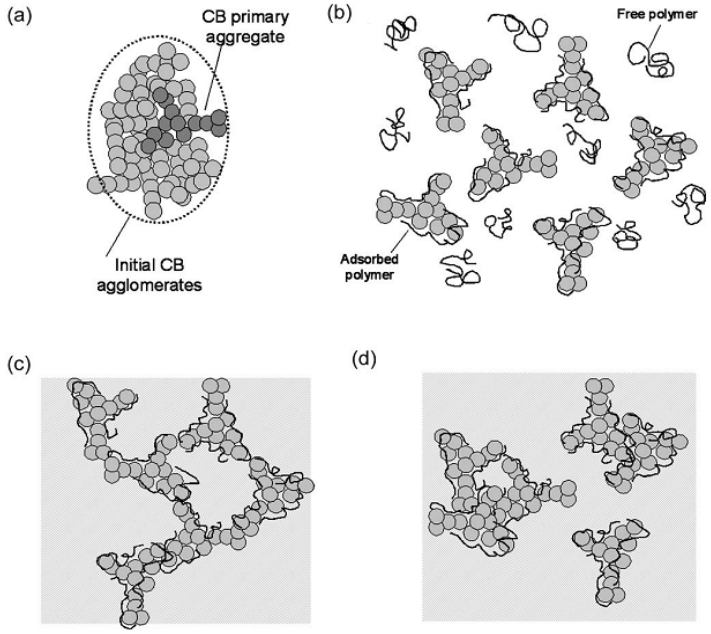

Figure 1.18 Schematic drawing summarizing the different kinds of CB dispersion state: (a) the initial CB powder, (b) dispersion and polymer adsorption of the aggregate in the solution. After solvent evaporation, (c) dispersion in plastified blends and (d) dispersion in non-plastified blends.[91]

During the past two decades, $Li_{1.2}V_3O_8$ was investigated as a promising positive electrode material due to its high theoretical capacity of 360 mAh/g. However, the experimental capacity generally remains much lower, i.e.180 mAh/g, than the theoretical value. $Li_{1.2}V_3O_8$ is thus a good material to be optimized through the binder on composite electrode capacity. Hence, a new polymeric binder was designed based on pre-plastified PEO with electrolyte solvent, and an optimized PEO/CB ratio. The more homogeneous and efficient CB distribution resulted in better CB/$Li_{1.2}V_3O_8$ interfaces and collection of active material grains. This is mainly ascribed to PEO/CB interactions, optimized plasticized PEO and PEO/CB ratios. As a result, the optimized composite electrode reached a specific capacity of 280 mAh/g

instead of 180 mAh/g at RT.[70] Besides, different types of CB dispersion states have been examined and schematically summarized in Figure 1.18.[91]

1.5. Application of binders for anodes

1.5.1. Carbonaceous materials

Firstly, a classification of carbonaceous materials is inevitable due to the variety of available carbons anodes in LIBs. Most carbonaceous materials can be classified as graphite and non-graphite. Graphite is composed of a stack of hexagonally bonded sheets of carbon connected by van der Walls forces. The lithium occupies an interstitial site between two planes of graphite. Hence, lithium ions can only combine on every second carbon hexagon in the graphite sheet which limits the amount of lithium ions to 1 for every 6 carbon atoms. This results in a limited theoretical capacity. The different structural features of non-graphite carbon, i.e. soft and hard carbon, result in different lithium storage mechanisms. The adhesion strength of the PVDF-based carbonaceous anodes could be tailored at the molecular level.[65]

Water-based CMC was firstly investigated by Drofenik et al. to demonstrate the different binding mechanism with gelatin. It seems that CMC tends to form networks. Gelatin bind the neighbouring particles through the “bridge” mechanism.[92] Due to the hydroxyl groups, the CMC binder could take part in the formation of the surface film. This should be beneficial to the formation of SEI film[93] The modification of CMC was conducted through the attachment of lithium ion. LiCMC was successfully synthesized by Courtel et al. as an aqueous binder for MCMB anode. However, when considering the cycle performance achieved at C/12 after 100 cycles, the order of performance for the Li/MCMB cells fabricated based on different binders is: xanthan>PVDF>PEDOT>NaCMC>LiCMC. It’s worth noting that the electrode

based on the conjugated polymer poly (3,4-ethylendioxythiophene) PEDOT could not deliver a high specific capacity despite the electronic conductivity contribution to the electrode.[94] [95] [96].

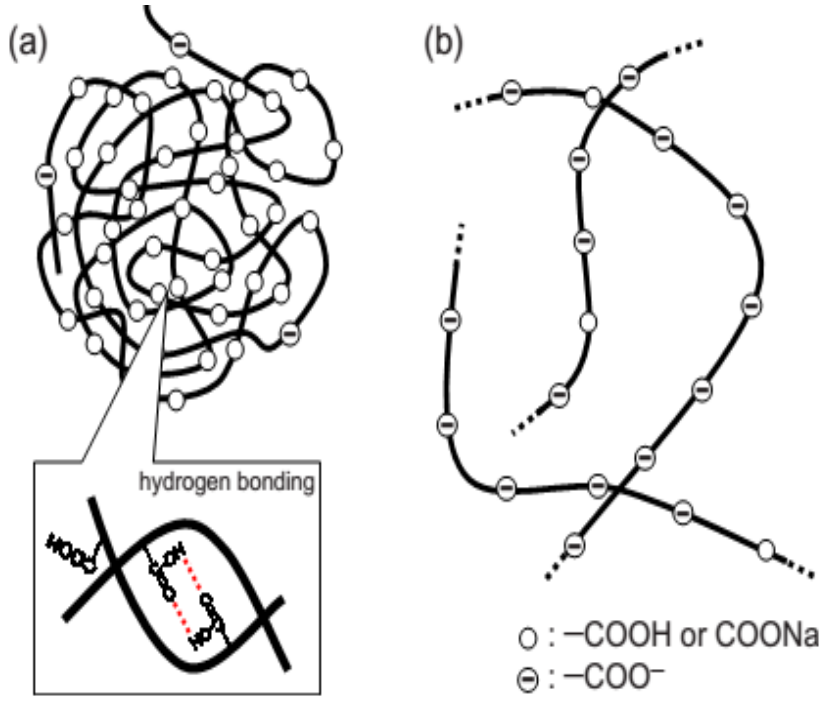

Figure 1.19 Schematic illustration of polymer chain conformation of (a) PAAH and (b) sodium polyacrylate dissolved in water.[97]

Electrodes containing spherical natural graphite and LFP fabricated with PVDF, water soluble polyacrylic acid (PAAH) and PAA (Li, Na, and K) were evaluated for LIBs performance. The electrochemical performance showed that PAA (H, Li, Na and K) binders could significantly improve the first cycle irreversible and reversible capacities except the rate capability. Among the PAAX series binders, PAALi and PAANa offered better cell performance, which could be attributed to a more favourable polymer distribution in composite. Also, the application of SBR could alleviate the cracks derived from the brittle PAAX based electrodes.[85] The advantages include improvement of capacity retention and the initial cycling efficiency of PAA based natural graphite electrodes which has also been verified by Ui et al.[98] Polyacrylates were applied as a binder for graphite electrodes in a LIB cell to modify the interface. Compared to PVDF, the efficiency of the initial cycle was improved by the polyacrylates in an ethylene carbonate based electrolyte. The

different confirmations of polyacrylates and PAA are demonstrated in Figure 1.19. Generally, carboxyl groups of PAAH show weak acidity and electrolytic dissociation, which is almost suppressed in a PAAH aqueous solution. The PAAH molecules are prone to aggregate through hydrogen bonding between two carboxyl groups. Electrolytic dissociation of PAANa and PAALi is induced in aqueous solutions which are weakly basic due to hydrolysis of the alkali salts occurs in their aqueous solution. Due to the differences in polymer conformation, i.e. the stretched polyacrylate increases the flowage resistance of the aqueous solution, the alkali polyacrylate solution was more viscosity than the PAAH solution.[99]

EPDM is a saturated amorphous elastomer with a glass-transition at ca. 50 ^{o}C. Through the CV tests in the cathodic region (3.0-5.5), oxidation reactions between non-fluorinated binder (EPDM), CB and $LiPF_6$ were demonstrated. These side reactions could be avoided through changing the electrolyte to $LiBF_6$.[100]

According to the work conducted by Zhang et al., poly(acrylonitrile-methyl methacrylate) (AMMA) is a promising binder candidate for graphite anodes in LIBs. AMMA was believed to have a similar bonding ability as the PVDF binder, e.g. low solubility in the liquid electrolyte and resistance to reactions with highly reactive lithiated graphite.[101] Based on the AMMA binder, a poly(acrylamide-co-diallyldimethylammonium chloride) (AMAC) binder was synthesized as a water-based binder for graphite anodes with better dispersion and distribution properties.[102]

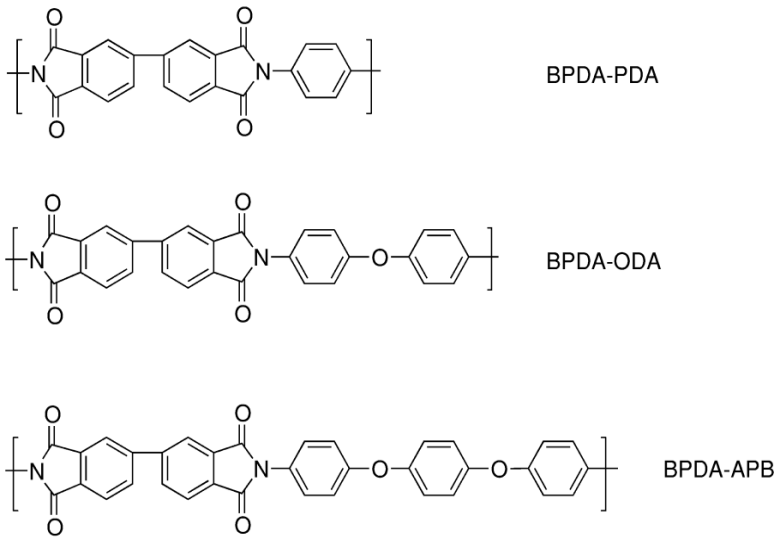

Figure 1.20 Molecular structure of polyimides used as binders in LIBs.[103]

To investigate the relationship between the amount of oxygen atoms in binders and the reversible capacity, a series of aromatic polyimides were synthesized from tetracarboxylic dianhydrides and aromatic diamines through dehydration of the intermediate polyamic acid by either a thermal or chemical method. These include 3,3'-4,4'-biphenyltetracarboxlic dianhydride (BPDA) as an acid and p-phenylenediamine (PDA), 4,4'-oxydianiline (ODA) and 1,4-bis (4-aminophenoxy) benzene (APB) as diamines (Figure 1.20). Since the aromatic polyimides are electrochemically active compared to the inert PVDF binder, there is additional capacity of the anodes based on the polyimides binder. It could be concluded that the active sites in polyimides are the carbonyl oxygen atoms in the diimide ring. [103]

Due to the strong hydrogen bonds between hydroxyl groups in PVA and active materials as well as the current collector, high molecular weight polyvinyl alcohol (PVA) was proved to be a promising binder for graphite.[104]

1.5.2. Silicon

Silicon (Si) has been researched intensively as an alternative anode material for LIBs in the last decade due to its high theoretical gravimetric specific capacity of 4200 mAh/g ($Li_{4.4}Si$), low lithiation/delithiation potential, its natural abundance, safety, environmental benignity and its small initial irreversible capacity compared with other metal- or alloy-based anode materials.[105,106] However, Si-based anodes also face grand challenges due to ca. 300% volume expansion during lithiation/delithiation processes, which commonly pulverizes, cracks and breaks electrical contact between the Si particles with conductive additive and the current collector, resulting in rapid capacity loss.[39,107,108] Recently, significant progress has been made through the synthesis of various Si nanostructures such as nanocrystals,[49] nanowires,[57] core-shell nano-fibres,[54,109] nano-tubes,[110] nano-spheres, nano-porous materials and Si/carbon nano-composites.[111-113] Although remarkable improvements in the electrochemical performance of Si-based anodes have been achieved, deformation of electrodes due to drastic volume changes persists. This is especially true for high Si loading electrodes.

Annealed PVDF-based Si electrodes were tested by Xu et al. The thermal treatment at 230 ^{o}C for 3h under argon gas was believed to improve the binding capacity of the PVDF-based electrode therefore the cycle performance.[114]

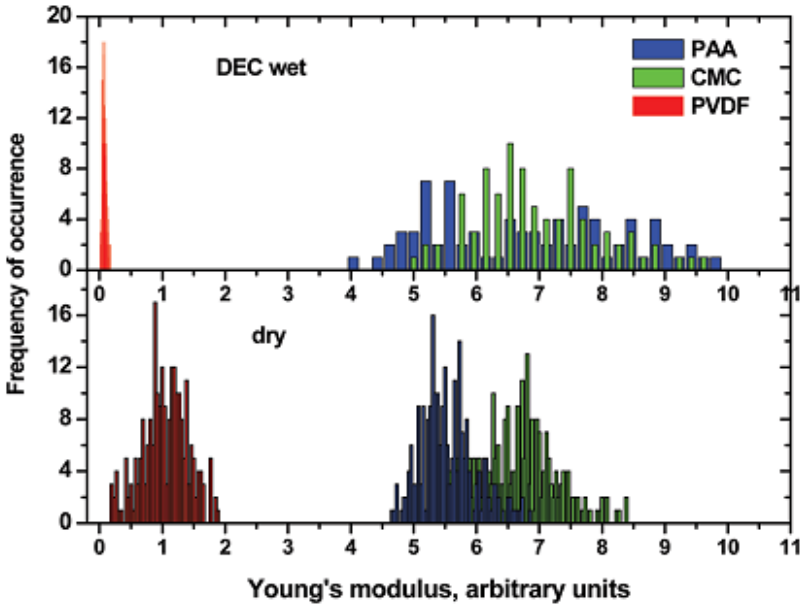

Figure 1.21 Results of AFM stiffness measurements for films made from PAA, CMC and PVDF. Results are normalized to stiffness of PVDF in dry states.[115]

Magasinki et al. demonstrated that pure PAA could be an attractive binder for Si-based anodes due to its abundant carboxylic groups. Swelling tests of the polymer films in DEC vapour were conducted to evaluate the interaction between PAA/CMC/PVDF and carbonates. Compared to PVDF, PAA and CMC have less swelling capability which indicates lower interaction with the electrolyte. As shown in Figure 1.21, the value of the Young's modulus for PVDF decreased rapidly after contact with DEC. However, the value of PAA and CMC are nearly constant after immerse in the electrolyte.[115] A better cycle performance for PAA compared to CMC was found by Komba et al. Since CMC and PAA have similar chemical structures and physical properties, further evidence of the advantages should be clarified. Based on the characterization using XRD and XPS, a different binding mechanism was proposed as shown in Figure 1.22. The chemical interaction inside PAA facilitated a film-like coating on the SiO surface, which could supress volume expansion and maintain the physical connection of the conductive additives during the

lithiation/delithiation processes.[116] Based on the promising performance of PAA, a polycarbodiimide (PCD) modified PAA binder was applied to Si/graphite composite anode materials. The cross-linked PAA-PCD composite binder could effectively modulates the rheological property of PAA slurry, thus achieving uniform dispersion and strong adhesion of the active materials.[117]

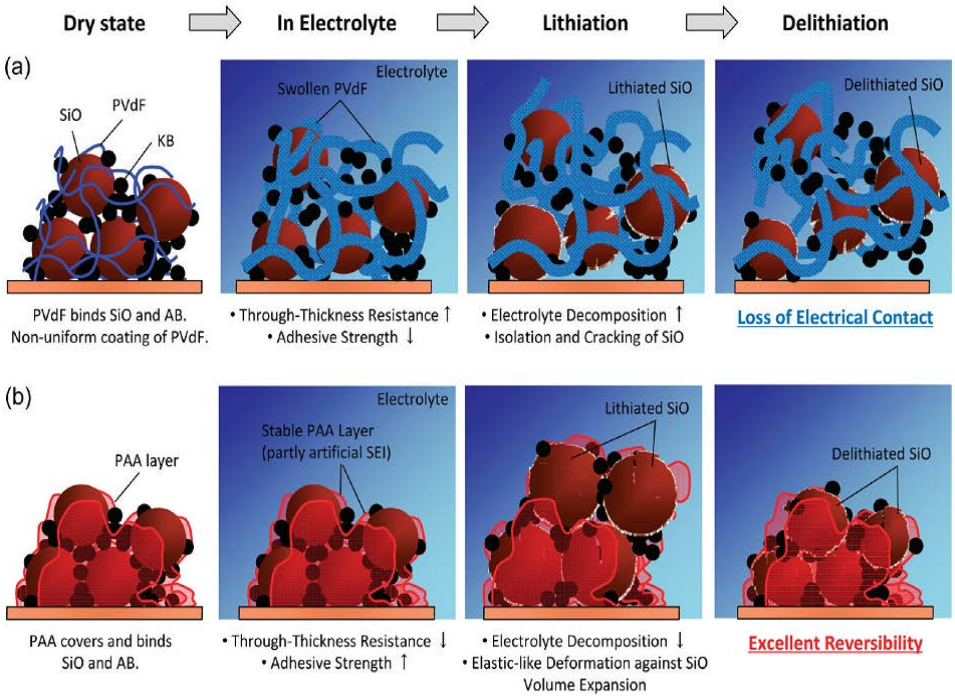

Figure 1.22 Schematic illustrations of the proposed mechanism for the improved cyclability for the SiO powder composite electrodes; (a) PVDF and (PAA) binders.[116]

Through thermal treatment of PAA and CMC, Koo et al. cross-linked these two polymers through a condensation reaction. Since the condensation between the free carboxylic acid groups of PAA-CMC and the OH groups of the silicon nanoparticles, the electrochemical performance of Si anodes based on the synthesized PAA-CMC composite binder was greatly improved.[118] Park et al. proposed a photo-cross linkable PAA-BP composite binder for Si-based anodes. Under UV irradiation, the PAA-BP binders formed an irreversible cross-linked structure through the

formation of a new three dimension C-C bond network between the benzophenone moiety and the PAA backbone (Figure 1.23).[119]

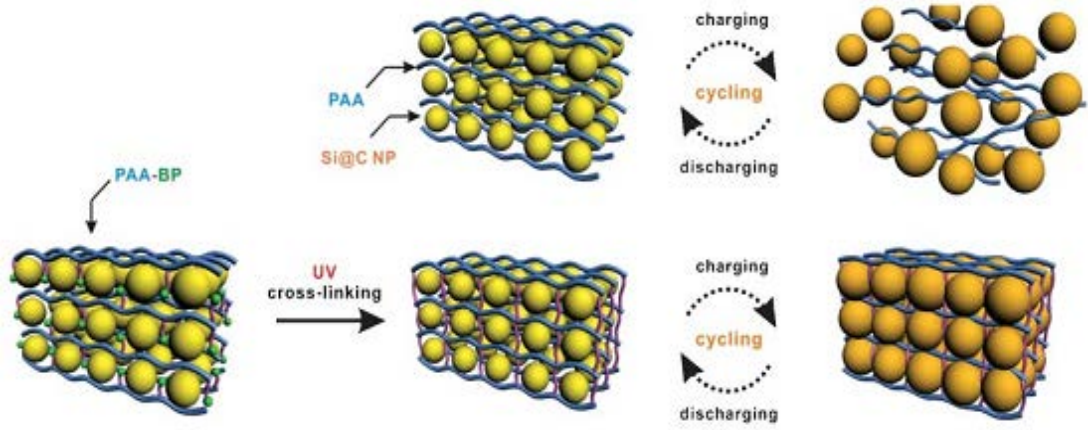

Figure 1.23 Schematic illustration of the irreversible cross-linked structure of the PAA-BP binder to accommodate volume expansion of the Si anode during charging-discharging cycles.[119]

Acrylic adhesive was investigated as a binder for silicon/carbon composite materials. The capacity retention after 50 cycles increases from 67% for PVDF-based electrodes to 79% and 90% for electrodes bound by acrylic adhesive and modified acrylic adhesive, respectively. CMC was believed to increase the adhesion strength of acrylic adhesive by 20%. Also, CMC was proved to be beneficial to prevent particle agglomeration and increase uniform distribution.[120] Liu et al. also reported that the addition of CMC to SBR could enhance the cycling life of Si-based electrodes. Compared to the conventional PVDF binder system, SBR could increase the binding strength and improve dispersion properties.[121]

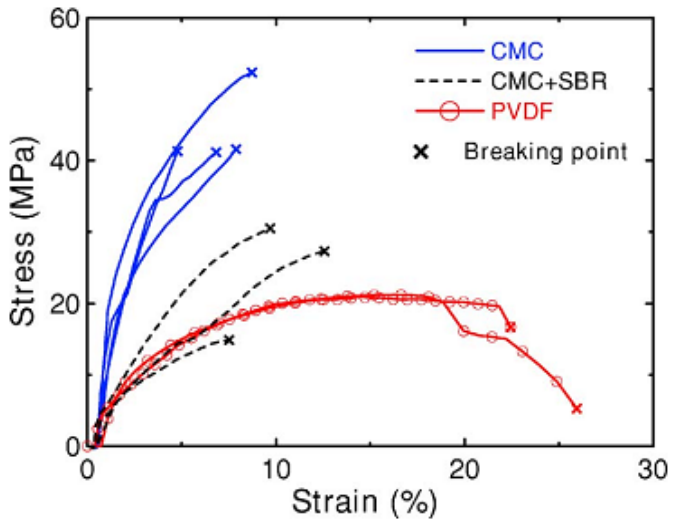

Figure 1.24 Stress vs strain for CMC, CMC-SBR and PVDF films. The X at the end of each curve indicates the breaking point.[122]

Lestriez et al. reported that the improved performance of CMC on Si-based materials is mainly attributed to an efficient CB-CMC-Si network and its extended conformation in solution.[123] According to Figure 1.24, CMC films are quite stiff and can only be extended by ca. 5-8% before breaking. Although SBR-CMC and PVDF are not elastomers, they are still less brittle than CMC. The cell performance of CMC binder-based Si anodes is superior to that of SBR-CMC and PVDF binders.[122] A self-healing process of the strong Si-CMC hydrogen binding was revealed by Bridel et al. where the chemical bonding between binder and Si could accommodate textural stresses.[124] Based on further understanding of the function of CMC on Si anodes, a CMC porous scaffold was obtained using the slurry spray technique as a binder for Si anodes (Figure 1.25). The slurry was sprayed onto the heated copper foil. Afterwards, the water evaporated instantly upon contact with the copper foil. As a result, a porous scaffold electrode was formed. According to the cycle performance, the scaffold structure could accommodate the volume change during lithiation/delithiation.[125]

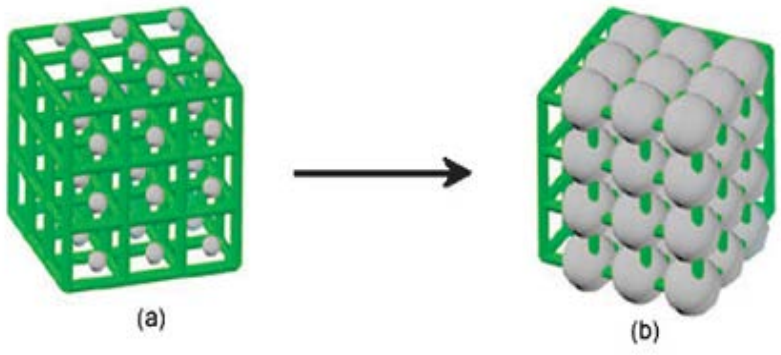

Figure 1.25 3D scaffold binder structure: silicon particles are bound in the porous polymer binder scaffold. The scaffold structure is able to accommodate volume expansion without demolishing the structure.[125]

Polyamide imide (PAI) had been applied in the Si electrode fabrication by Choi et al. Although PAI binder react with Li ions and electrons during the first cycle, the cycle performance is remarkably improved due to its strong binding force which can afford the volume expansion after lithiation.[126]

High molecular weight polyvinyl alcohol (PVA) was synthesized by two step polymerizations and employed as a binder for Si electrodes. The strong hydrogen bonding of hydroxyl groups in PVA contribute to the high binding capability. These hydroxyl groups form hydrogen bonds with active materials and the current collector. In contrast, the fluorine atoms in PVDF can only form weak hydrogen bonds.[104]

Cui et al. reported a novel method using amorphous silicon as an inorganic glue replacing conventional polymer binders The inorganic glue was prepared by addition of 10 wt% polyacrylonitrile (PAN) in dimethylformamide (DME) solvent. This inorganic glue can keep the contact in conventional silicon particle anodes and enables successful cycling of various sizes of silicon particles. The electrode was carbonized at 700 ^{o}C under an argon atmosphere. After carbonization, a layer of

boron doped Si was deposited onto the surface through CVD method. The mechanism of this novel binding is schematically illustrated in Figure 1.26.[127]

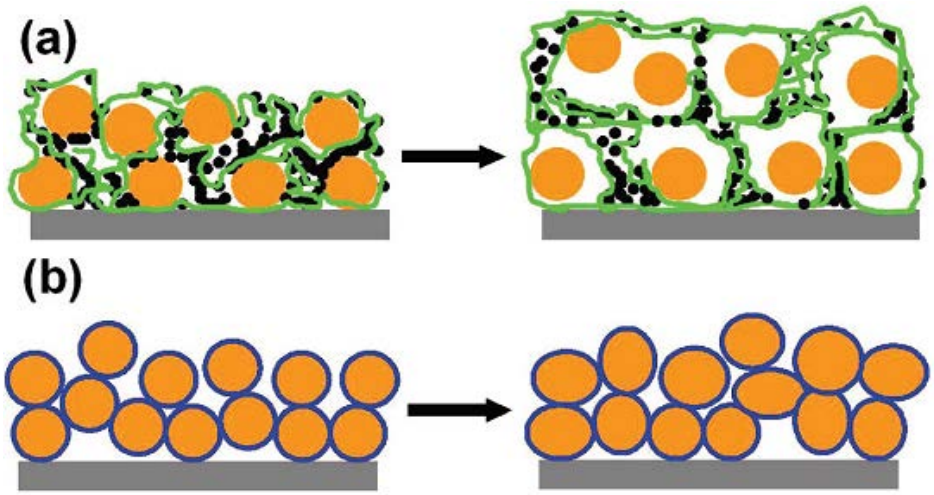

Figure 1.26 Schematic illustration of the morphology change of Si particle films before and after charge-discharge cycling. (a) Si particle films prepared with conventional binder systems. After cycling, the Si particles lose electrical contact with surrounding particles. (b) Si particles fused together and bonded by a-Si inorganic glue, where blue rings indicate a-Si coating. After cycling, the particle film still maintains an all-connecting porous structure, where no loss of electrical contact occurs.[127]

Komaba et al. demonstrated that the PAANa polymer was an efficient binder to enhance the electrode performance of Si-graphite composite negative electrodes. After the cycling, the PAANa composite electrode is firmly attached to the current collector. The PAANa polymer could cover the Si particles, which would reduce electrolyte decomposition and thus suppresses electrical isolation in the composite electrode.[128]

Bae et al. introduced polyethyleneimine (PEI) as a binder for silicon-CNT composite anodes due to the reaction between PEI and CNT. The larger surface area of CNT could accelerate the formation of SEI film which results in a low initial

Coulombic efficiency. Accordingly, half-cell tests demonstrated more improved capacity retention behaviour in the sample with PEI than that of PVDF binder.[129]

Polyimide binder (PI) was evaluated as a binder for modified Si anodes by Kim et al. The PI polymer binder supressed the side-reaction between the electrolyte and the modified high surface area Si anode materials.[130]

1.5.3. Other anodes

Spinel lithium titanate, $Li_4Ti_5O_{12}$, has attracted great interest as an anode material for rechargeable LIBs because it can offer a great safety improvement due to its high and flat Li insertion voltage at ca. 1.55 V versus Li/Li^+. Based on this promising anode candidate, binder effects tests were conducted using CMC, poly ethylene glycol, polyacrylonitrile and Acryl S020.

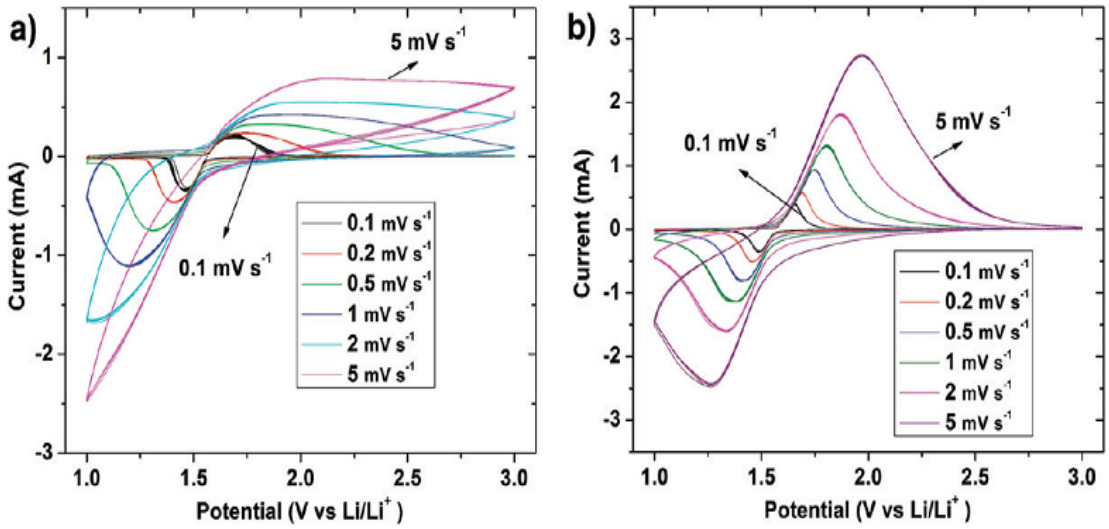

Figure 1.27 Cyclic voltammograms of $Li_4Ti_5O_{12}$ microsphere electrodes using (a) PVDF and (b) CMC as binders at different scan rates from 0.1 to 5 mV/s at 26 ^oC after charge and discharge for 80 cycles.[131]

Through the cyclic voltammograms (CVs) test of $Li_4Ti_5O_{12}$ electrodes using PVDF and CMC as binders (Figure 1.27), both profiles indicated the good reversibility of lithium intercalation into and delithiation from $Li_4Ti_5O_{12}$ at a scan rate of 0.1 mV/s. At an increased scan rate (5 mV/s), the CMC based electrode could maintains the symmetrical shape of the cathodic peaks and the anodic peaks in its CV profiles. However, the shapes of the cathodic peaks and the anodic peaks change greatly for the PVDF binder based electrode. This indicated good reversibility and good rate capability for CMC based electrodes. The activation energies, charge

transfer resistance and diffusion coefficient of the microsphere electrodes were calculated from EIS to further investigate the electrode kinetics. Comparatively, the CMC based electrode showed lower charge transfer resistance, activation energy and higher lithium ion diffusion coefficient.[131] Based on the promising performance of CMC on $Li_4Ti_5O_{12}$, a synergistic effect was also demonstrated when it was applied in electrolytic solutions based on ionic liquids. The application of ionic liquids provides a promising solution for the development of greener and safer batteries.[132] The effect of molecular weight (MW) and degree of substation (DS) of CMC binder have also been investigated. The LTO electrode showed excellent cycle performance when based on low MW and high DS CMC binder.[133]

Another type of aqueous fabrication of more than 200 micro-metre thick LTO electrodes using a novel poly (PEGMA-co-MMA-co-IBVE) copolymer binder has been demonstrated. High active material loading up to 28 mg/cm^2 and 4.2 mAh/cm^2 at *C*/2 rate were achieved after 10 tons/cm^2. The PEG based copolymer is a multifunctional material that plays critical roles, i.e. the effective dispersion of electrode slurries, ensuring cohesion of electrode materials and maintaining ionic conduction pathways throughout the electrode.[134]

According to study by Gong et al., the highly polar polyacrylonitrile (PAN) is a promising binder for LTO material. The excellent performance can be attributed to high polarity, resulting in strong adhesion and low irreversible capacity. Additionally, PAN-containing electrodes have shown good electrolyte wettability and low charge transfer resistance.[135]

Materials based on tin oxide have been proposed as promising alternative anode materials for LIBs owing to their high theoretical capacity (790 mAh/g). CMC was applied as an aqueous fabrication process for SnO_2 based LIBs to improve the

performance of SnO_2. Through the work by Liu et al.[136] and Chou et al.[137,138], the initial capacity and the cyclic retention of SnO_2 anodes using CMC as binders are better than those using PVDF as binders.

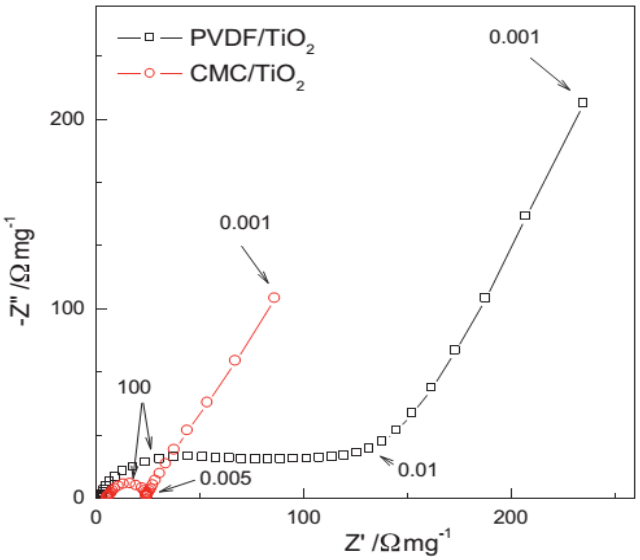

Figure 1.28 Nyquist plots of the TiO_2/PVDF and TiO_2/CMC electrodes. E = 1.78 V, T = 20 ^oC.[139]

The electrochemical performance of nanocrystalline anatase TiO_2 electrodes fabricated through sodium CMC binder and optimized with SBR has been investigated. The performance was compared with electrodes manufactured using traditional PVDF and its copolymer with hexafluoropropylene (PVDF-HFP). CMC and CMC/SBR based electrodes possess higher specific capacity, rate capability, and cycling stability than those prepared using PVDF or PVDF-HFP as binder. The CMC-based TiO_2 electrodes could achieve a total energy density of more than 120 Wh kg^{-1}.[140], EIS have been applied to investigate the interfacial kinetics of the two types of composite electrodes. The CMC based electrodes exhibit significant lower impedance than the PVDF based electrodes.[139,141](Figure 1.28)

1.6. Application of binders for Li-S battery

Lithium-sulfur batteries deliver the theoretical energy density 5 times higher than that of current commercialized LIBs (ca. 2,500 vs. ca. 500 Wh/kg). However, Li-S batteries suffer from a few frustrating problems, including the insulating properties of sulfur and its discharge products, ca. 76% volume expansion cycling from sulfur (S) to lithium sulfide (Li_2S), and polysulfide shuttle that transport sulfur species back and forth between electrodes. These lead to the destruction of sulfur cathode and the corrosion of lithium anode with short battery life. Binders have been proven to be effective in improving the tolerance of volume expansion and stop the polysulfide shuttle through chemical bonding. Thereby, application of binders in Lithium-sulfur batteries attracted more and more attention. Since divinyloxyhydroxyolysulfides were first developed as an alternative binder for Li-sulfur batteries,[142] polymers including gelatin, PEO, PAA, CMC, SBR and carbonyl-β-cyclodextrin have also been identified as promising binders. Gelatin could enhance the redox reversibility of sulfur cathodes through slowing down the reduction reaction of elemental sulfur during the discharging process and reforming S_8 after the delithiation process.[143] Gelatin is more electrochemically stable and possesses a higher adhesion force in contrast to PEO polymer binder.[144] The distribution property of gelatin-based electrodes has been investigated by Wang et al. At the beginning of the discharge for the gelatin based electrode, the porous sulfur cathode exhibited a homogenous distribution of sulfur, carbon and pores. As the extent of the discharge increased, the sulfur particles and pores gradually disappeared. The porous structure and elemental sulfur reappeared even after 50 charging cycles. The good distribution and reversibility of the gelatin-based electrode is the key factor to improve the cycle performance of Li-sulfur batteries.[145]

The influence of the pH on the gelatin solution on the cycle performance of the sulfur cathode for lithium-sulfur batteries was studied by Zhang et al. Scanning electron microscopy observations revealed that the cathode prepared with a pH 10.0 gelatin solution as a binder showed the most uniform distribution. An initial capacity of ca. 1130 mAh/g and a reversible capacity of ca. 650 mAh/g after 30 cycles were achieved, which were higher than those of the cathodes prepared at pH 5 and 8. When the pH value is 10, the dispersion is more uniform, which could result in higher initial discharge capacity of and better long-term performance than pH 5 and 8.[146]

The electrochemical properties of sulfur cathodes based on commercially available sulfur powder and water-soluble binders have been investigated. A mixture of SBR and CMC was used as the binder. Compared with conventional PVDF binders, the SBR/CMC binder significantly improved cycling performance of the sulfur cathode with a high specific capacity of 580 mAh/g after 60 cycles. The better performance could not only be ascribed to the high adhesion but also excellent dispersion property, which favours uniform distribution and good electrical contact, leading to high sulfur utilization. [147]

The low electronic resistance of the Li-sulfur electrode in aqueous binding system was also proven by PAA polymer binder. Ascribed to the better distribution property, the better kinetics characteristics were evidenced by the CV and EIS tests. [148]

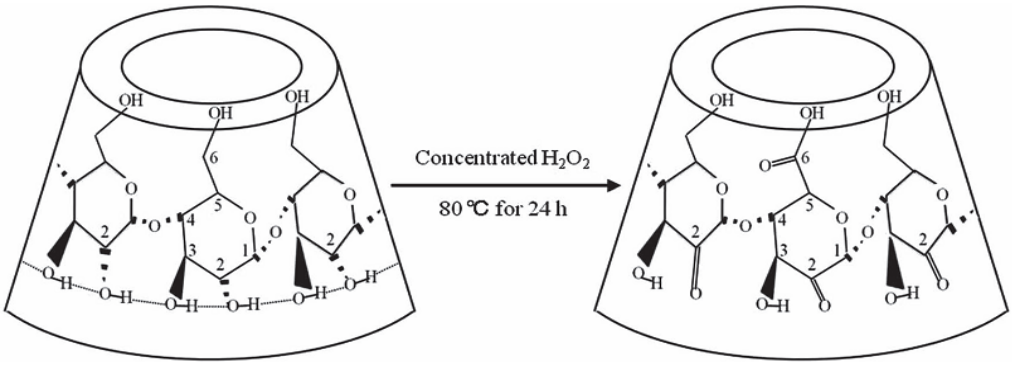

Figure 1.29 Schematic reaction of β-CD with H_2O_2.[149]

Through carbonylation reaction, the β-cyclodextrin (β-CD) was identified as a promising water soluble binder for sulfur composite cathodes. The carbonyl-β-cyclodextrin (C-β-CD) was achieved through partial oxidation in H_2O_2 solution. The carbonyl-β-cyclodextrin (C-β-CD) exhibit a water solubility ca. 100 times than that of β-CD at room temperature. (Figure 1.29) Sulfur composite cathodes based on C-β-CD binder demonstrate a high reversible capacity of 694.2 mAh/g_{sulfur} and 1542.7 mAh/$g_{composite}$, with a sulfur utilization approaching 92.2%. The discharge capacity remains at 1456 mAh/g_{sulfur} after 50 cycles, which is much higher than that of the cathode with unmodified β-CD as binder. The strong bonding strength and wide electrochemical windows also promote the total performance through confining polysulfide shuttle. Consider the low cost and environmental benignity, C-β-CD is also a promising binder for sulfur cathodes in rechargeable lithium batteries with high cycle performance.[149]

1.7. Trend of binder development

1.7.1. Adoption of sustainable binders

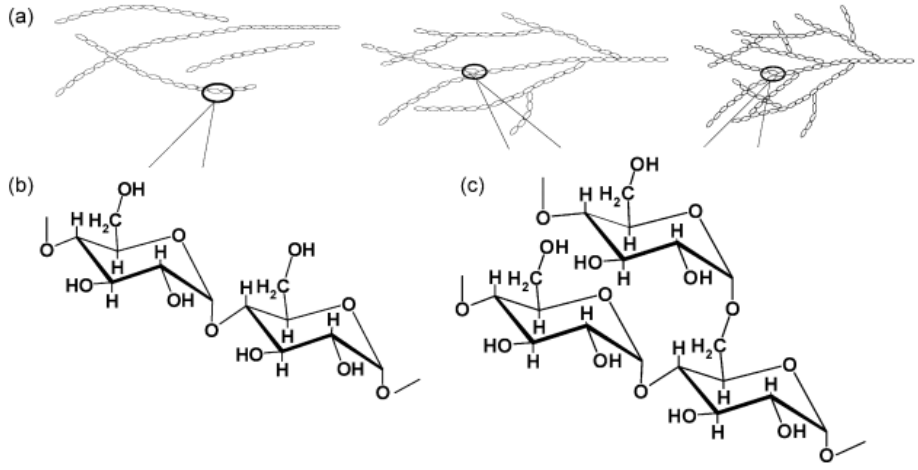

Figure 1.30 Schematic illustration of three different polysaccharides and their structural formulae: (a) amylose, (b) amylopectin, and (c) glycogen.[150]

A wide variety of natural derived sustainable polymers have been developed to improve the LIBs performance. Crop-derived polysaccharides were employed as binder for high capacity silicon-graphite based electrodes due to its natural abundant functional groups. (Figure 1.30) The advantage of the polysaccharides can be summarized as follows: (1) effectively reduced electrolyte decomposition in the initial cycle; (2) improved mechanical strength to cope with volume expansion; (3) excellent capacity retention.[150] Chitosan is a polysaccharide composed mainly of β-(1,4)-linked 2-deoxy-2-amino-D-glucopyranose units. Compared to using PVDF binder, the chitosan based graphite anode exhibited enhanced cycle performances, i.e. rate capability and first Columbic efficiency. The first Columbic efficiency of the chitosan based anode is 95.4%, which is 89.3% for the PVDF-based anode. After 200

lithiation/delithiation cycles at 0.5C, the capacity retention of the chitosan based electrode is significantly higher than that of the PVDF based electrode.[151]

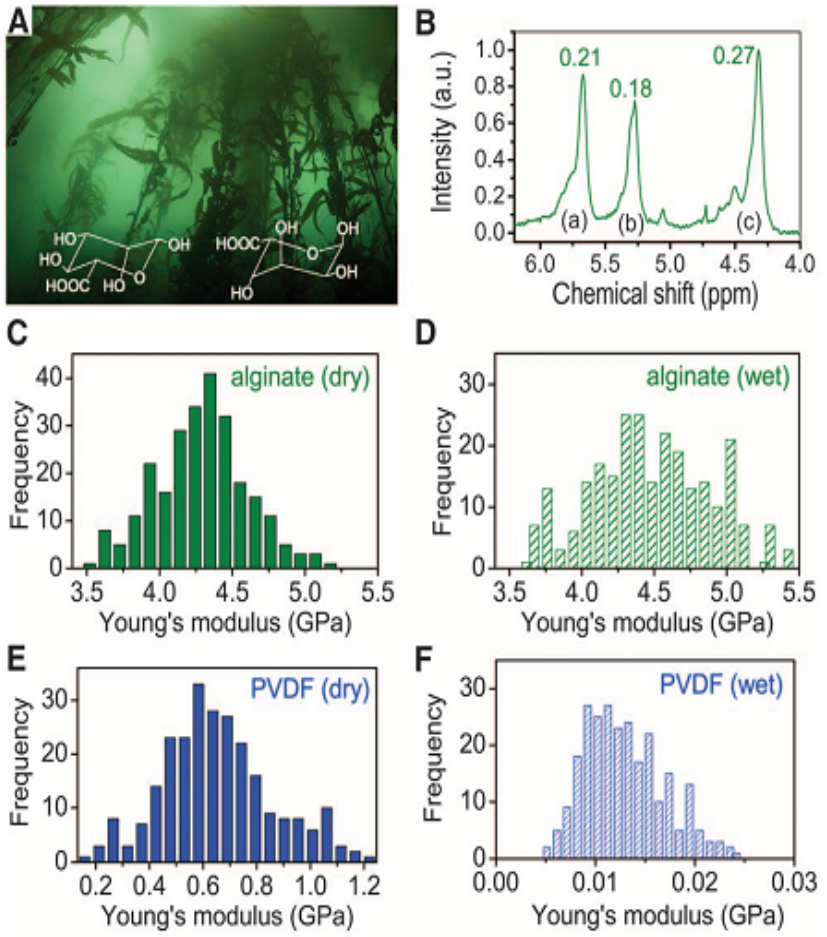

Figure 1.31 Alginate origin and characterization. (A) Giant kelp forest in the Pacific Ocean, photographed near the coast of California, USA. The insets show the chemical structure of alginate. (B) 1H NMR spectrum of sodium alginate. The numbers above the peaks marked as (a), (b) and (c) correspond to their integrated intensities. Ppm, parts per million; a.u., arbitrary units. (C to F) comparison between Young's modulus of sodium alginate and PVDF and in dry and wet state.[152]

Furthermore, a high-modulus natural polysaccharide was extracted from brown algae, yields a significant Si anode performance.[152] In contrast to the polysaccharides found in terrestrial plants, alginate is extracted from marine botany. It contains hydroxyl and carboxyl groups in each of the polymer's monomeric units.

(Figure 1.31a) The larger number of binder-Si bonds are mainly attributed to the increased content of carboxyl groups in the alginate, which resulted in better Si electrode stability. Besides, as showed in Figure 1.31C to F, sodium alginate present ca. 6.7 times higher stiffness than dry film of PVDF, which improves the tolerance of volume expansion of Si anode after volume change. At a current density of 1200 mA/g, with Li insertion capacity limited to 1200 mAh/g, the alginate-based Si anode operated safely for more than 1300 cycles.

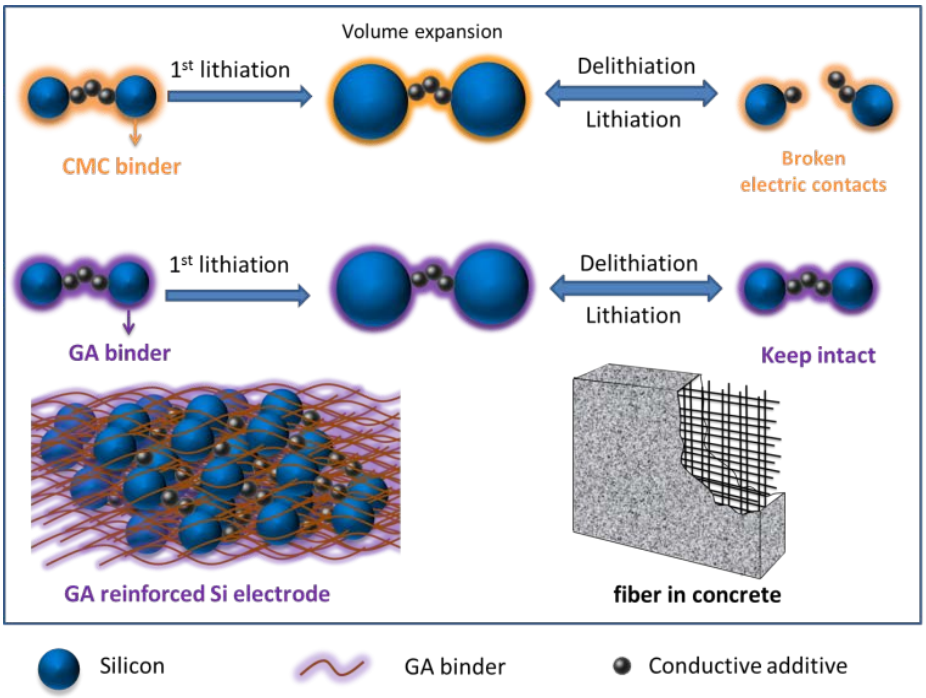

Figure 1.32 Schematics of the concept to address volume change issue in battery materials. GA with dual functionality could have both the strong chemical bonding and the ductile properties necessary to tolerate the expansion during lithiation/delithiation processes.[153]

Naturally abundant gum arabic (GA), composed of polysaccharides and glycoproteins, was applied as a dual-function binder to address the volume expansion issue of Si anodes. Firstly, the hydroxyl groups of the polysaccharide in GA are crucial in ensuring strong binding to Si. Secondly, similar to the function of fibre in

fibre-reinforced concrete (FRC), the long glycoproteins chain provide further mechanical tolerance to dramatic volume expansion by Si nanoparticles. (Figure 1.32) The resultant Si anodes present an outstanding capacity of ca. 2000 mAh/g at a 1 *C* rate and 1000 mAh/g at a 2 *C* rate, throughout 500 cycles. Excellent long-term stability is achieved by the maintenance of 1000 mAh/g specific capacity at a 1 *C* rate for over 1000 cycles. This low cost, naturally abundant and environmentally benign polymer is a promising binder for future LIBs.[153]

1.7.2. Enhancement of mechanical property

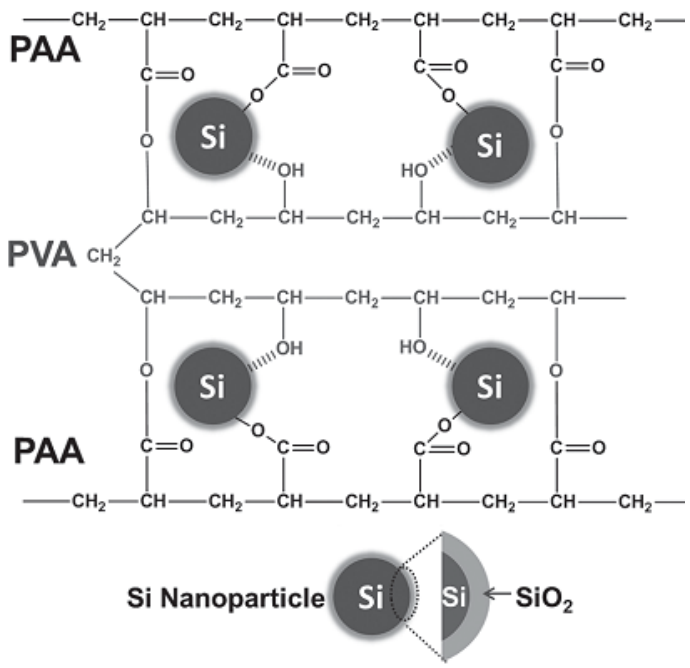

Figure 1.33 The chemical structure and interactions between cross-linked PAA-PVA and silicon particles.[154]

As illustrated above, the glycoproteins reinforced polysaccharides polymer have been demonstrated to enhance the tolerance of crack derived from the expansion of lithiated Si. Moreover, the crosslinking structure of the binder was believed to be benefit to the mechanical stability of the electrode. A facile *in situ* thermal-

crosslinking technique was developed by Wang et al. through combination of PAA and polyvinyl alcohol (PVA). (Figure 1.33) This designed binder can effectively accommodate the large volume change of silicon anodes upon lithiation/delithiation due to the deformable polymer network and strong binding between Si and the binder. As a result, high-areal-capacity of 4.3 mAh/cm^2 with good cycling stability was demonstrated at based on the PAA-PVA binder.[154]

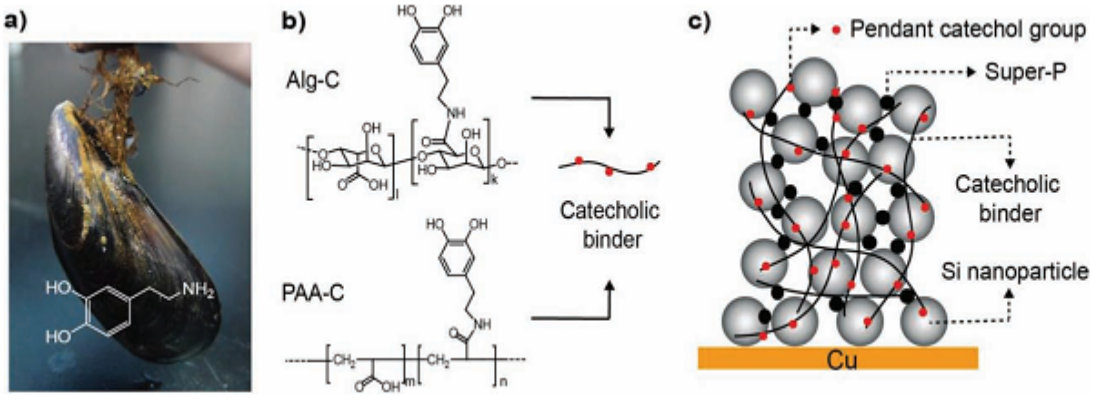

Figure 1.34 Catechol conjugated polymer binders and Si anode structure. a) Mussel, the inset shows the chemical structure of dopamine inspired by mussel foot proteins. (b) Structural formula of alginate-catechol and polyacrylic acid-catechol alongside a simplified structure of a conjugated polymer binder; the solid black line represents the polymer backbone with carboxylic acid functional groups attached and red circles represent catechol moieties conjugated to the backbone. (c) A graphical illustration of the Si NP anode structure.[155]

Inspired by the wetness-resistant adhesion feature of mussels, alginate and PAA were modified by the catechol, which is a determine factor in the distinguished wetness-resistant adhesion. The synthesis and binding mechanism is illustrated in Figure 1.34. The mussel-inspired binders with extraordinary wetness-resistant adhesion capability can significantly improve the capacities and cycle life of Si nano-

particles based anodes while remaining mechanical stability at wet organic environment. The cathechol-conjugated alginate (Alg-C) binder are demonstrated to achieve ca. 2 mg/cm^2 mass loading, which is equivalent to ca. 8.4 mAh/cm^2.In addition to the cathechol contribution to the energy density, the Alg-C based electrode exhibited superior capacity retention (84.5%) after 150 cycles.[155]

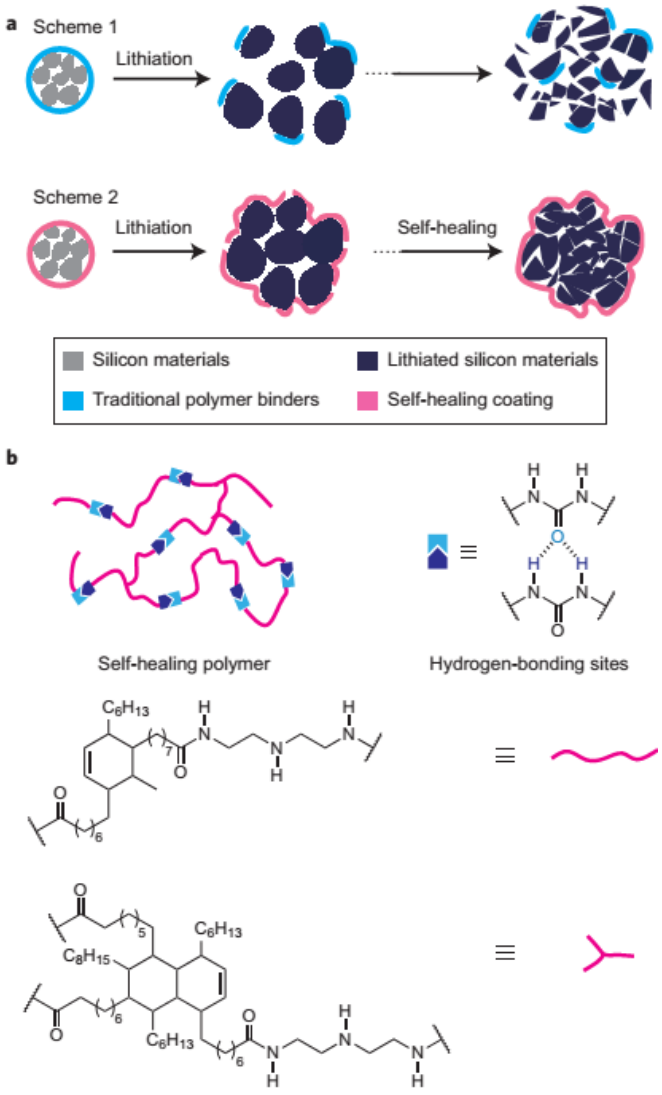

Figure 1.35 Design and structure of the self-healing electrode. (a) Scheme 1: schematic illustration of the design and behaviour of a conventional silicon electrode that shows failure of the electrode because of particles and polymer binder cracking, which results in loss of electrical contact. Scheme 2: schematic illustration of the design and behaviour of stretchable self-healing electrode that maintains electrical contact between the broken particles with no cracks in the polymer binder due to the

stretchability and incorporation of self-healing chemistry. (b) Chemical structure of the SHP. Magenta lines, polymer backbones; light-blue and dark-blue boxes, hydrogen-bonding sites.[156]

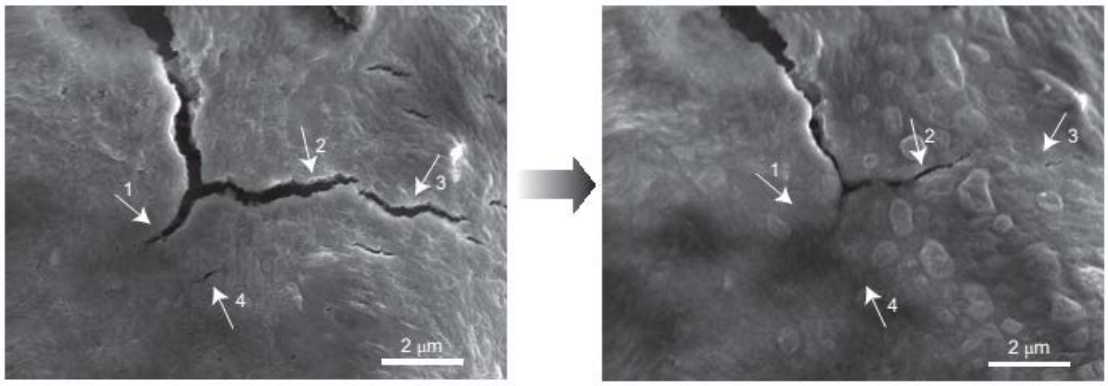

Figure 1.36 Left: cracks in the polymer layer in the lithiated state; right: after five hours the smaller cracks were healed, indicated by the arrows on the images.[156]

Actually, nature has offered other options to solve the mechanical fracture of electrodes, such as skin, have the ability to self-healing when damaged. Based on this natural phenomenon, Cui et al. applied the self-healing polymers (SHP) as binders to optimize the mechanical properties of Si based electrodes in LIBs.[156] (Figure 1.35) On deep galvanostatic cycling between 0.01 and 1 V, the delithiation capacity reached 2617 mAh/g for the first cycle at 0.1C. Also, the delithiation capacity retention was 100%, 95% and 80% after 20, 50 and 90 cycles, respectively. The improved cycling stability of the electrode can be attributed to two major features, i.e. stretchability and spontaneous self-healing capabilities. The SHP/CB coating can better withstand the large volumetric changes due to its superior mechanical stretchability as well as its strong interactions with the silicon surface. It could self-heal when the SHP/CB composite coating fractures. To provide further evidence, the morphologies of the electrodes with cycling were presented using SEM as seen Figure 1.36.

1.7.3. Optimization of ion conductivity

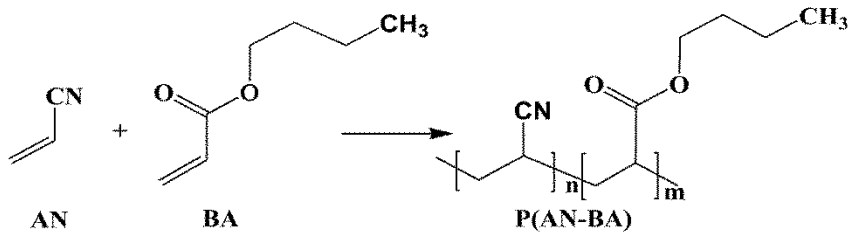

Figure 1.37 The molecular structure of AN, BA and P(AN-BA).[157]

The rate determining step in the electrodes of lithium ion batteries is supposed to be the lithium ion diffusion coefficient. The diffusion in binder is critical due to the coating of binders on the surface of active materials. The faster kinetics was achieved through modification of polyacrylonitrile and gum arabic. Polyacrylonitrile (PAN) is a good choice for a binder due to its high polarity, electrochemical stability and ability to facilitate Li ion transport. Unfortunately, PAN is a semicrystalline polymer with a high glass transition temperature (T_g) of 96.5 °C. Hence, butylacrylate (BA) was chosen to address this issue due to its low T_g of -45 °C. The molecular structure of AN, BA and P(AN-BA) is shown in Figure 1.37. The adhesion strength, electrical and electrochemical properties of electrodes can be improved through he copolymerization of acrylonitrile (AN) with BA. The advantages are mainly contribute by an increase in the diffusion coefficient and a decrease in the impedance of the graphite electrodes.[157]

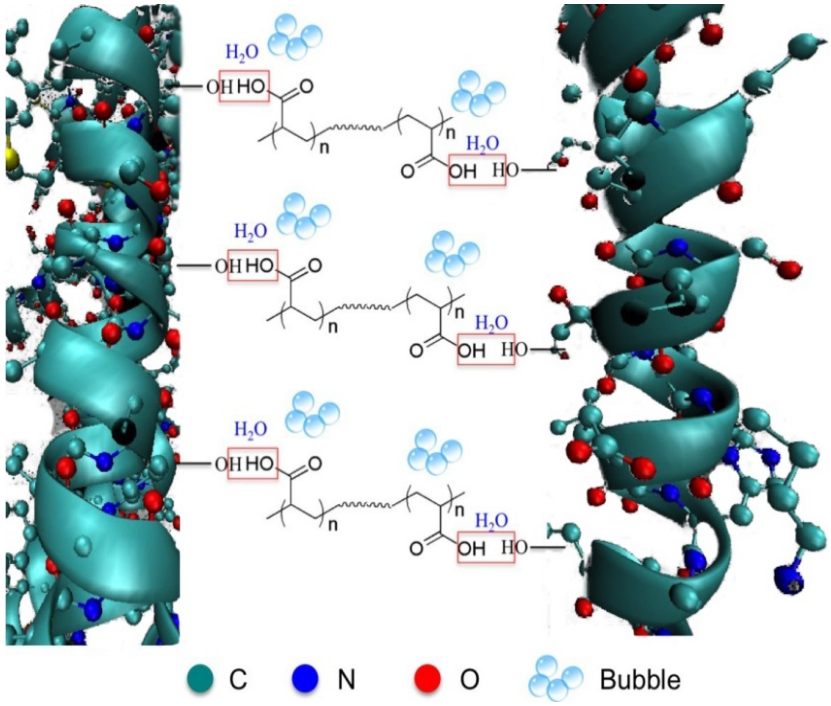

Figure 1.38 Schematic diagram of the polymeric reaction: the generation of water and formation of crack-blocking GA-PAA composite binder.[158]

The higher electrolyte uptake of the binder has been evidenced to be beneficial to the lithium ion transport. To improve the ion transport capability in GA, PAA is crosslinked through an *in situ* esterification reaction. Esterification reactions between GA and PAA established a flexible network resulting in improved lithium ion conductivity, reinforced mechanical strength and enhanced coherent strength. (Figure 1.38) The improved lithium ion coefficient is mainly ascribed to the enhanced polarity and generated micron-sized pores, which improve the electrolyte uptake. Besides, the generated pores can stop the crack propagation caused by the expansion of lithiated Si electrode. As a result of the crack-blocking effect, the resultant Si anodes had a superior volumetric capacity of 2890 Ah/L. In addition, charge/discharge cycling for more than 1000 cycles was achieved with Li insertion capacity limited to 1000 mAh/g at 1 *C* rate.[61]

1.7.4. Tailoring of electronic conductivity

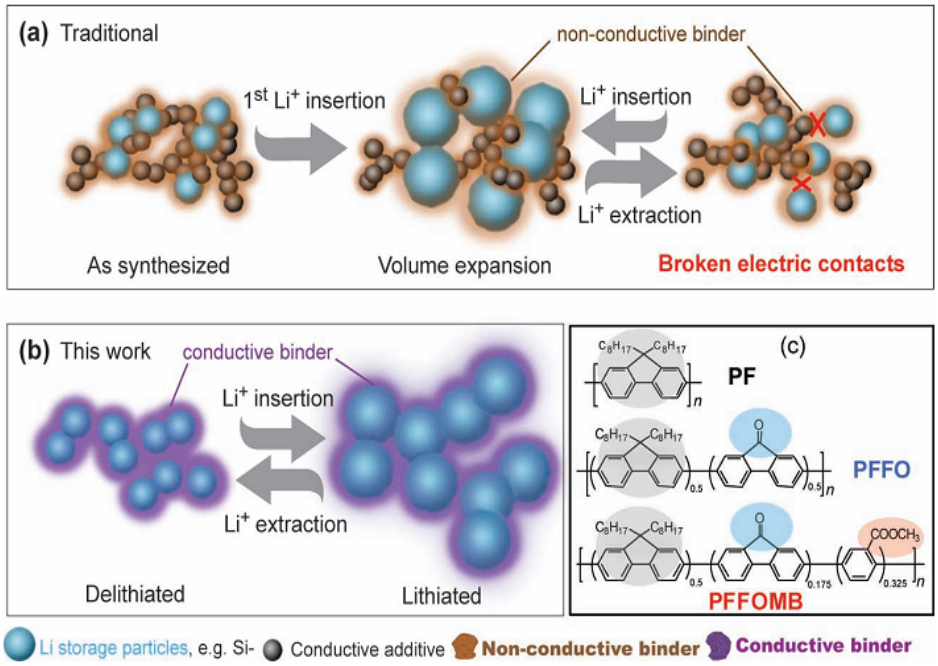

Figure 1.39 Schematics of the technical approaches to address volume change issue in battery materials. (a) Traditional approaches use acetylene black (AB) as the conductive additive and PVDF polymer as the mechanical binder. (b) Conductive polymer with dual functionality, as a conductor and binder, could maintain both electrical and mechanical integrity of the electrode during the battery cycles. (c) The molecular structure of the PF-type conductive polymers, with two key function groups in PFFOMB, carbonyl and methylbenoic ester, for tailoring the conduction band and improving the mechanical binding force, respectively.[62]

Liu et al. synthesized a multi-functional polymer binder based on polyfluorene (PF) type polymers. To achieve a properly tailored electronic structure, two key functional groups, carbonyl C=O and methylbenzoic ester -PhCOOCH$_3$ (MB) were introduced to the PF backbone as shown in Figure 1.39c. It was demonstrated by synchrotron-based soft X-ray absorption spectroscopy (XAS) that the carbonyl groups in PFFO and PFFOMB generated a new LUMO state at 284.7 eV. The as-synthesized

PFFOMB featured much improved electric conductivity and robust mechanical binding force, which simultaneously maintained electric connectivity and accommodated the Si volume change simultaneously.[62]

1.8. Scope of the thesis

The overall aim of this work is to develop green electrode fabrication technologies for low cost and high performance lithium ion batteries. Inevitably, this is a multidisciplinary effort, with various practical requirements. These requirements include adoption of various polymers, modification of the binding systems and design of electrode fabrication technologies. The detailed strategies are demonstrated in the following chapters.

Chapter 2 describes a commercialized aqueous *Eastman AQ^{TM}55S* (EAQ) polymer binder applied in the current commercialized graphite anode. EAQ is a water soluble polymer with abundant structured hydroxyl groups, in contrast, the conventional PVDF binder which is an organic-based polymer with an inert chemical structure. The specific objectives for this part of the work were:

I. To investigate the dispersion and distribution properties of the aqueous and organic based electrodes.

II. To demonstrate the advantages of functional groups among the binders and oxidized graphite.

Considering the benefits of the functional groups in the aqueous binding system above, Chapter 3 demonstrates a dual-functional gum arabic (GA) polymer binder system for Si anodes. Si is particularly attractive because of its highest known theoretical capacity of 4200 mAh/g. However, silicon anode materials suffer from substantial volume change (300 vol%) during lithiation/delithiation. This causes poor electrical contact of Si particles with the conducting matrix and severe pulverization of the Si. Besides the hydroxyl and carboxyl groups in GA, the other component, i.e. glycoprotein, can establish a fibre reinforced structure to enhance mechanical strength, leading to a high tolerance of volume expansion after lithiation.

Chapter 4 demonstrates the important role of binders based on both their physical and chemical properties in Li-S batteries. Lithium-sulfur (Li-S) batteries supply a theoretical energy density five times higher than that of current commercialized LIBs (2,500 vs. 500 Wh/kg). Nevertheless, Li-S batteries have critical flaws, including (i) the insulating properties of sulfur and its discharge products, (ii) ca. 76% volume change cycling from sulfur (S) to lithium sulfide (Li_2S), and (iii) polysulfide shuttles that transport sulfur species back and forth between electrodes. These lead to the destruction of sulfur cathodes and the corrosion of lithium anodes producing short battery life. The GA binder system is designed to endow sulfur electrodes with high binding strength and good ductility to buffer volume change, while its functional groups chemically immobilize sulfur species within the cathode to inhabit the polysulfide shuttle.

To make the Si electrode more attractive for practical application, high mass loading is necessary for the high areal capacity needed to advance the energy density of LIBs. Chapter 5 illustrates a three dimensional cross-linking structure via an *in situ* esterification process through water-based GA and polyarylic acid (PAA) polymers. The esterification reaction between hydroxyl groups in GA and carboxyl groups in PAA can provide reinforced mechanical strength and flexibility. Moreover, the micon-sized pores formed during the esterification process are proposed to block crack formation and propagation by relieving the stress of the dramatic volume expansion.

A multi-functinonal polymer binder system is developed for current commercialized $LiFePO_4$ (LFP) cathodes in Chapter 6. LFP has been considered a promising cathode material that could dominate large scale EV markets due to its low cost, high safety and high theoretical capacity (170 mAh/g). However, the low

electronic and ion conductivities have been an issue since its inception. The multi-functional polymer binder SA-ProDOT was synthesized from sodium alginate (SA) and 3,4-propylenedioxythiophene-2,5-dicarboxylic acid (ProDOT) using a cyclohexane/DBSA/water micro-emulsion system. The tailored electronic structure of the SA-ProDOT facilitates n-type lithium doping under the battery environment. The SA-ProDOT demonstrates significantly better binding capability, mechanical property, electrolyte uptake and lithium ion diffusion coefficients than other conventional binders.

1.9. References

1 Han, Z. & Reitz, R. D. (1995) 'Turbulence modeling of internal combustion engines using RNG k-epsilon models', *Combustion Science and Technology* 106, 267-295.

2 Akansu, S. O., Dulger, Z., Kahraman, N. & Veziroglu, T. N. (2004) 'Internal combustion engines fueled by natural gas - hydrogen mixtures', *International Journal of Hydrogen Energy* 29, 1527-1539.

3 Agarwal, A. K. (2007) 'Biofuels (alcohols and biodiesel) applications as fuels for internal combustion engines', *Progress in Energy and Combustion Science* 33, 233-271.

4 Etacheri, V., Marom, R., Elazari, R., Salitra, G. & Aurbach, D. (2011) 'Challenges in the development of advanced Li-ion batteries: a review', *Energy & Environmental Science* 4, 3243.

5 Song, H.-K., Lee, K. T., Kim, M. G., Nazar, L. F. & Cho, J. (2010) 'Recent Progress in Nanostructured Cathode Materials for Lithium Secondary Batteries', *Advanced Functional Materials* 20, 3818-3834.

6 Li, H. & Zhou, H. (2012) 'Enhancing the performances of Li-ion batteries by carbon-coating: present and future', *Chem Commun (Camb)* 48, 1201-1217.

7 Goodenough, J. B. & Kim, Y. (2010) 'Challenges for Rechargeable Li Batteries†', *Chemistry of Materials* 22, 587-603.

8 Myung, S.-T., Amine, K. & Sun, Y.-K. (2010) 'Surface modification of cathode materials from nano- to microscale for rechargeable lithium-ion batteries', *Journal of Materials Chemistry* 20, 7074.

9 Lee, K. T. & Cho, J. (2011) 'Roles of nanosize in lithium reactive nanomaterials for lithium ion batteries', *Nano Today* 6, 28-41.

10 Winter, M. & Brodd, R. J. (2004) 'What are batteries, fuel cells, and supercapacitors?', *Chemical Reviews* 104, 4245-4269.

11 Logan, B. E., Hamelers, B., Rozendal, R. A., Schrorder, U., Keller, J., Freguia, S., Aelterman, P., Verstraete, W. & Rabaey, K. (2006) 'Microbial fuel cells: Methodology and technology', *Environmental Science & Technology* 40, 5181-5192.

12 Minh, N. Q. (1993) 'CERAMIC FUEL-CELLS', *Journal of the American Ceramic Society* 76, 563-588.

13 Springer, T. E., Zawodzinski, T. A. & Gottesfeld, S. (1991) 'POLYMER ELECTROLYTE FUEL-CELL MODEL', *Journal of the Electrochemical Society* 138, 2334-2342.

14 Steele, B. C. H. & Heinzel, A. (2001) 'Materials for fuel-cell technologies', *Nature* 414, 345-352.

15 Chau, K. T., Chan, C. C. & Liu, C. (2008) 'Overview of permanent-magnet brushless drives for electric and hybrid electric vehicles', *Ieee Transactions on Industrial Electronics* 55, 2246-2257.

16 Emadi, A., Lee, Y. J. & Rajashekara, K. (2008) 'Power electronics and motor drives in electric, hybrid electric, and plug-in hybrid electric vehicles', *Ieee Transactions on Industrial Electronics* 55, 2237-2245.

17 Moreno, J., Ortuzar, M. E. & Dixon, J. W. (2006) 'Energy-management system for a hybrid electric vehicle, using ultracapacitors and neural networks', *Ieee Transactions on Industrial Electronics* 53, 614-623.

18 Chan, C. C. (2002) 'The state of the art of electric and hybrid vehicles', *Proceedings of the Ieee* 90, 247-275.

19 Chan, C. C. (2007) 'The state of the art of electric, hybrid, and fuel cell vehicles', *Proceedings of the Ieee* 95, 704-718.

20 Haidar, A. M. A., Muttaqi, K. M. & Sutanto, D. (2014) 'Technical challenges for electric power industries due to grid-integrated electric vehicles in low voltage distributions: A review', *Energy Conversion and Management* 86, 689-700.

21 Waag, W., Fleischer, C. & Sauer, D. U. (2014) 'Critical review of the methods for monitoring of lithium-ion batteries in electric and hybrid vehicles', *Journal of Power Sources* 258, 321-339.

22 Garcia-Villalobos, J., Zamora, I., San Martin, J. I., Asensio, F. J. & Aperribay, V. (2014) 'Plug-in electric vehicles in electric distribution networks: A review of smart charging approaches', *Renewable & Sustainable Energy Reviews* 38, 717-731.

23 Mwasilu, F., Justo, J. J., Kim, E.-K., Ton Duc, D. & Jung, J.-W. (2014) 'Electric vehicles and smart grid interaction: A review on vehicle to grid and renewable energy sources integration', *Renewable & Sustainable Energy Reviews* 34, 501-516.

24 Qi, Z. (2014) 'Advances on air conditioning and heat pump system in electric vehicles - A review', *Renewable & Sustainable Energy Reviews* 38, 754-764.

25 Cao, Q., Zhang, H. P., Wang, G. J., Xia, Q., Wu, Y. P. & Wu, H. Q. (2007) 'A novel carbon-coated LiCoO2 as cathode material for lithium ion battery', *Electrochemistry Communications* 9, 1228-1232.

26 Ozawa, K. (1994) 'LITHIUM-ION RECHARGEABLE BATTERIES WITH LICOO2 AND CARBON ELECTRODES - THE LICOO2 C SYSTEM', *Solid State Ionics* 69, 212-221.

27 Hosono, E., Kudo, T., Honma, I., Matsuda, H. & Zhou, H. (2009) 'Synthesis of Single Crystalline Spinel LiMn2O4 Nanowires for a Lithium Ion Battery with High Power Density', *Nano Letters* 9, 1045-1051.

28 Kim, D. K., Muralidharan, P., Lee, H.-W., Ruffo, R., Yang, Y., Chan, C. K., Peng, H., Huggins, R. A. & Cui, Y. (2008) 'Spinel LiMn2O4 Nanorods as Lithium Ion Battery Cathodes', *Nano Letters* 8, 3948-3952.

29 Wang, J. & Sun, X. (2012) 'Understanding and recent development of carbon coating on LiFePO4 cathode materials for lithium-ion batteries', *Energy & Environmental Science* 5, 5163-5185.

30 Yuan, L.-X., Wang, Z.-H., Zhang, W.-X., Hu, X.-L., Chen, J.-T., Huang, Y.-H. & Goodenough, J. B. (2011) 'Development and challenges of LiFePO4 cathode material for lithium-ion batteries', *Energy & Environmental Science* 4, 269-284.

31 Huang, J. & Jiang, Z. (2008) 'The preparation and characterization of Li4Ti5O12/carbon nano-tubes for lithium ion battery', *Electrochimica Acta* 53, 7756-7759.

32 Kim, C., Yang, K. S., Kojima, M., Yoshida, K., Kim, Y. J., Kim, Y. A. & Endo, M. (2006) 'Fabrication of electrospinning-derived carbon nanofiber webs for the anode material of lithium-ion secondary batteries', *Advanced Functional Materials* 16, 2393-2397.

33 Qie, L., Chen, W.-M., Wang, Z.-H., Shao, Q.-G., Li, X., Yuan, L.-X., Hu, X.-L., Zhang, W.-X. & Huang, Y.-H. (2012) 'Nitrogen-Doped Porous Carbon Nanofiber Webs as Anodes for Lithium Ion Batteries with a Superhigh Capacity and Rate Capability', *Advanced Materials* 24, 2047-2050.

34 Wang, G., Shen, X., Yao, J. & Park, J. (2009) 'Graphene nanosheets for enhanced lithium storage in lithium ion batteries', *Carbon* 47, 2049-2053.

35 Yoo, E., Kim, J., Hosono, E., Zhou, H.-s., Kudo, T. & Honma, I. (2008) 'Large reversible Li storage of graphene nanosheet families for use in rechargeable lithium ion batteries', *Nano Letters* 8, 2277-2282.

36 Idota, Y., Kubota, T., Matsufuji, A., Maekawa, Y. & Miyasaka, T. (1997) 'Tin-based amorphous oxide: A high-capacity lithium-ion-storage material', *Science* 276, 1395-1397.

37 Poizot, P., Laruelle, S., Grugeon, S., Dupont, L. & Tarascon, J. M. (2000) 'Nano-sized transition-metaloxides as negative-electrode materials for lithium-ion batteries', *Nature* 407, 496-499.

38 Miyachi, M., Yamamoto, H., Kawai, H., Ohta, T. & Shirakata, M. (2005) 'Analysis of SiO anodes for lithium-ion batteries', *Journal of the Electrochemical Society* 152, A2089-A2091.

39 Kasavajjula, U., Wang, C. & Appleby, A. J. (2007) 'Nano- and bulk-silicon-based insertion anodes for lithium-ion secondary cells', *Journal of Power Sources* 163, 1003-1039.

40 Meethong, N., Kao, Y.-H., Speakman, S. A. & Chiang, Y.-M. (2009) 'Aliovalent Substitutions in Olivine Lithium Iron Phosphate and Impact on Structure and Properties', *Advanced Functional Materials* 19, 1060-1070.

41 Chen, J. J. & Whittingham, M. S. (2006) 'Hydrothermal synthesis of lithium iron phosphate', *Electrochemistry Communications* 8, 855-858.

42 Yang, S. F., Song, Y. N., Zavalij, P. Y. & Whittingham, M. S. (2002) 'Reactivity, stability and electrochemical behavior of lithium iron phosphates', *Electrochemistry Communications* 4, 239-244.

43 Yang, S. F., Zavalij, P. Y. & Whittingham, M. S. (2001) 'Hydrothermal synthesis of lithium iron phosphate cathodes', *Electrochemistry Communications* 3, 505-508.

44 Kim, J.-K., Choi, J.-W., Chauhan, G. S., Ahn, J.-H., Hwang, G.-C., Choi, J.-B. & Ahn, H.-J. (2008) 'Enhancement of electrochemical performance of lithium iron phosphate by controlled sol-gel synthesis', *Electrochimica Acta* 53, 8258-8264.

45 Wang, G. X., Bewlay, S. L., Konstantinov, K., Liu, H. K., Dou, S. X. & Ahn, J. H. (2004) 'Physical and electrochemical properties of doped lithium iron phosphate electrodes', *Electrochimica Acta* 50, 443-447.

46 Arnold, G., Garche, J., Hemmer, R., Strobele, S., Vogler, C. & Wohlfahrt-Mehrens, A. (2003) 'Fine-particle lithium iron phosphate LiFePO4 synthesized by a new low-cost aqueous precipitation technique', *Journal of Power Sources* 119, 247-251.

47 Jugovic, D. & Uskokovic, D. (2009) 'A review of recent developments in the synthesis procedures of lithium iron phosphate powders', *Journal of Power Sources* 190, 538-544.

48 Lee, J. & Teja, A. S. (2005) 'Characteristics of lithium iron phosphate (LiFePO4)particles synthesized in subcritical and supercritical water', *Journal of Supercritical Fluids* 35, 83-90.

49 Kim, H., Han, B., Choo, J. & Cho, J. (2008) 'Three-Dimensional Porous Silicon Particles for Use in High-Performance Lithium Secondary Batteries', *Angewandte Chemie-International Edition* 47, 10151-10154.

50 Ng, S.-H., Wang, J., Wexler, D., Konstantinov, K., Guo, Z.-P. & Liu, H.-K. (2006) 'Highly reversible lithium storage in spheroidal carbon-coated silicon

nanocomposites as anodes for lithium-ion batteries', *Angewandte Chemie-International Edition* 45, 6896-6899.

51 Graetz, J., Ahn, C. C., Yazami, R. & Fultz, B. (2003) 'Highly reversible lithium storage in nanostructured silicon', *Electrochemical and Solid State Letters* 6, A194-A197.

52 Obrovac, M. N. & Christensen, L. (2004) 'Structural changes in silicon anodes during lithium insertion/extraction', *Electrochemical and Solid State Letters* 7, A93-A96.

53 Hatchard, T. D. & Dahn, J. R. (2004) 'In situ XRD and electrochemical study of the reaction of lithium with amorphous silicon', *Journal of the Electrochemical Society* 151, A838-A842.

54 Cui, L.-F., Yang, Y., Hsu, C.-M. & Cui, Y. (2009) 'Carbon-Silicon Core-Shell Nanowires as High Capacity Electrode for Lithium Ion Batteries', *Nano Letters* 9, 3370-3374.

55 Song, T., Xia, J., Lee, J.-H., Lee, D. H., Kwon, M.-S., Choi, J.-M., Wu, J., Doo, S. K., Chang, H., Il Park, W., Zang, D. S., Kim, H., Huang, Y., Hwang, K.-C., Rogers, J. A. & Paik, U. (2010) 'Arrays of Sealed Silicon Nanotubes As Anodes for Lithium Ion Batteries', *Nano Letters* 10, 1710-1716.

56 Yao, Y., McDowell, M. T., Ryu, I., Wu, H., Liu, N., Hu, L., Nix, W. D. & Cui, Y. (2011) 'Interconnected Silicon Hollow Nanospheres for Lithium-Ion Battery Anodes with Long Cycle Life', *Nano Letters* 11, 2949-2954.

57 Chan, C. K., Peng, H., Liu, G., McIlwrath, K., Zhang, X. F., Huggins, R. A. & Cui, Y. (2008) 'High-performance lithium battery anodes using silicon nanowires', *Nature Nanotechnology* 3, 31-35.

58 Goriparti, S., Miele, E., De Angelis, F., Di Fabrizio, E., Proietti Zaccaria, R. & Capiglia, C. (2014) 'Review on recent progress of nanostructured anode materials for Li-ion batteries', *Journal of Power Sources* 257, 421-443.

59 Lestriez, B. (2010) 'Functions of polymers in composite electrodes of lithium ion batteries', *Comptes Rendus Chimie* 13, 1341-1350.

60 Park, M., Zhang, X., Chung, M., Less, G. B. & Sastry, A. M. (2010) 'A review of conduction phenomena in Li-ion batteries', *Journal of Power Sources* 195, 7904-7929.

61 Ling, M., Xu, Y., Zhao, H., Gu, X., Qiu, J., Li, S., Wu, M., Song, X., Yan, C., Liu, G. & Zhang, S. (2015) 'Dual-functional gum arabic binder for silicon anodes in lithium ion batteries', *Nano Energy* 12, 178-185.

62 Liu, G., Xun, S., Vukmirovic, N., Song, X., Olalde-Velasco, P., Zheng, H., Battaglia, V. S., Wang, L. & Yang, W. (2011) 'Polymers with tailored electronic structure for high capacity lithium battery electrodes', *Adv Mater* 23, 4679-4683.

63 Liu, G., Zheng, H., Song, X. & Battaglia, V. S. (2012) 'Particles and Polymer Binder Interaction: A Controlling Factor in Lithium-Ion Electrode Performance', *Journal of the Electrochemical Society* 159, A214-A221.

64 Cho, K. Y., Kwon, Y. I., Youn, J. R. & Song, Y. S. (2013) 'Interaction analysis between binder and particles in multiphase slurries', *Analyst* 138, 2044-2050.

65 Yoo, M., Frank, C. W., Mori, S. & Yamaguchi, S. (2003) 'Effect of poly(vinylidene fluoride) binder crystallinity and graphite structure on the mechanical strength of the composite anode in a lithium ion battery', *Polymer* 44, 4197-4204.

66 Markevich, E., Salitra, G. & Aurbach, D. (2005) 'Influence of the PVdF binder on the stability of LiCoO2 electrodes', *Electrochemistry Communications* 7, 1298-1304.

67 Seki, S., Tabata, S., Matsui, S. & Watanabe, M. (2004) 'Effect of binder polymer structures used in composite cathodes on interfacial charge transfer processes in lithium polymer batteries', *Electrochimica Acta* 50, 379-383.

68 Kaneko, M., Nakayama, M. & Wakihara, M. (2007) 'Lithium-ion conduction in elastomeric binder in Li-ion batteries', *Journal of Solid State Electrochemistry* 11, 1071-1076.

69 Wu, M., Xiao, X., Vukmirovic, N., Xun, S., Das, P. K., Song, X., Olalde-Velasco, P., Wang, D., Weber, A. Z., Wang, L.-W., Battaglia, V. S., Yang, W. & Liu, G. (2013) 'Toward an Ideal Polymer Binder Design for High-Capacity Battery Anodes', *Journal of the American Chemical Society* 135, 12048-12056.

70 Guy, D., Lestriez, B., Bouchet, R., Gaudefroy, V. & Guyomard, D. (2005) 'Tailoring the binder of composite electrode for battery performance optimization', *Electrochemical and Solid State Letters* 8, A17-A21.

71 Liu, G., Zheng, H., Kim, S., Deng, Y., Minor, A. M., Song, X. & Battaglia, V. S. (2008) 'Effects of Various Conductive Additive and Polymeric Binder Contents on the Performance of a Lithium-Ion Composite Cathode', *Journal of the Electrochemical Society* 155, A887.

72 Witker, D. & Curtis, M. D. (2006) 'Lithium ion and electronic conductivity in 3-(oligoethylene oxide)thiophene comb-like polymers', *Journal of Power Sources* 156, 525-532.

73 Javier, A. E., Patel, S. N., Hallinan, D. T., Jr., Srinivasan, V. & Balsara, N. P. (2011) 'Simultaneous electronic and ionic conduction in a block copolymer: application in lithium battery electrodes', *Angew Chem Int Ed Engl* 50, 9848-9851.

74 Zheng, H. H., Yang, R. Z., Liu, G., Song, X. Y. & Battaglia, V. S. (2012) 'Cooperation between Active Material, Polymeric Binder and Conductive Carbon Additive in Lithium Ion Battery Cathode', *Journal of Physical Chemistry C* 116, 4875-4882.

75 Li, C.-C. & Wang, Y.-W. (2011) 'Binder Distributions in Water-Based and Organic-Based LiCoO2 Electrode Sheets and Their Effects on Cell Performance', *Journal of the Electrochemical Society* 158, A1361.

76 Lee, J.-T., Chu, Y.-J., Peng, X.-W., Wang, F.-M., Yang, C.-R. & Li, C.-C. (2007) 'A novel and efficient water-based composite binder for LiCoO2 cathodes in lithium-ion batteries', *Journal of Power Sources* 173, 985-989.

77 Tran, B., Oladeji, I. O., Wang, Z., Calderon, J., Chai, G., Atherton, D. & Zhai, L. (2012) 'Thick LiCoO2/Nickel Foam Cathode Prepared by an Adhesive and Water-Soluble PEG-Based Copolymer Binder', *Journal of the Electrochemical Society* 159, A1928-A1933.

78 Xu, J., Chou, S.-L., Gu, Q.-f., Liu, H.-K. & Dou, S.-X. (2013) 'The effect of different binders on electrochemical properties of LiNi1/3Mn1/3C1/3O2 cathode material in lithium ion batteries', *Journal of Power Sources* 225, 172-178.

79 Wang, Z. L., Dupre, N., Gaillot, A. C., Lestriez, B., Martin, J. F., Daniel, L., Patoux, S. & Guyomard, D. (2012) 'CMC as a binder in LiNi0.4Mn1.6O4 5V

cathodes and their electrochemical performance for Li-ion batteries', *Electrochimica Acta* 62, 77-83.

80 Xue, Z., Zhang, Z. & Amine, K. (2013) 'Cross-linkable urethane acrylate oligomers as binders for lithium-ion battery', *Electrochemistry Communications* 34, 86-89.

81 Hu, S., Li, Y., Yin, J., Wang, H., Yuan, X. & Li, Q. (2014) 'Effect of different binders on electrochemical properties of LiFePO4/C cathode material in lithium ion batteries', *Chemical Engineering Journal* 237, 497-502.

82 Guerfi, A., Kaneko, M., Petitclerc, M., Mori, M. & Zaghib, K. (2007) 'LiFePO4 water-soluble binder electrode for Li-ion batteries', *Journal of Power Sources* 163, 1047-1052.

83 Cai, Z. P., Liang, Y., Li, W. S., Xing, L. D. & Liao, Y. H. (2009) 'Preparation and performances of LiFePO4 cathode in aqueous solvent with polyacrylic acid as a binder', *Journal of Power Sources* 189, 547-551.

84 Zhang, Z., Zeng, T., Qu, C., Lu, H., Jia, M., Lai, Y. & Li, J. (2012) 'Cycle performance improvement of LiFePO4 cathode with polyacrylic acid as binder', *Electrochimica Acta* 80, 440-444.

85 Chong, J., Xun, S., Zheng, H., Song, X., Liu, G., Ridgway, P., Wang, J. Q. & Battaglia, V. S. (2011) 'A comparative study of polyacrylic acid and poly(vinylidene difluoride) binders for spherical natural graphite/LiFePO4 electrodes and cells', *Journal of Power Sources* 196, 7707-7714.

86 Lux, S. F., Schappacher, F., Balducci, A., Passerini, S. & Winter, M. (2010) 'Low Cost, Environmentally Benign Binders for Lithium-Ion Batteries', *Journal of the Electrochemical Society* 157, A320-A325.

87 Li, C.-C. & Lin, Y.-S. (2012) 'Interactions between organic additives and active powders in water-based lithium iron phosphate electrode slurries', *Journal of Power Sources* 220, 413-421.

88 Jung-Min, O., Geiculescu, O., DesMarteau, D. & Creager, S. (2011) 'Ionomer Binders Can Improve Discharge Rate Capability in Lithium-Ion Battery Cathodes', *Journal of the Electrochemical Society* 158, A207-A213.

89 Pejovnik, S., Dominko, R., Bele, M., Gaberscek, M. & Jamnik, J. (2008) 'Electrochemical binding and wiring in battery materials', *Journal of Power Sources* 184, 593-597.

90 Zhian, Z., Tao, Z., Yanqing, L., Ming, J. & Jie, L. (2014) 'A comparative study of different binders and their effects on electrochemical properties of LiMn 2O 4 cathode in lithium ion batteries', *Journal of Power Sources* 247, 1-8.

91 Guy, D., Lestriez, B., Bouchet, R. & Guyomard, D. (2006) 'Critical Role of Polymeric Binders on the Electronic Transport Properties of Composites Electrode', *Journal of the Electrochemical Society* 153, A679.

92 Drofenik, J., Gaberscek, M., Dominko, R., Poulsen, F. W., Mogensen, M., Pejovnik, S. & Jamnik, J. (2003) 'Cellulose as a binding material in graphitic anodes for Li ion batteries: a performance and degradation study', *Electrochimica Acta* 48, 883-889.

93 El Ouatani, L., Dedryvère, R., Ledeuil, J. B., Siret, C., Biensan, P., Desbrières, J. & Gonbeau, D. (2009) 'Surface film formation on a carbonaceous electrode: Influence of the binder chemistry', *Journal of Power Sources* 189, 72-80.

94 Courtel, F. M., Niketic, S., Duguay, D., Abu-Lebdeh, Y. & Davidson, I. J. (2011) 'Water-soluble binders for MCMB carbon anodes for lithium-ion batteries', *Journal of Power Sources* 196, 2128-2134.

95 Yen, J. P., Lee, C. M., Wu, T. L., Wu, H. C., Su, C. Y., Wu, N. L. & Hong, J. L. (2012) 'Enhanced High-Temperature Cycle-Life of Mesophase Graphite Anode with Styrene-Butadiene Rubber/Carboxymethyl Cellulose Binder', *ECS Electrochemistry Letters* 1, A80-A82.

96 Jabbour, L., Gerbaldi, C., Chaussy, D., Zeno, E., Bodoardo, S. & Beneventi, D. (2010) 'Microfibrillated cellulose–graphite nanocomposites for highly flexible paper-like Li-ion battery electrodes', *Journal of Materials Chemistry* 20, 7344.

97 Komaba, S., Okushi, K., Ozeki, T., Yui, H., Katayama, Y., Miura, T., Saito, T. & Groult, H. (2009) 'Polyacrylate Modifier for Graphite Anode of Lithium-Ion Batteries', *Electrochemical and Solid-State Letters* 12, A107.

98 Ui, K., Towada, J., Agatsuma, S., Kumagai, N., Yamamoto, K., Haruyama, H., Takeuchi, K. & Koura, N. (2011) 'Influence of the binder types on the electrochemical characteristics of natural graphite electrode in room-temperature ionic liquid', *Journal of Power Sources* 196, 3900-3905.

99 Komaba, S., Ozeki, T., Yabuuchi, N. & Shimomura, K. (2011) 'Polyacrylate as Functional Binder for Silicon and Graphite Composite Electrode in Lithium-Ion Batteries', *Electrochemistry* 79, 6-9.

100 Fransson, L., Eriksson, T., Edstrom, K., Gustafsson, T. & Thomas, J. O. (2001) 'Influence of carbon black and binder on Li-ion batteries', *Journal of Power Sources* 101, 1-9.

101 Zhang, S. S., Xu, K. & Jow, T. R. (2003) 'Poly(acrylonitrile-methyl methacrylate) as a non-fluorinated binder for the graphite anode of Li-ion batteries', *Journal of Applied Electrochemistry* 33, 1099-1101.

102 Zhang, S. S., Xu, K. & Jow, T. R. (2004) 'Evaluation on a water-based binder for the graphite anode of Li-ion batteries', *Journal of Power Sources* 138, 226-231.

103 Ohta, N., Sogabe, T. & Kuroda, K. (2001) 'A novel binder for the graphite anode of rechargeable lithium ion batteries for the improvement of reversible capacity', *Carbon* 39, 1434-1436.

104 Hye-Kyoung, P., Byung-Seon, K. & Eun-Suok, O. (2011) 'Effect of high adhesive polyvinyl alcohol binder on the anodes of lithium ion batteries', *Electrochemistry Communications* 13, 1051-1053.

105 Qiu, J. X., Zhang, P., Ling, M., Li, S., Liu, P. R., Zhao, H. J. & Zhang, S. Q. (2012) 'Photocatalytic Synthesis of TiO2 and Reduced Graphene Oxide Nanocomposite for Lithium Ion Battery', *Acs Applied Materials & Interfaces* 4, 3636-3642.

106 Arico, A. S., Bruce, P., Scrosati, B., Tarascon, J. M. & Van Schalkwijk, W. (2005) 'Nanostructured materials for advanced energy conversion and storage devices', *Nature Materials* 4, 366-377.

107 Aurbach, D. (2000) 'Review of selected electrode-solution interactions which determine the performance of Li and Li ion batteries', *Journal of Power Sources* 89, 206-218.

108 Kasavajjula, U., Wang, C. S. & Appleby, A. J. (2007) 'Nano- and bulk-silicon-based insertion anodes for lithium-ion secondary cells', *Journal of Power Sources* 163, 1003-1039.

109 Cui, L.-F., Ruffo, R., Chan, C. K., Peng, H. & Cui, Y. (2009) 'Crystalline-Amorphous Core-Shell Silicon Nanowires for High Capacity and High Current Battery Electrodes', *Nano Letters* 9, 491-495.

110 Park, M.-H., Kim, M. G., Joo, J., Kim, K., Kim, J., Ahn, S., Cui, Y. & Cho, J. (2009) 'Silicon Nanotube Battery Anodes', *Nano Letters* 9, 3844-3847.

111 Liu, N., Wu, H., McDowell, M. T., Yao, Y., Wang, C. & Cui, Y. (2012) 'A Yolk-Shell Design for Stabilized and Scalable Li-Ion Battery Alloy Anodes', *Nano Letters* 12, 3315-3321.

112 Magasinski, A., Dixon, P., Hertzberg, B., Kvit, A., Ayala, J. & Yushin, G. (2010) 'High-performance lithium-ion anodes using a hierarchical bottom-up approach', *Nature Materials* 9, 353-358.

113 Guo, J. & Wang, C. (2010) 'A polymer scaffold binder structure for high capacity silicon anode of lithium-ion battery', *Chemical Communications* 46, 1428-1430.

114 Xu, Y., Yin, G., Ma, Y., Zuo, P. & Cheng, X. (2010) 'Simple annealing process for performance improvement of silicon anode based on polyvinylidene fluoride binder', *Journal of Power Sources* 195, 2069-2073.

115 Magasinski, A., Zdyrko, B., Kovalenko, I., Hertzberg, B., Burtovyy, R., Huebner, C. F., Fuller, T. F., Luzinov, I. & Yushin, G. (2010) 'Toward Efficient Binders for Li-Ion Battery Si-Based Anodes: Polyacrylic Acid', *Acs Applied Materials & Interfaces* 2, 3004-3010.

116 Komaba, S., Shimomura, K., Yabuuchi, N., Ozeki, T., Yui, H. & Konno, K. (2011) 'Study on Polymer Binders for High-Capacity SiO Negative Electrode of Li-Ion Batteries', *Journal of Physical Chemistry C* 115, 13487-13495.

117 Han, Z. J., Yabuuchi, N., Hashimoto, S., Sasaki, T. & Komaba, S. (2012) 'Cross-Linked Poly(acrylic acid) with Polycarbodiimide as Advanced Binder for Si/Graphite Composite Negative Electrodes in Li-Ion Batteries', *ECS Electrochemistry Letters* 2, A17-A20.

118 Bonjae, K., Hyunjung, K., Younghyun, C., Kyu Tae, L., Nam-Soon, C. & Jaephil, C. (2012) 'A Highly Cross-Linked Polymeric Binder for High-Performance Silicon Negative Electrodes in Lithium Ion Batteries', *Angewandte Chemie International Edition* 51, 8762-8767.

119 Park, Y., Lee, S., Kim, S.-H., Jang, B. Y., Kim, J. S., Oh, S. M., Kim, J.-Y., Choi, N.-S., Lee, K. T. & Kim, B.-S. (2013) 'A photo-cross-linkable polymeric binder for silicon anodes in lithium ion batteries', *Rsc Advances* 3, 12625-12630.

120 Chen, L. B., Xie, X. H., Xie, J. Y., Wang, K. & Yang, J. (2006) 'Binder effect on cycling performance of silicon/carbon composite anodes for lithium ion batteries', *Journal of Applied Electrochemistry* 36, 1099-1104.

121 Li, T., Yang, J.-y. & Lu, S.-g. (2012) 'Effect of modified elastomeric binders on the electrochemical properties of silicon anodes for lithium-ion batteries', *International Journal of Minerals Metallurgy and Materials* 19, 752-756.

122 Li, J., Lewis, R. B. & Dahn, J. R. (2007) 'Sodium carboxymethyl cellulose - A potential binder for Si negative electrodes for Li-ion batteries', *Electrochemical and Solid State Letters* 10, A17-A20.

123 Lestriez, B., Bahri, S., Sandu, I., Roue, L. & Guyomard, D. (2007) 'On the binding mechanism of CMC in Si negative electrodes for Li-ion batteries', *Electrochemistry Communications* 9, 2801-2806.

124 Bridel, J. S., Azaïs, T., Morcrette, M., Tarascon, J. M. & Larcher, D. (2010) 'Key Parameters Governing the Reversibility of Si/Carbon/CMC Electrodes for Li-Ion Batteries†', *Chemistry of Materials* 22, 1229-1241.

125 Guo, J. C. & Wang, C. S. (2010) 'A polymer scaffold binder structure for high capacity silicon anode of lithium-ion battery', *Chemical Communications* 46, 1428-1430.

126 Wei-Ren, L., Mo-Hua, Y., Hung-Chun, W., Chiao, S. M. & Nae-Lih, W. (2005) 'Enhanced cycle life of Si anode for Li-ion batteries by using modified elastomeric binder', *Electrochemical and Solid-State Letters* 8, A100-A103.

127 Cui, L.-F., Hu, L., Wu, H., Choi, J. W. & Cui, Y. (2011) 'Inorganic Glue Enabling High Performance of Silicon Particles as Lithium Ion Battery Anode', *Journal of the Electrochemical Society* 158, A592.

128 Komaba, S., Yabuuchi, N., Ozeki, T., Han, Z. J., Shimomura, K., Yui, H., Katayama, Y. & Miura, T. (2012) 'Comparative Study of Sodium Polyacrylate and Poly(vinylidene fluoride) as Binders for High Capacity Si-Graphite Composite Negative Electrodes in Li-Ion Batteries', *Journal of Physical Chemistry C* 116, 1380-1389.

129 Bae, J., Cha, S.-H. & Park, J. (2013) 'A new polymeric binder for silicon-carbon nanotube composites in lithium ion battery', *Macromolecular Research* 21, 826-831.

130 Jung Sub, K., Wonchang, C., Kyu Young, C., Dongjin, B., JongChoo, L. & Joong Kee, L. (2013) 'Effect of polyimide binder on electrochemical characteristics of surface-modified silicon anode for lithium ion batteries', *Journal of Power Sources* 244, 521-526.

131 Chou, S. L., Wang, J. Z., Liu, H. K. & Dou, S. X. (2011) 'Rapid Synthesis of Li4Ti5O12 Microspheres as Anode Materials and Its Binder Effect for Lithium-Ion Battery', *Journal of Physical Chemistry C* 115, 16220-16227.

132 Kim, G. T., Jeong, S. S., Joost, M., Rocca, E., Winter, M., Passerini, S. & Balducci, A. (2011) 'Use of natural binders and ionic liquid electrolytes for greener and safer lithium-ion batteries', *Journal of Power Sources* 196, 2187-2194.

133 Lee, B.-R. & Oh, E.-S. (2013) 'Effect of Molecular Weight and Degree of Substitution of a Sodium-Carboxymethyl Cellulose Binder on Li4Ti5O12Anodic Performance', *The Journal of Physical Chemistry C* 117, 4404-4409.

134 Tran, B., Oladeji, I. O., Wang, Z., Calderon, J., Chai, G., Atherton, D. & Zhai, L. (2013) 'Adhesive PEG-based binder for aqueous fabrication of thick Li4Ti5O12 electrode', *Electrochimica Acta* 88, 536-542.

135 Gong, L., Nguyen, M. H. T. & Oh, E. S. (2013) 'High polar polyacrylonitrile as a potential binder for negative electrodes in lithium ion batteries', *Electrochemistry Communications* 29, 45-47.

136 Liu, G. C., Shen, X. X., Ui, K., Wang, L. D. & Kumagai, N. (2012) 'Influence of the binder types on the electrochemical characteristics of tin nanoparticle negative electrode for lithium secondary batteries', *Journal of Power Sources* 217, 108-113.

137 Chou, S. L., Wang, J. Z., Zhong, C., Rahman, M. M., Liu, H. K. & Dou, S. X. (2009) 'A facile route to carbon-coated SnO2 nanoparticles combined with a new binder for enhanced cyclability of Li-ion rechargeable batteries', *Electrochimica Acta* 54, 7519-7524.

138 Chou, S. L., Gao, X. W., Wang, J. Z., Wexler, D., Wang, Z. X., Chen, L. Q. & Liu, H. K. (2011) 'Tin/polypyrrole composite anode using sodium carboxymethyl cellulose binder for lithium-ion batteries', *Dalton Transactions* 40, 12801-12807.

139 Mancini, M., Nobili, F., Tossici, R. & Marassi, R. (2012) 'Study of the electrochemical behavior at low temperatures of green anodes for Lithium ion batteries prepared with anatase TiO2 and water soluble sodium carboxymethyl cellulose binder', *Electrochimica Acta* 85, 566-571.

140 Moretti, A., Kim, G.-T., Bresser, D., Renger, K., Paillard, E., Marassi, R., Winter, M. & Passerini, S. (2013) 'Investigation of different binding agents for nanocrystalline anatase TiO2 anodes and its application in a novel, green lithium-ion battery', *Journal of Power Sources* 221, 419-426.

141 Mancini, M., Nobili, F., Tossici, R., Wohlfahrt-Mehrens, M. & Marassi, R. (2011) 'High performance, environmentally friendly and low cost anodes for lithium-ion battery based on TiO2 anatase and water soluble binder carboxymethyl cellulose', *Journal of Power Sources* 196, 9665-9671.

142 Trofimov, B. A., Morozova, L. V., Markova, M. V., Mikhaleva, A. I., Myachina, G. F., Tatarinova, I. V. & Skotheim, T. A. (2006) 'Vinyl ethers with polysulfide and hydroxyl functions and polymers therefrom as binders for lithium-sulfur batteries', *Journal of Applied Polymer Science* 101, 4051-4055.

143 Huang, Y., Sun, J., Wang, W., Wang, Y., Yu, Z., Zhang, H., Wang, A. & Yuan, K. (2008) 'Discharge Process of the Sulfur Cathode with a Gelatin Binder', *Journal of the Electrochemical Society* 155, A764.

144 Sun, J., Huang, Y. Q., Wang, W. K., Yu, Z. B., Wang, A. B. & Yuan, K. G. (2008) 'Application of gelatin as a binder for the sulfur cathode in lithium-sulfur batteries', *Electrochimica Acta* 53, 7084-7088.

145 Wang, Y., Huang, Y., Wang, W., Huang, C., Yu, Z., Zhang, H., Sun, J., Wang, A. & Yuan, K. (2009) 'Structural change of the porous sulfur cathode using gelatin as a binder during discharge and charge', *Electrochimica Acta* 54, 4062-4066.

146 Zhang, W., Huang, Y., Wang, W., Huang, C., Wang, Y., Yu, Z. & Zhang, H. (2010) 'Influence of pH of Gelatin Solution on Cycle Performance of the Sulfur Cathode', *Journal of the Electrochemical Society* 157, A443.

147 He, M., Yuan, L.-X., Zhang, W.-X., Hu, X.-L. & Huang, Y.-H. (2011) 'Enhanced Cyclability for Sulfur Cathode Achieved by a Water-Soluble Binder', *The Journal of Physical Chemistry C* 115, 15703-15709.

148 Zhang, Z., Bao, W., Lu, H., Jia, M., Xie, K., Lai, Y. & Li, J. (2012) 'Water-Soluble Polyacrylic Acid as a Binder for Sulfur Cathode in Lithium-Sulfur Battery', *ECS Electrochemistry Letters* 1, A34-A37.

149 Jiulin, W., Zhendong, Y., Monroe, C. W., Jun, Y. & Nuli, Y. (2013) 'Carbonyl-beta-cyclodextrin as a novel binder for sulfur composite cathodes in rechargeable lithium batteries', *Advanced Functional Materials* 23, 1194-1201.

150 Murase, M., Yabuuchi, N., Han, Z.-J., Son, J.-Y., Cui, Y.-T., Oji, H. & Komaba, S. (2012) 'Crop-Derived Polysaccharides as Binders for High-Capacity Silicon/Graphite-Based Electrodes in Lithium-Ion Batteries', *Chemsuschem* 5, 2307-2311.

151 Chai, L., Qu, Q., Zhang, L., Shen, M., Zhang, L. & Zheng, H. (2013) 'Chitosan, a new and environmental benign electrode binder for use with graphite anode in lithium-ion batteries', *Electrochimica Acta* 105, 378-383.

152 Kovalenko, I., Zdyrko, B., Magasinski, A., Hertzberg, B., Milicev, Z., Burtovyy, R., Luzinov, I. & Yushin, G. (2011) 'A major constituent of brown algae for use in high-capacity Li-ion batteries', *Science* 334, 75-79.

153 Ling, M., Xu, Y., Zhao, H., Gu, X., Qiu, J., Li, S., Wu, M., Song, X., Yan, C., Liu, G. & Zhang, S. (2015) 'Dual-functional gum arabic binder for silicon anodes in lithium ion batteries', *Nano Energy* 12, 178-185.

154 Song, J., Zhou, M., Yi, R., Xu, T., Gordin, M. L., Tang, D., Yu, Z., Regula, M. & Wang, D. (2014) 'Interpenetrated Gel Polymer Binder for High-Performance Silicon Anodes in Lithium-ion Batteries', *Advanced Functional Materials* 24, 5904-5910.

155 Ryou, M. H., Kim, J., Lee, I., Kim, S., Jeong, Y. K., Hong, S., Ryu, J. H., Kim, T. S., Park, J. K., Lee, H. & Choi, J. W. (2013) 'Mussel-Inspired Adhesive Binders for High-Performance Silicon Nanoparticle Anodes in Lithium-Ion Batteries', *Advanced Materials* 25, 1571-1576.

156 Wang, C., Wu, H., Chen, Z., McDowell, M. T., Cui, Y. & Bao, Z. (2013) 'Self-healing chemistry enables the stable operation of silicon microparticle anodes for high-energy lithium-ion batteries', *Nature Chemistry* 5, 1043-1049.

157 Minh Hien Thi, N. & Oh, E.-S. (2013) 'Application of a new acrylonitrile/butylacrylate water-based binder for negative electrodes of lithium-ion batteries', *Electrochemistry Communications* 35, 45-48.

158 Ling, M., Zhao, H., Xiaoc, X., Shi, F., Wu, M., Qiu, J., Li, S., Song, X., Liu, G. & Zhang, S. (2014) 'Low cost and environmentally benign crack-blocking

structures for long life and high power Si electrodes in lithium ion batteries', *J. Mater. Chem. A* 3, 2036-2042.

CHAPTER 2: AN ENVIRONMENTALLY BENIGN LIB FABRICATION PROCESS USING A LOW COST, WATER SOLUBLE AND EFFICIENT BINDER

Journal of Materials Chemistry A 2013, 1, 11543−11547

STATEMENT OF CONTRIBUTION TO CO-AUTHORED PUBLISHED PAPER

This chapter includes a co-authored paper. The bibliographic details of the co-authored paper, including all authors, are:

Min Ling, Jingxia Qiu, Sheng Li, Hui Zhao, Gao Liu* and Shanqing Zhang*

An Environmentally benign LIB fabrication process using a low cost, water soluble and efficient binder

Published in *Journal of Materials Chemistry A* 2013, 1, 11543−11547

My contribution to the paper involved:

Experimental design and implementation;

Collection and analysis of data;

Preparation of manuscript.

(Signed) _____ (Date)_____

Name of Student: Min Ling

(Countersigned) _____ (Date)_____
Corresponding author of paper: Shanqing Zhang

(Countersigned) _____ (Date)_____
Supervisor: Shanqing Zhang

Pages 97-109 of this chapter which consists of the published paper, "An Environmentally benign LIB fabrication process using a low cost, water soluble and efficient binder" have been removed from this copy for copyright reasons.

CHAPTER 3: DUAL-FUNCTIONAL GUM ARABIC BINDER FOR SILICON ANODES IN LITHIUM ION BATTERIES

Nano Energy, 2013, doi: 10.1016/j.nanoen.2014.12.011

STATEMENT OF CONTRIBUTION TO CO-AUTHORED PUBLISHED PAPER

This chapter includes a co-authored paper. The bibliographic details of the co-authored paper, including all authors, are:

Min Ling, Yanan Xu, Hui Zhao, Xingxing Gu, Jingxia Qiu, Sheng Li, Mingyan Wu, Xiangyun Song, Cheng Yan, Gao Liu* and Shanqing Zhang*

Dual-functional gum Arabic binder for silicon anodes in lithium ion batteries

Published in *Nano Energy, 2013, doi: 10.1016/j.nanoen.2014.12.011*

My contribution to the paper involved:

Initial concept, experimental design and implementation;

Collection and analysis of data;

Preparation of manuscript.

(Signed) _____ (Date)_____

Name of Student: Min Ling

(Countersigned) _____ (Date)_____
Corresponding author of paper: Shanqing Zhang

(Countersigned) _____ (Date)_____
Supervisor: Shanqing Zhang

Pages 112-135 of this chapter which consists of the published paper, "Dual-functional gum Arabic binder for silicon anodes in lithium ion batteries" have been removed from this copy for copyright reasons.

CHAPTER 4: ACACIA SENEGAL INSPIRED BI-FUNCTIONAL BINDER FOR LONGEVITY OF LITHIUM SULFUR BATTERIES

4.1. Introduction

Lithium-ion batteries (LIBs) have been successfully commercialized and widely used in portable electronics.[1,2] The demands for high energy density with low cost, however, prohibits their large-scale applications in the rapidly expanding market of electric vehicles.[3] Lithium-sulfur (Li-S) batteries, which have a theoretical energy density five times higher than that of Li-ion batteries (2,500 vs. 500 Wh/kg), could meet these needs while significantly reducing battery cost. For this reason, the combination of lithium and sulfur has been considered as one of the most promising battery chemistries for the full electrification of vehicles.[4-6] Li-S batteries however, also have critical flaws, including the insulating properties of sulfur and its discharge products, a ca. 76% volume change cycling from sulfur (S) to lithium sulfide (Li_2S), and polysulfide shuttles that transport sulfur species back and forth between electrodes. These lead to the destruction of sulfur cathodes and the corrosion of lithium anodes resulting in short battery life.

In traditional Li-S cells, a typical sulfur electrode consists of three components, i.e. the electrochemically active sulfur material, the conductive carbon additive, and the polymeric binder.[7,8] Through the syntheses of nano-architectured carbon additives, the electrochemical performance and cycle life of Li-S batteries have been successfully improved.[9-13] These nano-carbon additives improve the insulating properties of the sulfur electrode as well as physically and/or chemically secure sulfur species in the cathode. Though effective, to date most research activities have focused on the synthesis of nanostructured carbon/sulfur composites; while less attention has been devoted to the electrically inactive components of the sulfur electrode, such as the binder. Recent studies however, show that important characteristics of the Si anode in Li-ion batteries, such as high initial reversible capacity and excellent

cyclability, are greatly dependent on the binder's ability to buffer up to 300% volume change and maintain electrode integrity.[14-17] In comparison, the sulfur electrode in Li-S batteries exhibits its own characteristic volume change during cycling with two opposing volume change during cycling, i.e. ca. 76% volume expansion during cycling of S to Li_2S and volume shrinkage of the polysulfide dissolution into liquid electrolyte. Moreover, the dissolved polysulfides migrate from the sulfur cathode to the lithium anode, where the sulfur electrochemically reacts with the metallic Li anode subsequently leading to poor cyclability. Overall, binders play a critically important role in maintaining electrode integrity and retaining sulfur species during Li-S battery cycling.

Polyvinylidene fluoride (PVDF) is widely used as the binder in state-of-the-art LIBs. When introduced from Li-ion to Li-S systems, the electrochemical performance of Li-S cells is far from satisfactory due to the relatively poor adhesion strength of PVDF.[18] Furthermore, the rapid decline of non-regenerable resources has triggered the adoption of environmentally friendly, sustainable bio-derived materials for energy storage devices.[19,20] These bio-derived binders are usually water-soluble and have the additional advantages of enhanced safety and low cost. For example, sodium alginates (Na-alginates) are a promising bio-derived polymer binder for the Si anode in Li-ion batteries.[21] Sulfur cathodes with alginate as a binder also exhibit better cyclability than those using PVDF binders.[22] Other bio-derived polymers, including gelatin,[23,24] sodium carboxyl methyl cellulose (CMC),[25] and carbonyl-β-cyclodextrin (CβC),[26] also have promising characteristics as green binders for sulfur cathodes i.e. lower electronic and ionic resistance and better mass transport kinetics.

Despite the aforementioned advantages, bio-derived aqueous polymer binders have not been used in Li-S batteries and the relevant mechanisms have not been

investigated. Generally these polymers have high functional group content such as hydroxyl, carbonyl, and carboxylic groups. In this study we report on a new bio-derived polymer binder, i.e. gum arabic (GA), for high performance Li-S cells. This aqueous polymer binder has excellent binding strength, good ductility, and wide electrochemical windows for sulfur cathodes. An outstanding cycling performance, i.e. 843 mAh/g at *C*/5 and 503 mAh/g at 1 *C* after 500 cycles, is achieved due to the bi-functionalities of the GA binder. The good mechanical properties of GA help accommodate volume change and preserve electrode integrity during cycling, while its functional groups chemically retain sulfur species and inhibit the polysulfide from shuttling, thereby improving the longevity of Li-S cells. To the best of our knowledge, the GA binder has the best cycling performance when compared with previously bio-derived and non-bio-derived aqueous binders in Li-S batteries. More importantly, we demonstrate for the first time the important role of the binder, due to its physical and chemical properties, in the preparation of high-performance Li-S cells.

4.2. Results and discussion

GA is a nontoxic natural polymer extracted from *Acacia senegal*, a deciduous legume in Northeast Africa that is widely used in food and medicine as a soluble dietary fibre. GA has abundant functional groups, confirmed by XPS and FTIR spectroscopy (Figure 4.1). The XPS spectrum in Figure 4.1a shows sharp 1s peaks at 532 and 286 eV, which provide strong evidence of elemental O and C, respectively.[27] The FTIR spectroscopy supports molecular geometry for the functional groups of GA (Figure 4.1b). The broad and strong peaks located at 3,406 and 2,934 cm^{-1} are attributed to the stretching vibrations of O-H and C-H bond. The peak at 1,258 cm^{-1} is

related to the O-C-H deformation of pyranose rings; and the peaks at 1,628, 1,420, and 1,072 cm^{-1} are from the symmetric/asymmetric vibrations of O-C-O bonds. Additional weak absorption peaks appearing at the low frequency range of 900-500 cm^{-1} are ascribed to C-O and C-O-C symmetric/asymmetric vibrations.[28,29] The FTIR spectrum exhibits the features of a polysaccharide, which is the main component of GA. As a result, the molecular structure of GA can be described as backbone units of (1, 3)-linked D-galactopyranose, with side units of d-galactopyranose, D-glucuronic acid, and L-arabofuranose (Figure 4.1c).[28,30]

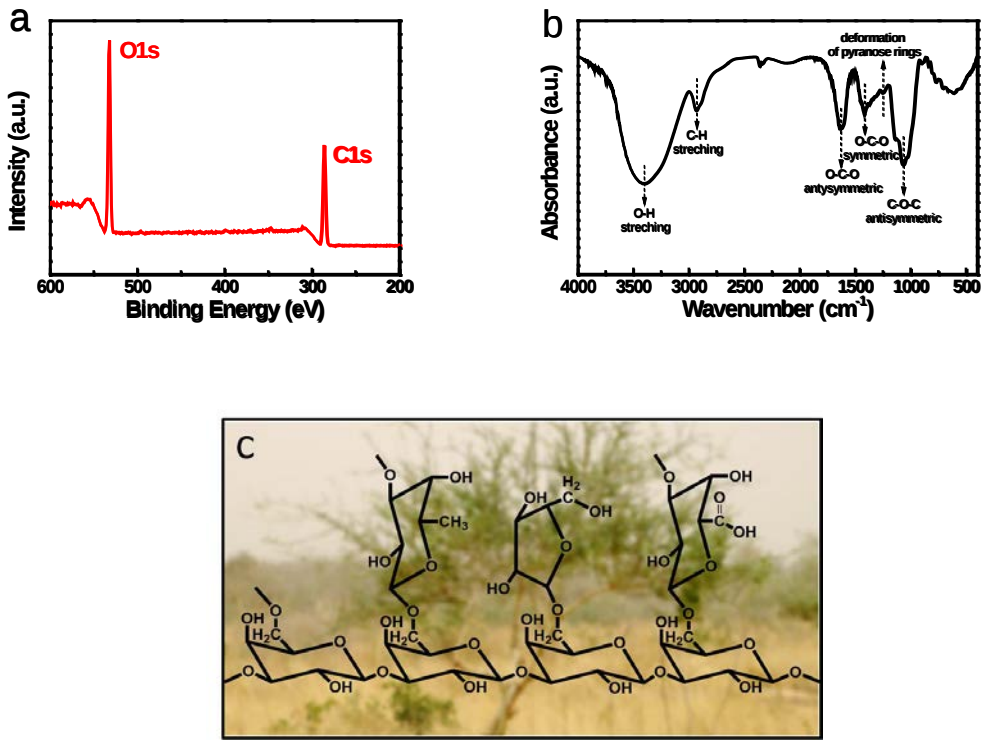

Figure 4.1 Characterization of aqueous polymer GA. (a) XPS and (b) FTIR spectra of GA. (c) Proposed chemical structure of GA with the background of *Acacia senegal*.

In this work, GA was used as a green binder for sulfur cathode in Li-S batteries. Before utilization, the electrochemical stability of GA was evaluated by cyclic voltammetry (CV) at 0.1 mV/s within the voltage window of 1.5-3.0 V (vs. Li/Li^{+}).

The results in Figure S4.1 confirm its high electrochemical stability for application in Li-S cells. In the Li-S cells, the sulfur cathode was fabricated using sulfur powder as the active material, super P carbon as the conductive additive, and GA as the binder. Figure 4.2a shows the charge/discharge profile of the sulfur electrode with the GA binder (S@GA) within the voltage window of 1.8-2.6 V at *C*/5 (1 *C* = 1,675 mA/g). This sulfur electrode shows a typical two-plateau discharge curve in conventional Li-S cells, i.e. the formation of soluble long-chain polysulfides (Li_2S_x, $4 \leq x \leq 8$) at ~2.3 V and insoluble short-chain Li_2S_2/Li_2S at ~2.1 V. The redox peaks in Figure 4.2b conform well to the plateaus in the charge/discharge profile. When scanning forwards, the oxidation peak near 2.4 V is caused by the transformation of sulfur species to Li_2S_x ($x>2$). When scanning backwards, two clear reduction peaks are found: one is ca. 2.3 V representing the transformation of S to higher-order Li_2S_x ($4 \leq x \leq 8$), and the other at ca. 2.1 V caused by the further reduction of higher-order lithium polysulfides to lower-order Li_2S_x ($x \leq 4$), and to Li_2S.

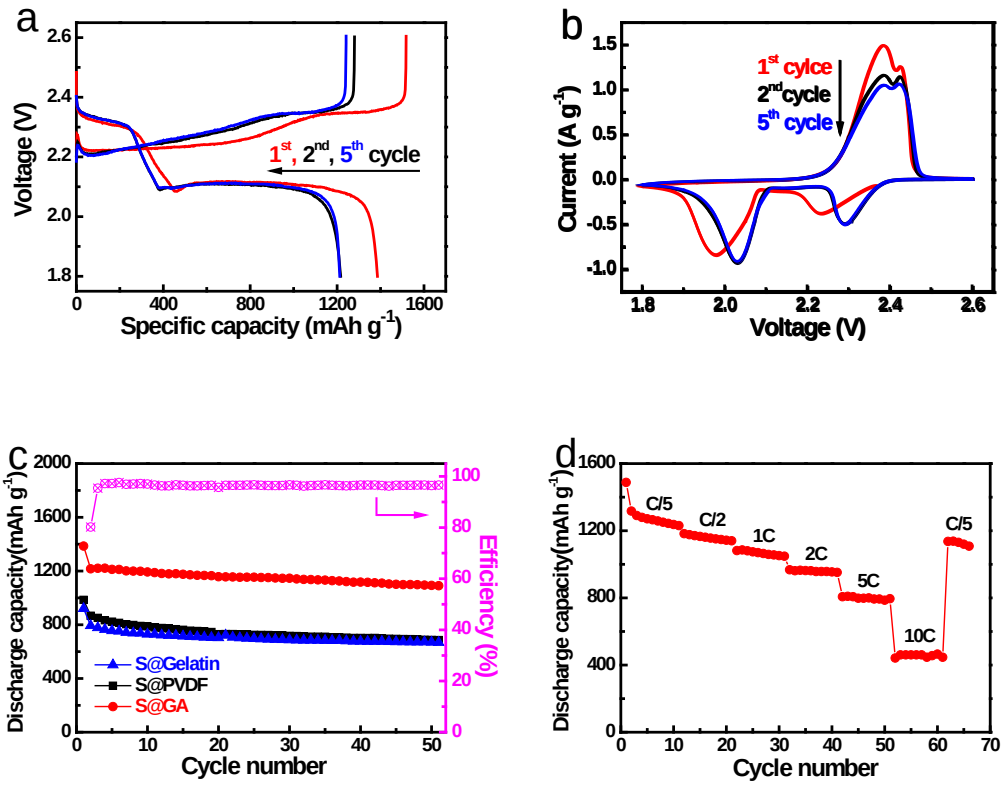

Figure 4.2 Electrochemical performances of sulfur electrodes with different binders. (a) the charge-discharge profiles of the S@GA electrode at *C*/5, (b) The cyclic voltammograms of the S@GA electrode in the voltage range of 1.8-2.6 V vs. Li/Li^+ at 0.1 mV/s,. (c) the cycling performance of the S@GA, S@PVDF, and S@gelatin electrodes and the Coulombic efficiency of the S@GA electrode at *C*/5, and (d) The discharge capacities of the S@GA electrode at various *C* rates.

The cycling performance of the sulfur electrode with PVDF (S@PVDF) and gelatin (S@gelatin) as binders was also tested under the same conditions as shown in Figure 4.2c. The S@GA electrode delivered an initial discharge capacity as high as 1386 mAh/g (normalized to S), which is nearly 82.7% of its theoretical maximum (1675 mAh/g). This is much higher than the S@PVDF (984 mAh/g) or S@gelatin (921 mAh/g) electrodes. After 50 deep charge/discharges, a reversible discharge capacity of 1090 mAh/g was obtained for the S@GA electrode with a fading rate of 0.2% per cycle after the second cycle. The capacities of the S@PVDF and S@gelatin electrodes quickly decrease to ca. 668 mAh/g. The GA binder therefore demonstrates higher sulfur utilization and better capacity retention than the conventional binders such as PVDF and gelatin. In addition to high capacity, the S@GA cathode maintained a high Coulombic efficiency of >95% during the whole cycling. The rate capability of the S@GA cathode is shown in Figure 4.2d. A highly reversible capacity of 952 mAh/g was obtained at 2 *C*, while 460 mAh/g could still be achieved when the *C* rate was as high as 10*C*. The capacity recovered to 1108 mAh/g when the *C* rate was switched back to *C*/5, indicating excellent electrode integrity and fast reaction kinetics in the S@GA electrode.[31,32]

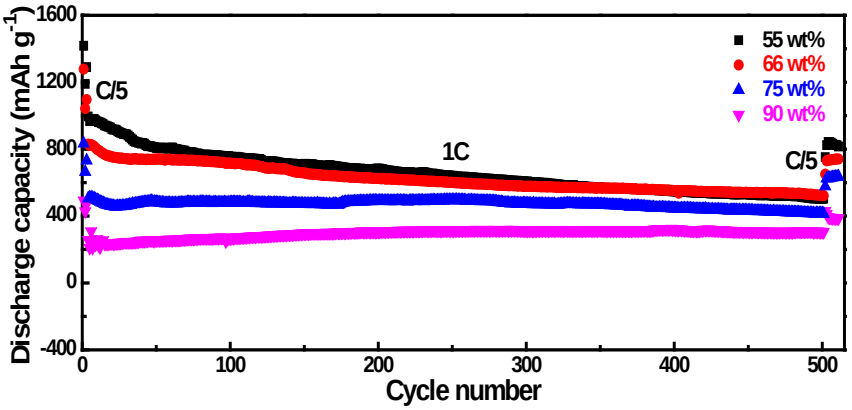

Figure 4.3 The long term cycling performance of the S@GA electrodes with different amounts of sulfur loading in sulfur/carbon composites, i.e. 55, 66, 75, and 90 wt%, respectively.

The S@GA cathodes with different sulfur loadings in sulfur/carbon composites (i.e. 60, 70, 80, and 90 wt%) were evaluated for long term cycling, as shown in Figure 4.3. The electrodes were first intentionally cycled at *C*/5 to have high utilization of active materials, and then cycled for 500 cycles at 1 *C* before cycling back at *C*/5. When the sulfur loading was 55 wt%, the S@GA cathode delivered an initial capacity of 996 mAh/g at 1 *C* rate at the fourth cycle, which is ca. 60% of its theoretical maximum. After 500 cycles, the capacity stabilized at 504 mAh/g at 1 *C* with a capacity retention of 50.6%. An obvious increase in capacity to 843 mAh/g after 500 cycles was observed when decreasing the current rate from 1 *C* to *C*/5. With the increase in sulfur loading, cycling performances were much more stable albeit at the expense of lower sulfur utilization. The S@GA cathodes delivered a reversible capacity of 741, 637, and 430 mAh/g at *C*/5 after 500 charge/discharges when sulfur content increased to 66, 75, and 90 wt%, respectively. This result indicates the excellent stability of sulfur cathodes with the GA binder for improving the longevity of Li-S batteries. Figure S4.2 shows the cycling comparison of sulfur cathodes with the GA binder to different bio-derived and non-bio-derived aqueous binders that have

been applied in Li-S batteries to date. Since most sulfur electrodes show cycling performance within 50 cycles, we focused the comparison on the initial discharge capacity and capacity at the fiftieth cycle. The GA binder demonstrated the best cycling performance among aqueous binders in Li-S batteries: i) the S@GA electrode demonstrated cycling performance after 500 cycles had a capacity of 843 mAh/g and capacity retention of 60% at *C*/5; ii) the high sulfur loading of 90 wt% in sulfur/carbon composites with 500 stable cycles was also achieved; and iii) the S@GA electrode shows higher capacity than most sulfur electrodes. It is worth noting that when normalized to sulfur, the initial capacity of the S@GA electrode is much lower than that of Ref. 17 in Figure S4.2a (1386 vs. 1543 mAh/g). However, when taking composites into consideration, the capacity of the S@GA electrode is much higher than that of Ref. 17 (762 vs. 694 mAh/g).

Polysulfides (Li_2S_x, x>2) have good dissolution in organic electrolytes and migrate to the Li anode, where they electrochemically react with metallic Li subsequently resulting in poor cyclability and low Coulombic efficiency (always < 90%). Considering its excellent cycling performance (ca. 60% capacity retention after 500 cycles) and high Coulombic efficiency (> 95%), we believed that the importance of the GA binder stems from its ability to maintain electrode integrity and immobilize polysulfides within the cathode. Therefore, we shifted out our attention to the physical and chemical properties of GA to study possible mechanisms to improve in cycling performance.

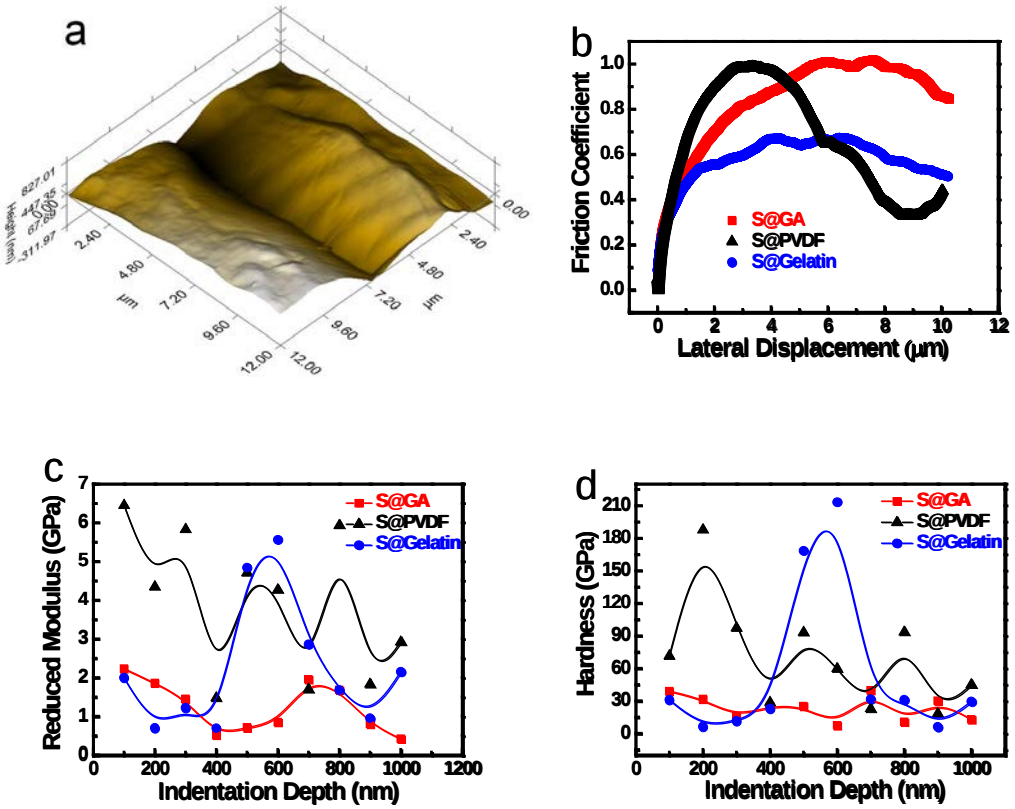

Figure 4.4 Characterization of GA's physical properties. (a) *In situ* 3D nano-scratch images of the S@GA electrode by SPM microscopy, (b) friction coefficients of the S@GA, S@PVDF, and S@gelatin electrodes obtained by the nano-scratch test, (c) Average reduced modulus, and (d) hardness variations of the S@GA, S@PVDF, and S@gelatin electrodes obtained by the nano-indentation test.

Nano-scratch and nano-indentation tests were carried out to quantify the mechanical properties of resultant sulfur cathodes with different binders, and used SPM microscopy to obtain *in situ* 3D nano-scratch images of the electrode, as shown in Figure 4.4. The scratch force was set to 1000 μN and the scratch length was set to 10μm. The scratch track of the S@GA electrode is smooth with limited cracks (Figure 4.4a), which is comparable to that of the S@PVDF and S@gelatin electrodes (Figures S4.3a and S4.3b). Lateral force was recorded in real time for the calculation of the friction coefficient during the scratch test

(Figure 4.4b). The friction coefficient of the S@GA electrode remained more constant comparing with that of the S@PVDF electrode, while the average friction coefficient of the S@GA electrode was much higher than that of the S@gelatin electrode. This demonstrates more compliance and greater tolerance to volume change by the GA binder than the PVDF and gelatin binder. The nano-indentation test was done under the force of 2000 μN; and ten individual indents were adopted for accurate calculation. The indentation depth (*Er*) is a combined modulus of the indenter and specimen, which is given in Equation 1:

$$\frac{1}{E_r} = \frac{(1-v^2)}{E} + \frac{(1-v'^2)}{E'} \quad (1)$$

Where E and v are the Young's modulus and Poisson's ratio of the specimen, and E' and v' are the elastic modulus and Poisson's ratio of the indenter. For a standard diamond indenter, E' is 1140 GPa and v' is 0.07. Meanwhile, the measurement of hardness (H) is given in Equation 2:

$$H = \frac{P_{max}}{A} \quad (2)$$

Where A is the projected area of contact and P_{max} is the maximum load. The averaged reduced modulus E_r and hardness H varying with indentation depths are shown in Figures 4.4c and 4.4d. The lowest modulus and hardness of the S@GA electrode demonstrates the superior mechanical properties of GA compared to PVDF and gelatin, which is highly beneficial for tolerance of delamination needed for long cycle life.

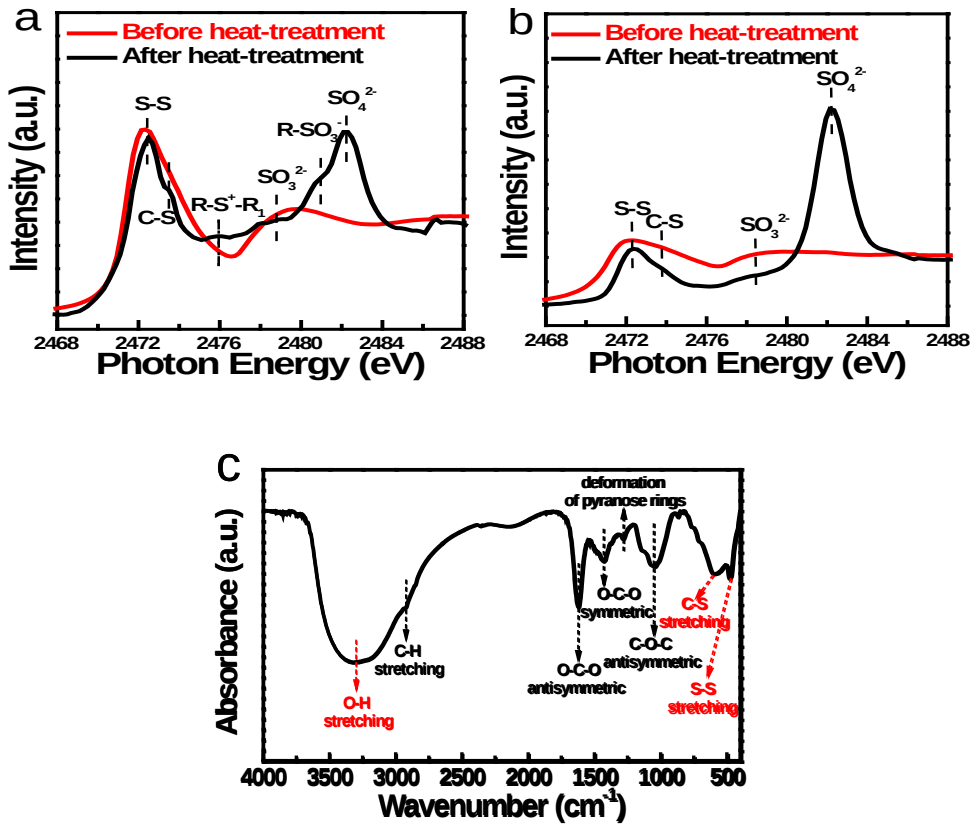

Figure 4.5 Characterization of chemical bonding between GA and S. (a) TEY and (b) TFY S K-edge XAS spectra for the mixture of GA and S before and after heat-treatment at 80 ^{o}C, and (c) FTIR spectroscopy of the mixture of GA and polysulfides (Li_2S_x, x = 8) after heat-treatment at 80 ^{o}C.

S K-edge X-ray absorption spectroscopy (XAS) was applied to monitor the S atom bonding evolution and study the possible chemical reactions between GA and S. We simulated sample preparation processes by mixing GA with S and heat treated them at 80 ^{o}C for 2 hours. The total-electron-yield (TEY) and total-fluorescence-yield (TFY) S K-edge XAS data of the mixtures before and after heat-treatment are presented in Figure 4.5. Before annealing, both TEY and TFY spectra show only a broad peak located at 2472.37 eV, which is attributed to the typical bonding of elemental S.[33] After heat-treatment, the peak intensity of the elemental S decreased while four new peaks were identified in the TEY spectrum. The new peaks located at 2473.41, 2478.17, 2480.56, and 2481.97 eV are attributed to the transitions from S 1s

to $R\text{-}S^{-}_{C\text{-}S\sigma^*}$, $SO_3^{2-}{}_{O\text{-}S\sigma^*}$, $R\text{-}SO_3^{-}{}_{O\text{-}S\sigma^*}$, and $SO_4^{2-}{}_{C\text{-}S\sigma^*}$, respectively.[33,34] These new peaks demonstrate the chemical bonding between the functional groups of GA and S. The same peaks are further confirmed by the TFY spectrum in Figure 4.5b. As the TFY mode is more bulk-sensitive than the TEY mode, the dominant peak at 2481.97 eV further confirmed the strong bonding between GA and S.[35] We used the FTIR spectroscopy to identify chemical bonding between the functional groups of GA and polysulfides (Li_2S_x, x = 8), as shown in Figure 4.5c. Compared to pure GA in Figure 4.1b, the spectrum of heat-treated GA-Li_2S_8 composites reveals an obvious red shift of the O-H stretching vibrations peak from 3406 to 3316 cm^{-1}, while two new absorption peaks related to S-C stretching and S-S bending vibrations appear at 600 and 484 cm^{-1}.[28,36,37] The chemical reactions between GA and polysulfides help trap polysulfides and immobilize sulfur species within the cathode. This hinders the out-diffusion of polysulfides from the S cathode to the Li anode, leading to the low loss of active sulfur species and subsequent excellent long term cycling.

The physical and chemical properties of the GA binder are responsible for the integrity of the sulfur electrode and immobilization of sulfur species onto the current collector, which can be confirmed by Li-S cells before and after cycling. EIS measurements were performed on the cells with GA, PVDF, and gelatin binders before and after cycling (Figure S4.4). The EIS data show the smallest semi-circle of the S@GA cell both before and after cycling, indicating its lower interfacial resistance compared with the PVDF and gelatin cells.[38,39] The GA binder provides stronger binding strength between S and C as well as electrode mixture and current collector, which restricts volume change and preserves electrode integrity during cycling. The surface morphology of the S@GA cathode before and after cycling was observed using SEM as shown in Figure S4.5. There was no obvious morphology

change in the S@GA cathode before and after long cycling. However, the re-deposition of polysulfides on the carbon surface was still observed. Through the chemical bonding of GA and sulfur species, the extent of the shuttle effect can be substantially controlled. The uniform re-dispersion and immobilization of sulfur species also reduce cell resistance as verified by EIS measurements and benefitted from the utilization of active sulfur material. All the results provide strong supports for the excellent mechanical properties of GA and chemical bonding between GA and S, which play a critical role in maintaining the integrity of sulfur electrode as well as restraining the polysulfide shuttle to improve the longevity of Li-S batteries.

4.3. Conclusions

In summary, the naturally available GA polymer is introduced as a green binder for high performance sulfur cathode in Li-S batteries. Using the same preparation procedure as in traditional Li-S cells, the resulting S@GA cathode demonstrates significantly better electrochemical performance compared to S@PVDF and S@gelatin electrodes. The S@GA electrode delivered an initial capacity of 1386 mAh/g at *C*/5, and 843 mAh/g at *C*/5 and 504 mAh/g at 1 *C* through 500 cycles when sulfur loading was 55 wt% in sulfur/carbon composites. The highly reversible capacity of 430 mAh/g at *C*/5 was also obtained after 500 charge/discharges when sulfur loading was enhanced to 90 wt%. To the best of our knowledge, the GA binder in this work demonstrates a better cycling performance than all previously used bio-derived and nonbio-derived aqueous binders in Li-S batteries. This result indicates the excellent stability of sulfur cathodes with GA binder for the longevity of Li-S batteries, which is attributed to the unique physical and chemical properties of GA. The excellent mechanical properties of GA endow sulfur electrodes with high binding

strength and good ductility to buffer volume change, while its functional groups chemically immobilize sulfur species within the cathode to inhibit the polysulfide shuttle. In this work, we demonstrate for the first time the important role of binder from both its physical and chemical properties in Li-S batteries. We believe this discovery will increase interest in the battery research community's search for natural binders to meet the requirements of Li-S cells.

References

1 Chu, S. & Majumdar, A. (2012) 'Opportunities and challenges for a sustainable energy future', *Nature* 488, 294-303.

2 Dunn, B., Kamath, H. & Tarascon, J. M. (2011) 'Electrical Energy Storage for the Grid: A Battery of Choices', *Science* 334, 928-935.

3 Ji, L. W., Lin, Z., Alcoutlabi, M. & Zhang, X. W. (2011) 'Recent developments in nanostructured anode materials for rechargeable lithium-ion batteries', *Energy & Environmental Science* 4, 2682-2699.

4 Manthiram, A., Fu, Y., Chung, S.-H., Zu, C. & Su, Y.-S. (2014) 'Rechargeable lithium-sulfur batteries', *Chemical Reviews*, 10.1021/cr500062v.

5 Yang, Y., Zheng, G. Y. & Cui, Y. (2013) 'Nanostructured sulfur cathodes', *Chemical Society Reviews* 42, 3018-3032.

6 Yin, Y. X., Xin, S., Guo, Y. G. & Wan, L. J. (2013) 'Lithium-Sulfur Batteries: Electrochemistry, Materials, and Prospects', *Angewandte Chemie-International Edition* 52, 13186-13200.

7 Chen, L. & Shaw, L. L. (2014) 'Recent advances in lithium-sulfur batteries', *Journal of Power Sources* 267, 770-783.

8 Lin, Z. & Liang, C. (2014) 'Lithium–sulfur batteries: from liquid to solid cells', *Journal of Materials Chemistry A*, DOI: 10.1039/c1034ta04727c.

9 Ji, X. L., Lee, K. T. & Nazar, L. F. (2009) 'A highly ordered nanostructured carbon-sulphur cathode for lithium-sulphur batteries', *Nature Materials* 8, 500-506.

10 Sun, L., Li, M. Y., Jiang, Y., Kong, W. B., Jiang, K. L., Wang, J. P. & Fan, S. S. (2014) 'Sulfur Nanocrystals Confined in Carbon Nanotube Network As a

Binder-Free Electrode for High-Performance Lithium Sulfur Batteries', *Nano letters* 14, 4044-4049.

11 Wang, H. L., Yang, Y., Liang, Y. Y., Robinson, J. T., Li, Y. G., Jackson, A., Cui, Y. & Dai, H. J. (2011) 'Graphene-Wrapped Sulfur Particles as a Rechargeable Lithium-Sulfur Battery Cathode Material with High Capacity and Cycling Stability', *Nano letters* 11, 2644-2647.

12 Zhao, M. Q., Zhang, Q., Huang, J. Q., Tian, G. L., Nie, J. Q., Peng, H. J. & Wei, F. (2014) 'Unstacked double-layer templated graphene for high-rate lithium-sulphur batteries', *Nature Communications* 5, DOI: 10.1038/Ncomms4410.

13 Zhou, G. M., Yin, L. C., Wang, D. W., Li, L., Pei, S. F., Gentle, I. R., Li, F. & Cheng, H. M. (2013) 'Fibrous Hybrid of Graphene and Sulfur Nanocrystals for High-Performance Lithium-Sulfur Batteries', *Acs Nano* 7, 5367-5375.

14 Chou, S. L., Pan, Y. D., Wang, J. Z., Liu, H. K. & Dou, S. X. (2014) 'Small things make a big difference: binder effects on the performance of Li and Na batteries', *Physical Chemistry Chemical Physics* 16, 20347-20359.

15 Jeong, Y. K., Kwon, T. W., Lee, I., Kim, T. S., Coskun, A. & Choi, J. W. (2014) 'Hyperbranched beta-Cyclodextrin Polymer as an Effective Multidimensional Binder for Silicon Anodes in Lithium Rechargeable Batteries', *Nano letters* 14, 864-870.

16 Shen, L. Y., Shen, L., Wang, Z. X. & Chen, L. Q. (2014) 'In Situ Thermally Cross-linked Polyacrylonitrile as Binder for High-Performance Silicon as Lithium Ion Battery Anode', *Chemsuschem* 7, 1951-1956.

17 Wu, M. Y., Xiao, X. C., Vukmirovic, N., Xun, S. D., Das, P. K., Song, X. Y., Olalde-Velasco, P., Wang, D. D., Weber, A. Z., Wang, L. W., Battaglia, V. S.,

Yang, W. L. & Liu, G. (2013) 'Toward an Ideal Polymer Binder Design for High-Capacity Battery Anodes', *Journal of the American Chemical Society* 135, 12048-12056.

18 Song, M. K., Cairns, E. J. & Zhang, Y. G. (2013) 'Lithium/sulfur batteries with high specific energy: old challenges and new opportunities', *Nanoscale* 5, 2186-2204.

19 Kim, G. T., Jeong, S. S., Joost, M., Rocca, E., Winter, M., Passerini, S. & Balducci, A. (2011) 'Use of natural binders and ionic liquid electrolytes for greener and safer lithium-ion batteries', *Journal of Power Sources* 196, 2187-2194.

20 Lux, S. F., Schappacher, F., Balducci, A., Passerini, S. & Winter, M. (2010) 'Low Cost, Environmentally Benign Binders for Lithium-Ion Batteries', *Journal of the Electrochemical Society* 157, A320-A325.

21 Kovalenko, I., Zdyrko, B., Magasinski, A., Hertzberg, B., Milicev, Z., Burtovyy, R., Luzinov, I. & Yushin, G. (2011) 'A Major Constituent of Brown Algae for Use in High-Capacity Li-Ion Batteries', *Science* 334, 75-79.

22 Bao, W. Z., Zhang, Z. A., Gan, Y. Q., Wang, X. W. & Lia, J. (2013) 'Enhanced cyclability of sulfur cathodes in lithium-sulfur batteries with Na-alginate as a binder', *Journal of Energy Chemistry* 22, 790-794.

23 Sun, J., Huang, Y. Q., Wang, W. K., Yu, Z. B., Wang, A. B. & Yuan, K. G. (2008) 'Application of gelatin as a binder for the sulfur cathode in lithium-sulfur batteries', *Electrochimica Acta* 53, 7084-7088.

24 Wang, Q. Q., Wang, W. K., Huang, Y. Q., Wang, F., Zhang, H., Yu, Z. B., Wang, A. B. & Yuan, K. G. (2011) 'Improve Rate Capability of the Sulfur

Cathode Using a Gelatin Binder', *Journal of the Electrochemical Society* 158, A775-A779.

25 He, M., Yuan, L. X., Zhang, W. X., Hu, X. L. & Huang, Y. H. (2011) 'Enhanced Cyclability for Sulfur Cathode Achieved by a Water-Soluble Binder', *Journal of Physical Chemistry C* 115, 15703-15709.

26 Wang, J. L., Yao, Z. D., Monroe, C. W., Yang, J. & Nuli, Y. (2013) 'Carbonyl-beta-Cyclodextrin as a Novel Binder for Sulfur Composite Cathodes in Rechargeable Lithium Batteries', *Advanced Functional Materials* 23, 1194-1201.

27 Ryou, M. H., Kim, J., Lee, I., Kim, S., Jeong, Y. K., Hong, S., Ryu, J. H., Kim, T. S., Park, J. K., Lee, H. & Choi, J. W. (2013) 'Mussel-Inspired Adhesive Binders for High-Performance Silicon Nanoparticle Anodes in Lithium-Ion Batteries', *Advanced Materials* 25, 1571-1576.

28 Abu-Dalo, M. A., Othman, A. A. & Al-Rawashdeh, N. A. F. (2012) 'Exudate Gum from Acacia Trees as Green Corrosion Inhibitor for Mild Steel in Acidic Media', *International Journal of Electrochemical Science* 7, 9303-9324.

29 Almuslet, N. A., Hassan, E. A., Abd-El-Magied, A. S., Al-Sherbini & Muhgoub, M. G. A. (2012) 'Diode Laser (532 nm) Induced Grafting of Polyacrylamide onto Gum Arabic', *Journal of Physical Science* 23.

30 Renard, D., Lavenant-Gourgeon, L., Ralet, M. C. & Sanchez, C. (2006) 'Acacia senegal gum: Continuum of molecular species differing by their protein to sugar ratio, molecular weight, and charges', *Biomacromolecules* 7, 2637-2649.

31 Lin, Z., Nan, C., Ye, Y., Guo, J., Zhu, J. & Cairns, E. J. (2014) 'High-performance lithium/sulfur cells with a bi-functionally immobilized sulfur cathode', *Nano Energy* 9, 408-416.

32 Nan, C., Lin, Z., Liao, H., Song, M.-K., Li, Y. & Cairns, E. J. (2014) 'Durable Carbon-Coated Li2S Core−Shell Spheres for High Performance Lithium/Sulfur Cells', *J. Am. Chem. Soc.* 136, 4659-4663.

33 Jalilehvand, F. (2006) 'Sulfur: not a "silent" element any more', *Chemical Society Reviews* 35, 1256-1268.

34 Feng, X. F., Song, M. K., Stolte, W. C., Gardenghi, D., Zhang, D., Sun, X. H., Zhu, J. F., Cairns, E. J. & Guo, J. H. (2014) 'Understanding the degradation mechanism of rechargeable lithium/sulfur cells: a comprehensive study of the sulfur-graphene oxide cathode after discharge-charge cycling', *Physical Chemistry Chemical Physics* 16, 16931-16940.

35 Dey, A., Chow, M., Taniguchi, K., Lugo-Mas, P., Davin, S., Maeda, M., Kovacs, J. A., Odaka, M., Hodgson, K. O., Hedman, B. & Solomon, E. I. (2006) 'Sulfur K-Edge XAS and DFT calculations on nitrile hydratase: Geometric and electronic structure of the non-heme iron active site', *Journal of the American Chemical Society* 128, 533-541.

36 Coelho, R. R., Hovell, I., de Souza, A. L. & Rajagopal, K. (2006) 'PETR 34-Characterization of the functional chemical structure of sulphur in polyaromatic compounds from heavy petroleum fractions', *Abstracts of Papers of the American Chemical Society* 232.

37 Qian, W. L. & Krimm, S. (1992) 'Conformation Dependence of the Sh and Cs Stretch Frequencies of the Cysteine Residue', *Biopolymers* 32, 1503-1518.

38 Canas, N. A., Hirose, K., Pascucci, B., Wagner, N., Friedrich, K. A. & Hiesgen, R. (2013) 'Investigations of lithium-sulfur batteries using electrochemical impedance spectroscopy', *Electrochimica Acta* 97, 42-51.

39 Yuan, L. X., Qiu, X. P., Chen, L. Q. & Zhu, W. T. (2009) 'New insight into the discharge process of sulfur cathode by electrochemical impedance spectroscopy', *Journal of Power Sources* 189, 127-132.

Supporting Information

Acacia Senegal-Inspired Bi-functional Binder for Longevity of Lithium-Sulfur Batteries

Experimental

Electrode Preparation

Gum arabic (GA, No. 51198), extruded from *Acacia senegal*, was obtained from Sigma-Aldrich. Elemental sulfur (Aladdin, China) and super P carbon (TIMCAL, Switzerland) were used as active material and conductive additive for the sulfur electrode. Polyvinylidene fluoride (PVDF, HSV900, Arkema Inc. France) and gelatin (Gelatin, Aladdin, China) were also used as binders for comparison.

To prepare the sulfur electrode, GA was first dissolved in deionized water to 40 mg/ml as the binder solution. The aqueous slurry, containing defined amount of sulfur active material, super P carbon, and polymer binder, was simply mixed and casted on 1 μm carbon-coated Al foil. Deionized water and N-methyl-2-pyrrolidone (NMP) were used as dispersant for gelatin and PVDF, respectively. The working electrodes consisted of 80 wt% sulfur/carbon composites and 20 wt% polymer binder. The ratio of polymer binder was kept constant at 20 wt% for all electrodes. The sulfur loading in the sulfur/carbon composites of 60 wt% (i.e. the sulfur content in the electrode is 48 wt%) were used with different binders for comparison. The sulfur loadings in sulfur/carbon composites of 70, 80, and 90 wt% (i.e. the sulfur content in the electrode was increased to 56, 64, and 72 wt%) were also tested for their long term cycling. The electrodes were dried in vacuum at 60 °C overnight, and 2 hours at 80 °C

under ambient conditions before use. The mass loadings of the electrodes were 1.0-2.5 mg/cm^2.

Electrochemical evaluation

Coin cell test. The electrochemical performance of sulfur electrodes were tested in CR2025 coin cells under galvanostatic charge/discharge at room temperature using LAND battery cycler (China). Cells were assembled in an Ar-filled glove box using metallic lithium wafer as counter electrode. The electrolyte contained 1M lithium bis(trifluoromethane sulfonyl) imide (LiTFSI) in a binary solvent of 1,3-dioxolane (DOL) and dimethoxyethane (DME) (1:1 in volume) with 1 wt% lithium nitrate ($LiNO_3$) as additive. Celgard 2400 membrane was used as separator. Current density and specific capacity were calculated based on the mass of S active material.

CV test. Cyclic voltammetry (CV) study of the electrode was recorded by CHI660E electrochemical work station (Chinstruments, China) in the voltage range of 1.8-2.6 V vs. Li/Li$^+$ at a scan rate of 0.1 mV/s^1.

EIS test. Electrochemical impedance spectroscopy (EIS) of the electrode was recorded by CHI660E electrochemical work station with amplitude of 5 mV at the frequency range of 0.01Hz-100kHz.

Materials Characterization

XPS. X-ray photoelectron spectroscopy (XPS) was acquired in an ESCALAB-250Xi X-ray photoelectron spectrometer (ThermoFisher, UK) operating at an Al Kα radiation source, with an energy resolution of 1 eV for the survey and 0.1 eV for individual characteristic peaks.

FTIR. Fourier transform infrared spectrometry (FTIR) analyses were performed using a Tensor 27 (Bruker, Germany). 1 mg sample was mixed with 100 mg KBr and pressed into a pellet under pressure of 10 MPa. For each spectrum, the scan was collected at a resolution of 4 cm^{-1} from 4000 to 400 cm^{-1}. For the FTIR test on chemical bondage between GA and polysulfides, Li_2S_x (x = 8) solution was first prepared by proportionally adding S and Li_2S into THF solvent and stirring vigorously. GA was then added into the solution and continuously stirred for 4 hours. The obtained homogeneous suspension was subsequently volatilized and heated at 80 °C for one more hour until the brown mixture of GA and polysulfides was collected. All the above FTIR experiments were carried out in an Ar-filled glove box.

XAS. GA was mixed with sulfur powder in the glove box, and then heat-treated at 80 ^{o}C for 2 hours. After cooling down to room temperature, the mixture was pressed into In foil and formed some thin films. The thin films were transferred to beamline 9.3.1 in Advanced Light Source, Lawrence Berkeley National Laboratory. S K-edge X-ray absorption spectroscopy (XAS) data were collected in the beamline. Total electrons yield (TEY) signals were detected by monitoring the offset sample drain current while total fluorescence yield (TFY) signals were collected using a silicon drift detector.

Indentation test. In nano-scratch tests, a conical indenter (with radius approximately 1 μm, 90° cone angle) was used to scratch over the sample surface to obtain friction coefficient information. During the scratch process, the normal load was kept constant as 1000 μN and the lateral displacement was set as 10 μm. The nano-indentation tests were undertaken using a Hysitron TI 950 nano-indentation system with Berkovich indenter (three-sided pyramidal tip with radius approximately 150 nm, 142.3º total included angles).

SEM. SEM studies of the sulfur electrodes before and after cycling were carried out using an Utral 55 SEM microscope (CorlzeisD, Germany). The in-lens secondary electron detector was performed using an accelerating voltage of 5 kV and a working distance of ca. 7 mm. After cycling electrodes were washed three times using DEM/DOL solution before the SEM study.

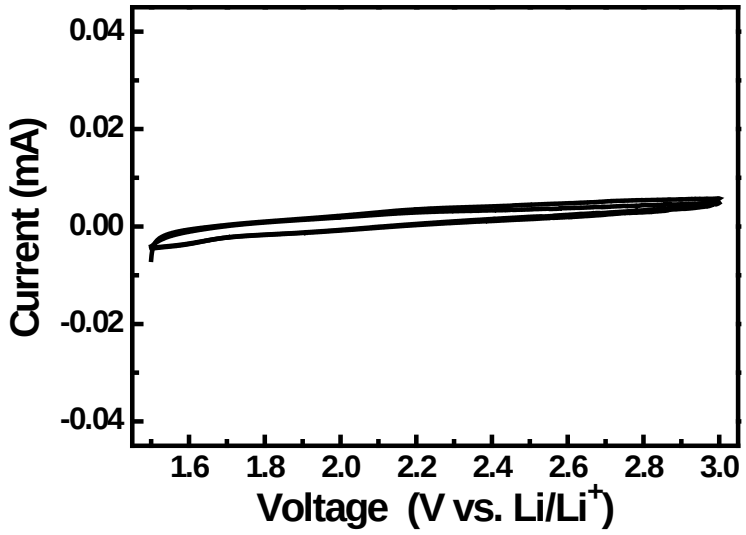

Figure S4.1 Cyclic voltammetry study of GA in the voltage range of 1.5-3.0 V vs. Li/Li^+ at the scan rate of 0.1mV/s.

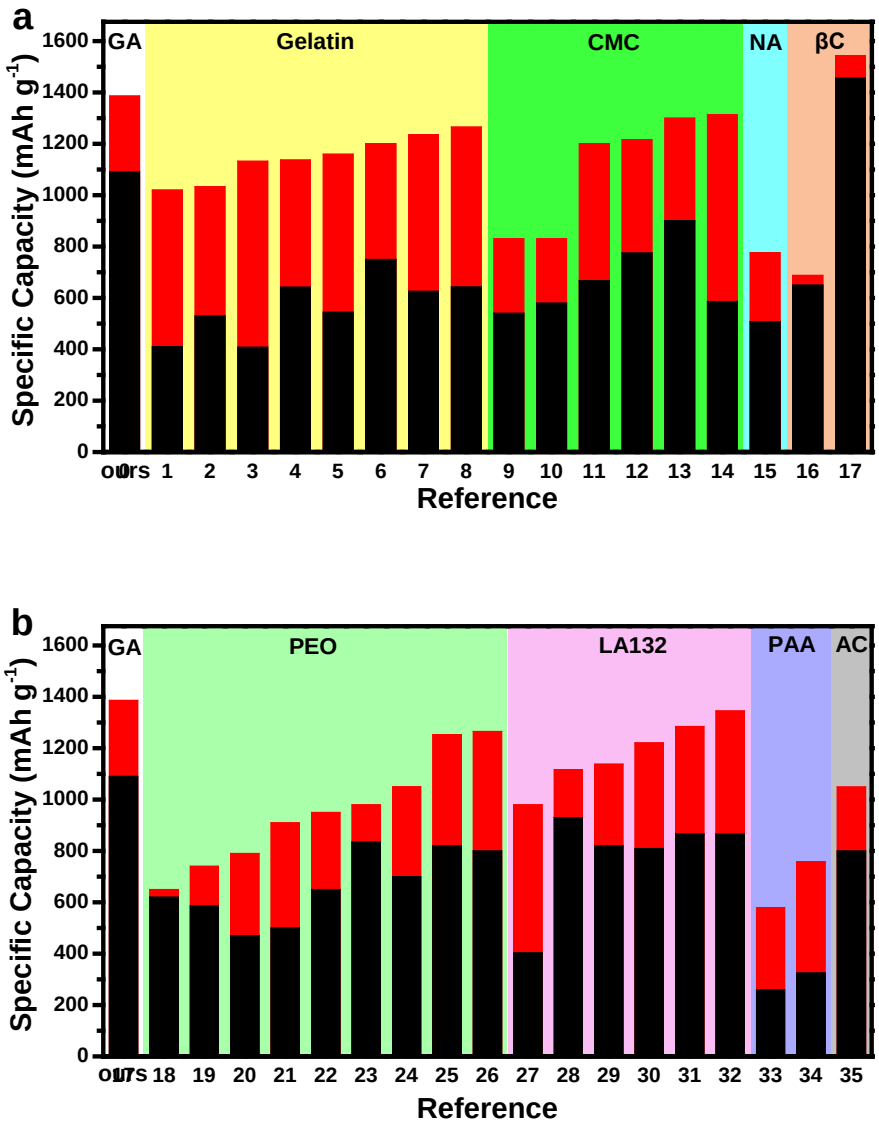

Figure S4.2 Comparisons of the GA binder with (a) bio-derived binders, including gelatin (Gelatin, Ref. 1-8), carboxy methyl cellulose (CMC, Ref. 9-14), sodium alginates (NA, Ref. 15), and β-cyclodextrin (βC, Ref. 16-17);[1-17] and (b) nonbio-derived aqueous binders, including poly(ethylene oxide) (PEO, Ref. 18-26), acrylonitrile copolymer (LA132, Ref. 27-32), poly(acrylic acid) (PAA, Ref. 33-34), and poly(acrylamide-co-diallyldimethylammonium chloride) (AC Ref. 35). ENREF 6 18[18-3518-35] The capacities for comparison are from the 1st (denoted as ■) and 50th cycle (denoted as ■) at low current rates.

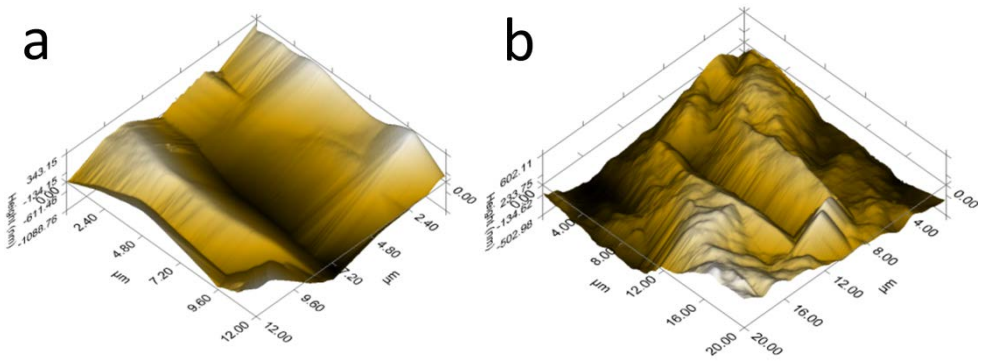

Figure S4.3 *In situ* 3D nano-scratch images of the (a) S@PVDF and (b) S@gelatin electrode by the SPM microscopy.

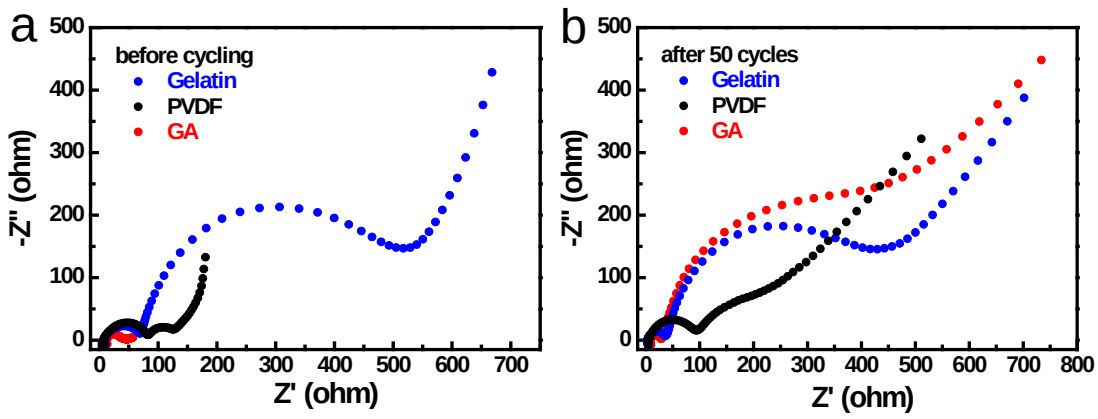

Figure S4.4 Electrochemical impedance spectroscopy studies of electrodes with different binders (a) before and (b) after 50 cycles.

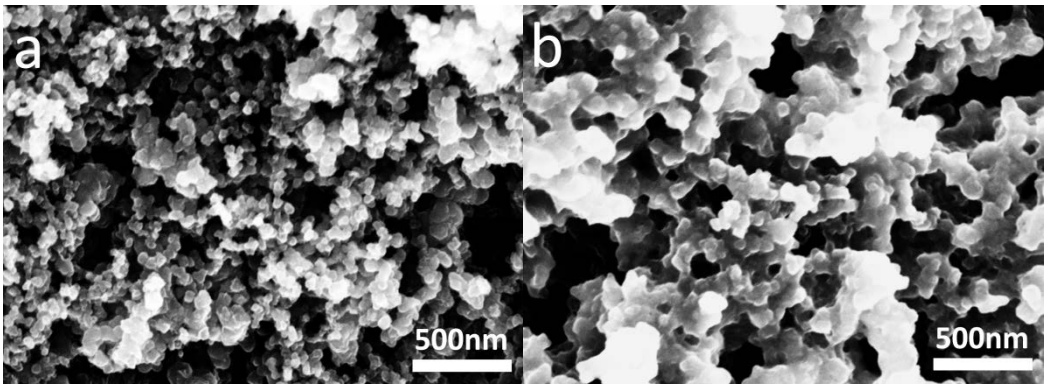

Figure S4.5 SEM images of the S@GA electrode (a) before and (b) after 50 cycles.

References

1 Nelson, J., Misra, S., Yang, Y., Jackson, A., Liu, Y. J., Wang, H. L., Dai, H. J., Andrews, J. C., Cui, Y. & Toney, M. F. (2012) 'In Operando X-ray Diffraction and Transmission X-ray Microscopy of Lithium Sulfur Batteries', *Journal of the American Chemical Society* 134, 6337-6343.

2 Jiang, S. Y., Gao, M. Y., Huang, Y. Q., Wang, W. K., Zhang, H., Yu, Z. B., Wang, A. B., Yuan, K. G. & Chen, X. N. (2013) 'Enhanced performance of the sulfur cathode with L-cysteine-modified gelatin binder', *Journal of Adhesion Science and Technology* 27, 1006-1011.

3 Sun, J., Huang, Y. Q., Wang, W. K., Yu, Z. B., Wang, A. B. & Yuan, K. G. (2008) 'Application of gelatin as a binder for the sulfur cathode in lithium-sulfur batteries', *Electrochimica Acta* 53, 7084-7088.

4 Zhang, W. Y., Huang, Y. Q., Wang, W. K., Huang, C. J., Wang, Y., Yu, Z. B. & Zhang, H. (2010) 'Influence of pH of Gelatin Solution on Cycle Performance of the Sulfur Cathode', *Journal of the Electrochemical Society* 157, A443-A446.

5 Wang, Q. Q., Wang, W. K., Huang, Y. Q., Wang, F., Zhang, H., Yu, Z. B., Wang, A. B. & Yuan, K. G. (2011) 'Improve Rate Capability of the Sulfur Cathode Using a Gelatin Binder', *Journal of the Electrochemical Society* 158, A775-A779.

6 Wang, W. K., Wang, Y., Huang, Y. Q., Huang, C. J., Yu, Z. B., Zhang, H., Wang, A. B. & Yuan, K. G. (2010) 'The electrochemical performance of lithium-sulfur batteries with LiClO4 DOL/DME electrolyte', *Journal of Applied Electrochemistry* 40, 321-325.

7 Sun, J., Huang, Y. Q., Wang, W. K., Yu, Z. B., Wang, A. B. & Yuan, K. G. (2008) 'Preparation and electrochemical characterization of the porous sulfur cathode using a gelatin binder', *Electrochemistry Communications* 10, 930-933.

8 Wei, S. C., Zhang, H., Huang, Y. Q., Wang, W. K., Xia, Y. Z. & Yu, Z. B. (2011) 'Pig bone derived hierarchical porous carbon and its enhanced cycling performance of lithium-sulfur batteries', *Energy & Environmental Science* 4, 736-740.

9 Schneider, H., Garsuch, A., Panchenko, A., Gronwald, O., Janssen, N. & Novak, P. (2012) 'Influence of different electrode compositions and binder materials on the performance of lithium-sulfur batteries', *Journal of Power Sources* 205, 420-425.

10 He, M., Yuan, L. X., Zhang, W. X., Hu, X. L. & Huang, Y. H. (2011) 'Enhanced Cyclability for Sulfur Cathode Achieved by a Water-Soluble Binder', *Journal of Physical Chemistry C* 115, 15703-15709.

11 Rao, M. M., Song, X. Y. & Cairns, E. J. (2012) 'Nano-carbon/sulfur composite cathode materials with carbon nanofiber as electrical conductor for advanced secondary lithium/sulfur cells', *Journal of Power Sources* 205, 474-478.

12 Lacey, M. J., Jeschull, F., Edstrom, K. & Brandell, D. (2014) 'Functional, water-soluble binders for improved capacity and stability of lithium-sulfur batteries', *Journal of Power Sources* 264, 8-14.

13 Rao, M. M., Li, W. S. & Cairns, E. J. (2012) 'Porous carbon-sulfur composite cathode for lithium/sulfur cells', *Electrochemistry Communications* 17, 1-5.

14 Rao, M. M., Song, X. Y., Liao, H. G. & Cairns, E. J. (2012) 'Carbon nanofiber-sulfur composite cathode materials with different binders for secondary Li/S cells', *Electrochimica Acta* 65, 228-233.

15 Wu, Y. L., Yang, J., Wang, J. L., Yin, L. C. & Nuli, Y. N. (2010) 'Composite Cathode Structure and Binder for High Performance Lithium-Sulfur Battery', *Acta Physico-Chimica Sinica* 26, 283-290.

16 Bao, W. Z., Zhang, Z. A., Gan, Y. Q., Wang, X. W. & Lia, J. (2013) 'Enhanced cyclability of sulfur cathodes in lithium-sulfur batteries with Na-alginate as a binder', *Journal of Energy Chemistry* 22, 790-794.

17 Wang, J. L., Yao, Z. D., Monroe, C. W., Yang, J. & Nuli, Y. (2013) 'Carbonyl-beta-Cyclodextrin as a Novel Binder for Sulfur Composite Cathodes in Rechargeable Lithium Batteries', *Advanced Functional Materials* 23, 1194-1201.

18 Zhou, X., Wan, L.-J. & Guo, Y.-G. (2013) 'Electrospun Silicon Nanoparticle/Porous Carbon Hybrid Nanofibers for Lithium-Ion Batteries', *Small* 9, 2684-2688.

19 Cheon, S. E., Cho, J. H., Ko, K. S., Kwon, C. W., Chang, D. R., Kim, H. T. & Kim, S. W. (2002) 'Structural factors of sulfur cathodes with poly(ethylene oxide) binder for performance of rechargeable lithium sulfur batteries', *Journal of the Electrochemical Society* 149, A1437-A1441.

20 Choi, Y. J., Kim, K. W., Ahn, H. J. & Ahn, J. H. (2008) 'Improvement of cycle property of sulfur electrode for lithium/sulfur battery', *Journal of Alloys and Compounds* 449, 313-316.

21 Liang, X., Wen, Z. Y., Liu, Y., Wang, X. Y., Zhang, H., Wu, M. F. & Huang, L. Z. (2011) 'Preparation and characterization of sulfur-polypyrrole

composites with controlled morphology as high capacity cathode for lithium batteries', *Solid State Ionics* 192, 347-350.

22 Lacey, M. J., Jeschull, F., Edstrom, K. & Brandell, D. (2013) 'Why PEO as a binder or polymer coating increases capacity in the Li-S system', *Chemical Communications* 49, 8531-8533.

23 Park, M. S., Jeong, B. O., Kim, T. J., Kim, S., Kim, K. J., Yu, J. S., Jung, Y. & Kim, Y. J. (2014) 'Disordered mesoporous carbon as polysulfide reservoir for improved cyclic performance of lithium-sulfur batteries', *Carbon* 68, 265-272.

24 Urbonaite, S. & Novak, P. (2014) 'Importance of 'unimportant' experimental parameters in Li-S battery development', *Journal of Power Sources* 249, 497-502.

25 Park, M. S., Yu, J. S., Kim, K. J., Jeong, G., Kim, J. H., Jo, Y. N., Hwang, U., Kang, S., Woo, T. & Kim, Y. J. (2012) 'One-step synthesis of a sulfur-impregnated graphene cathode for lithium-sulfur batteries', *Physical Chemistry Chemical Physics* 14, 6796-6804.

26 Liang, X. A., Wen, Z. Y., Liu, Y., Zhang, H., Huang, L. Z. & Jin, J. (2011) 'Highly dispersed sulfur in ordered mesoporous carbon sphere as a composite cathode for rechargeable polymer Li/S battery', *Journal of Power Sources* 196, 3655-3658.

27 Zhang, S. C., Zhang, L., Wang, W. K. & Xue, W. J. (2010) 'A Novel cathode material based on polyaniline used for lithium/sulfur secondary battery', *Synthetic Metals* 160, 2041-2044.

28 Chen, H. W., Dong, W. L., Ge, J., Wang, C. H., Wu, X. D., Lu, W. & Chen, L. W. (2013) 'Ultrafine Sulfur Nanoparticles in Conducting Polymer Shell as

Cathode Materials for High Performance Lithium/Sulfur Batteries', *Scientific Reports* 3.

29 Chen, S. R., Zhai, Y. P., Xu, G. L., Jiang, Y. X., Zhao, D. Y., Li, J. T., Huang, L. & Sun, S. G. (2011) 'Ordered mesoporous carbon/sulfur nanocomposite of high performances as cathode for lithium-sulfur battery', *Electrochimica Acta* 56, 9549-9555.

30 Miao, L. X., Wang, W. K., Wang, A. B., Yuan, K. G. & Yang, Y. S. (2013) 'A high sulfur content composite with core-shell structure as cathode material for Li-S batteries', *Journal of Materials Chemistry A* 1, 11659-11664.

31 Qiu, L. L., Zhang, S. C., Zhang, L., Sun, M. M. & Wang, W. K. (2010) 'Preparation and enhanced electrochemical properties of nano-sulfur/poly(pyrrole-co-aniline) cathode material for lithium/sulfur batteries', *Electrochimica Acta* 55, 4632-4636.

32 Xu, G. L., Xu, Y. F., Fang, J. C., Peng, X. X., Fu, F., Huang, L., Li, J. T. & Sun, S. G. (2013) 'Porous Graphitic Carbon Loading Ultra High Sulfur as High-Performance Cathode of Rechargeable Lithium-Sulfur Batteries', *Acs Applied Materials & Interfaces* 5, 10782-10793.

33 Lee, J. T., Zhao, Y. Y., Kim, H., Cho, W. I. & Yushin, G. (2014) 'Sulfur infiltrated activated carbon cathodes for lithium sulfur cells: The combined effects of pore size distribution and electrolyte molarity', *Journal of Power Sources* 248, 752-761.

34 Zhang, Z. A., Bao, W. Z., Lu, H., Jia, M., Xie, K. Y., Lai, Y. Q. & Li, J. (2012) 'Water-Soluble Polyacrylic Acid as a Binder for Sulfur Cathode in Lithium-Sulfur Battery', *Ecs Electrochemistry Letters* 1, A34-A37.

35 Zhang, S. S. (2012) 'Binder Based on Polyelectrolyte for High Capacity Density Lithium/Sulfur Battery', *Journal of the Electrochemical Society* 159, A1226-A1229.

CHAPTER 5: LOW COST AND ENVIRONMENTALLY BENIGN CRACK-BLOCKING STRUCTURES FOR LONG LIFE AND HIGH POWER SI ELECTRODES IN LITHIUM ION BATTERIES

Journal of Materials Chemistry A, 2014, doi: 10.1039/c4ta05817h

STATEMENT OF CONTRIBUTION TO CO-AUTHORED PUBLISHED PAPER

This chapter includes a co-authored paper. The bibliographic details of the co-authored paper, including all authors, are:

Min Ling, Hui Zhao, Xingcheng Xiao, Feifei Shi, Mingyan Wu, Jingxia Qiu, Sheng Li, Xiangyun Song, Gao Liu* and Shanqing Zhang*

Low cost and environmentally benign crack-blocking structures for long life and high power Si electrodes in lithium ion batteries

Published in *Journal of Materials Chemistry A, 2014, doi: 10.1039/c4ta05817h*

My contribution to the paper involved:

Initial concept, experimental design and implementation;

Collection and analysis of data;

Preparation of manuscript.

(Signed) _____ (Date)_____

Name of Student: Min Ling

(Countersigned) _____ (Date)_____
Corresponding author of paper: Shanqing Zhang

(Countersigned) _____ (Date)_____
Supervisor: Shanqing Zhang

Pages 174-195 of this chapter which consists of the published paper, “Low cost and environmentally benign crack-blocking structures for long life and high power Si electrodes in lithium ion batteries” have been removed from this copy for copyright reasons.

CHAPTER 6: A MULTI-FUNCTIONAL SA-PRODOT BINDER FOR LITHIUM ION BATTERIES

Submitted in *Nano Letters, Manuscript Number: nl-2015-00795w*

STATEMENT OF CONTRIBUTION TO CO-AUTHORED PUBLISHED PAPER

This chapter includes a co-authored paper. The bibliographic details of the co-authored paper, including all authors, are:

Min Ling, Sheng Li, Jingxia Qiu, Cheng Yan, Milton Kiefel, Gao Liu*, Shanqing Zhang*

A Multi-functional SA-ProDOT Binder for Lithium Ion Batteries

Submitted in *Nano Letters, Manuscript Number: nl-2015-00795w*

My contribution to the paper involved:

Initial concept, experimental design and implementation;

Collection and analysis of data;

Preparation of manuscript.

(Signed) _____ (Date)_____

Name of Student: Min Ling

(Countersigned) _____ (Date)_____
Corresponding author of paper: Shanqing Zhang

(Countersigned) _____ (Date)_____
Supervisor: Shanqing Zhang

Pages 198-230 of this chapter which consists of the published paper, "A Multi-functional SA-ProDOT Binder for Lithium Ion Batteries" have been removed from this copy for copyright reasons.

CHAPTER 7: CONCLUSIONS AND FUTURE WORK

7.1 General conclusions

To achieve economical and green lithium ion batteries fabrication technology, we developed a series of promising binder systems as a substitute to the conventional binder systems. The innovated binder systems, including Eastman AQ^{TM} *55S* (EAQ), gum arabic (GA), gum arabic and polyacrylic composite (GA-PAA) and sodium alginate conjugated ProDOT (SA-ProDOT), meet the critical criteria such as binding capability, mechanical property, and lithium ion and electronic conductivity. The EAQ and SA-ProDOT binders can improve the performance of graphite and lithium ion phosphate (LFP) compared to the currently applied active materials in industry. With respect to the high energy density batteries, the GA and GA-PAA binder system could improve Si anode material chemical bonding and improved conductivity. The GA binder system is also proven promising for the application in sulfur batteries.

The major findings can be summarized as follows:

1. We demonstrate that the green polymer Eastman $AQ^{TM}55S$ (EAQ) has potential for use as a LIB binder substitute for conventional LIB binders. The EAQ polymer binder is operation-environment friendly because it uses aqueous solvents, instead of N-methyl-2-pyrrolidinone (NMP) solvents which are used for PVDF binders. Moreover, the EAQ polymer binder has abundant active hydroxyl groups on its surface, which is different to the inert PVDF binder. We used oxidized graphite with carboxyl groups on its surface as the anode material. The specific capacity of the EAQ-based electrode increased by ca. 50% compared to the PVDF-based electrode. We demonstrate that the formation of the chemical bonds between the carboxyl groups on the oxidized graphite surface and the hydroxyl groups on the EAQ polymer surface is the key factor in this improved performance. The water soluble EAQ

polymer binder has the potential to convert the traditional LIB production process from an organic solvent and binder-based process into a green and water-based production technology.

2. A glycoprotein-reinforced Si electrode with high binding strength and ductility was produced based on the gum arabic (GA) natural polymer binder. The concept of *Fibre-Reinforced Concrete* (FRC) was applied to the LIB electrode fabrication process. There are two main benefits of GA that enhance performance: hydroxyl groups in polysaccharide increase the binding force and glycoproteins improve the mechanical properties including the tolerance of volume expansion. The resultant anodes, i.e. Si@GA anodes, have excellent adhesion to Si nanoparticles and current collector, increased ductility and more importantly, can endure dramatic the volume changes (up to 300%) of Si thereby prohibiting physical fracture during lithiation/delithiation processes. These outstanding properties stem from the concrete tensile structures formed by the abundant functional groups as well as the glycoprotein chain. A stable cycling performance was demonstrated at various *C* rates while a promising long-term performance of 1000 cycles was observed when limiting the specific capacity to 1000 mAh/g at 1 *C*.

3. The naturally available GA polymer was introduced as a green binder for high performance sulfur cathodes in Li-S batteries. Using the same preparation procedure as in traditional Li-S cells, the resulting S@GA cathode demonstrated significantly better electrochemical performance compared with S@PVDF and S@Gelatin electrodes. The S@GA electrode delivered an initial capacity of 1386 mAh/g at *C*/5, and 843 mAh/g at *C*/5 and 504 mAh/g at 1 *C* through 500 cycles when sulfur loading was 55 wt% in sulfur/carbon composites. The highly reversible capacity of 430 mAh/g at *C*/5 was also obtained after 500 charge/discharges when sulfur loading was

enhanced to 90 wt%. To the best of our knowledge, the GA binder in our work has a better cycling performance than all other previously used bio-derived and nonbio-derived aqueous binders in Li-S batteries. This result indicates the excellent stability of sulfur cathodes with GA binder to improve the longevity of Li-S batteries. The excellent mechanical properties of GA endow the sulfur electrode with high binding strength and good ductility to buffer volume change, while its functional groups chemically immobilize sulfur species within the cathode to inhibit the polysulfide shuttle. In this work, we demonstrate for the first time the importance of binders in Li-S batteries due to both their physical and chemical properties.

4. High areal Si loading anodes with high volumetric capacity for LIBs were successfully assembled via a simple *in situ* esterification process using the water-based natural polymers GA and PAA at 150 ^{o}C under vacuum. The esterification reaction between hydroxyl groups in GA and carboxylic acid groups in PAA provides reinforced mechanical strength and lithium diffusion capability. The micron-sized pores formed during the process block crack formation and propagation by relieving the stress of the electrode due to the dramatic volume change of Si particles during lithiation/delithiation processes. The excellent thermal, electrochemical and mechanical stability of the GA–PAA composite facilitated high volumetric capacity and long-term cycle performance that demonstrated promising potential for industrial applications.

5. The multifunctional polymer SA-ProDOT, was synthesized from sodium alginate **(**SA) and 3,4-propylenedioxythiophene-2,5-dicarboxylic acid (ProDOT) using a cyclohexane/DBSA/water micro-emulsion system as a conducting polymer binder in $LiFePO_4$ (LFP) electrodes. A long-term cycle with high specific capacity of ca. 120 mAh/g at 1 *C* cycle was achieved without the conductive additives when

using SA-ProDOT as a binder. The optimized performances compared with SA, SA plus carbon black (CB) and PVDF plus CB are due to improved Li-ion conduction, diffusion efficiency and lower electro-chemical impedance. The synthesized SA-ProDOT is very promising for applied universal application in low cost and environmentally benign LIB manufacturing.

7.2 Future work

The mechanism of the improved binding property will be further studied based on the binder systems developed in our lab. Since most of the experiments were conducted at the lab scale, the prospect for industrialization of the binder systems still needs investigation. I will also expand my research scope to further understand the Li-ion mass transport and electronic conductivity of the electrode and apply the proposed strategies to industrial manufacturing. The details are as follows:

1. Based on the excellent dispersion and distribution property of gum arabic (GA), modification of GA will be conducted to achieve higher energy/power density LIBs e.g. lithium ion conductivity, electronic conductivity and glass transmission temperature (T_g).
2. The relationship between the lithium ion diffusion coefficient and lithium ion conductivity will be studied especially with the existence of binder.
3. The value of lithium ion conductivity and electronic conductivity with various binder systems will be calculated to reveal the synergetic relationship.